

44722

National Library
of CanadaBibliothèque nationale
du Canada

Canadian Theses Division Division des thèses canadiennes

Ottawa, Canada
K1A 0N4**PERMISSION TO MICROFILM — AUTORISATION DE MICROFILMER**

- Please print or type — Écrire en lettres mouillées ou dactylographier

Full Name of Author — Nom complet de l'auteur

George Paul DEMETRE

Date of Birth — Date de naissance

1951.02.16

Country of Birth — Lieu de naissance

CANADA

Permanent Address — Résidence fixe

46 DEPT. OF MINERAL ENG.
UNIVERSITY OF ALBERTA
EDMONTON
T6G 2G6

Title of Thesis — Titre de la thèse

Scaling and Instability of
Simultaneous Flow in
Porous Media

University — Université

University of Alberta

Degree for which thesis was presented — Grade pour lequel cette thèse fut présentée

M.Sc.

Year this degree conferred — Année d'obtention de ce grade

1980

Name of Supervisor — Nom du directeur de thèse

DR. R. G. BENTSEN.

Permission is hereby granted to the NATIONAL LIBRARY OF
CANADA to microfilm this thesis and to lend or sell copies of
the film.

The author reserves other publication rights, and neither the
thesis nor extensive extracts from it may be printed or other-
wise reproduced without the author's written permission.

L'autorisation est, par la présente, accordée à la BIBLIOTHÈ-
QUE NATIONALE DU CANADA de microfilmer cette thèse et de
prêter ou de vendre des exemplaires du film.

L'auteur se réserve les autres droits de publication; ni la thèse
ni de longs extraits de celle-ci ne doivent être imprimés ou
autrement reproduits sans l'autorisation écrite de l'auteur.

Date

April 17/1980

Signature

George Demetre.



NOTICE

The quality of this microfiche is heavily dependent upon the quality of the original thesis submitted for microfilming. Every effort has been made to ensure the highest quality of reproduction possible.

If pages are missing, contact the university which granted the degree.

Some pages may have indistinct print especially if the original pages were typed with a poor typewriter ribbon or if the university sent us a poor photocopy.

Previously copyrighted materials (journal articles, published tests, etc.) are not filmed.

Reproduction in full or in part of this film is governed by the Canadian Copyright Act, R.S.C. 1970, c. C-30. Please read the authorization forms which accompany this thesis.

**THIS DISSERTATION
HAS BEEN MICROFILMED
EXACTLY AS RECEIVED**

AVIS

La qualité de cette microfiche dépend grandement de la qualité de la thèse soumise au microfilmage. Nous avons tout fait pour assurer une qualité supérieure de reproduction.

S'il manque des pages, veuillez communiquer avec l'université qui a conféré le grade.

La qualité d'impression de certaines pages peut laisser à désirer, surtout si les pages originales ont été dactylographiées à l'aide d'un ruban usé ou si l'université nous a fait parvenir une photocopie de mauvaise qualité.

Les documents qui font déjà l'objet d'un droit d'auteur (articles de revue, examens publiés, etc.) ne sont pas microfilmés.

La reproduction, même partielle, de ce microfilm est soumise à la Loi canadienne sur le droit d'auteur, SRC 1970, c. C-30. Veuillez prendre connaissance des formules d'autorisation qui accompagnent cette thèse.

**LA THÈSE A ÉTÉ
MICROFILMÉE TELLE QUE
NOUS L'AVONS REÇUE**

THE UNIVERSITY OF ALBERTA

SCALING AND INSTABILITY OF SIMULTANEOUS FLOW IN POROUS MEDIA

by

C

George Paul DEMETRE

A THESIS

SUBMITTED TO THE FACULTY OF GRADUATE STUDIES AND RESEARCH
IN PARTIAL FULFILMENT OF THE REQUIREMENTS FOR THE DEGREE
OF MASTER OF SCIENCE

IN

PETROLEUM ENGINEERING

DEPARTMENT OF MINERAL ENGINEERING

EDMONTON, ALBERTA

SPRING, 1980

THE UNIVERSITY OF ALBERTA
FACULTY OF GRADUATE STUDIES AND RESEARCH

The undersigned certify that they have read, and recommend to the Faculty of Graduate Studies and Research, for acceptance, a thesis entitled SCALING AND INSTABILITY OF SIMULTANEOUS FLOW IN POROUS MEDIA submitted by George Paul DEMETRE in partial fulfilment of the requirements for the degree of MASTER OF SCIENCE in PETROLEUM ENGINEERING.

.....
.....
Supervisor: Dr. R.G. Bentsen
.....
.....
.....

Date March 28, 1980

Ah, not in knowledge is happiness, but in the acquisition of knowledge. In for ever knowing, we are for ever blessed; but to know all, were the curse of a fiend.

From "The Power of Words"
Edgar Allan Poe (1809-1849)

Abstract

Laboratory studies must be scaled, if they are to be useful in predicting fluid flow behaviour in petroleum reservoirs. To this end, an extended set of scaling groups has been derived which includes all of the variables in the immiscible fluid displacement problem. Of particular note is the result that the geometric factor is unimportant when comparing a model and prototype, provided that the displacement is stable.

To verify this result, and to investigate the effect of stability on the immiscible displacement problem, a series of experiments was undertaken. Distilled water was used to displace a Dow Corning 200 oil from tubular, unconsolidated sandpacks. The experimental results show that the geometric factor is not important, provided that the displacement is either stable or pseudo-stable (fully developed fingering). Furthermore, it is demonstrated that neither the linear nor the radial scaling groups are good correlating parameters in the transition zone between stable and pseudo-stable displacements ($13.56 < N_s < 900$). Finally, the experimental results corroborate earlier experimental work, delimiting stable and unstable displacements, undertaken in this laboratory.

Acknowledgements

The author would like to thank Dr. D.L. Flock for providing the initial motivation for this study.

Acknowledgement is gratefully given to Dr. R.G. Bentsen for his innumerable consultations throughout the course of this study.

Special thanks to Mr. G.T. Walsh for the design and modifications to the experimental apparatus and to Hans Nerenberg for his most helpful suggestions in the laboratory.

Finally, the author gratefully acknowledges the financial assistance of the Alberta Oil Sands Technology and Research Authority and the National Research Council.

Table of Contents

Chapter	Page
1. Introduction	1
1.1 Purpose of This Study	1
1.2 Stabilization and Stability--Terminology Defined ...	3
2. Theory and Literature Review	4
2.1 Theory of Immiscible Displacement	4
2.1.1 Fundamental Equations	4
2.1.2 Relative Permeability and Mobility Ratio	5
2.1.3 Partial Differential Equation	9
2.1.4 Fractional Flow Equation	9
2.1.5 Capillary Pressure Models	10
2.2 Immiscible Displacement Mechanisms	12
2.2.1 Muskat Displacement Mechanism	12
2.2.2 Buckley-Leverett and Dietz Displacement Mechanisms	17
2.3 Scaled Models and Scaling Groups	22
2.3.1 Derivation of Scaling Groups	23
2.3.2 Dimensionless Form of the Fluid Displacement Equations	25
2.3.3 Remarks on Scaling Groups	28
2.4 Stability Theory of Immiscible Displacement	31
2.4.1 Experimental Observations and Mathematical Descriptions of Instability	32
3. Experimental Equipment, Materials and Procedure	43
3.1 Porous Media	43
3.1.1 Sand	43
3.1.2 Coreholders	43

3.1.3 Packing Procedure	43
3.2 Fluids	44
3.3 Pumping System	45
3.4 Sandpack Property Determination	47
3.5 Displacement Procedure	48
3.6 Core Extraction Technique	49
4. Presentation and Discussion of Results	50
4.1 Sandpack Properties	50
4.2 Wettability of the Porous Media	51
4.3 Displacement Results	54
4.4 Scaling in Porous Media--Theoretical Results	55
4.5 Scaling in Porous Media--Experimental Results	58
4.5.1 Water-wet System	59
4.5.2 Oil-wet System--Horizontal Displacements	68
4.5.3 Oil-wet System--Vertical Displacements	77
4.6 Stability of Displacement Tests	79
4.6.1 Water-wet System	79
4.6.2 Oil-wet System	82
5. Summary and Conclusions	84
Recommendations	88
References Cited	90
Selected Bibliography	93
Appendix A--Derivations	95
A.1 Derivation of Equation 2.16	95
A.2 Derivations of Scaling Groups	99
A.2.1 Dimensional Analysis	99
A.2.2 Inspectional Analysis	105

A.2.3 Modified Inspectional Analysis	110
Appendix B--Experimental Results From the Literature	120
Appendix C--Sample Calculation of Extrapolated Data	122

List of Tables

Table		Page
2.1	System Parameters--Peters, 1979	41
3.1	Pertinent Fluid Properties At 21.5°C	45
4.1	Summary of Sandpack Properties	52
4.2	Summary of Displacement Tests	56
B.1	Summary of Sandpack Properties--Data From Peters (1979)	120
B.2	Summary of Displacement Tests--Data from Peters (1979)	121

List of Figures

Figure		Page
2.1	Typical Relative Permeability Curves	8
2.2	Typical Normalized Relative Permeability Curves ..	8
2.3	Typical Capillary Pressure Curve	13
2.4	Typical Normalized Capillary Pressure Curve	13
2.5	Saturation Distribution for the Muskat and Buckley-Leverett Models	15
2.6	Effect of Mobility Ratio--Linear System (Muskat, 1937)	18
2.7	Saturation Distribution for the Buckley-Leverett and Dietz Models	21
2.8	Variation of Breakthrough Recovery with Reciprocal Capillary Number Showing the Effect of Mobility Ratio	30
3.1	Schematic of Apparatus	44
4.1	Recovery Correlated By The Inverse Linear Leverett Number--Water-Wet System	60
4.2	Recovery Correlated by the Inverse Radial Leverett Number--Water-Wet System	63
4.3	Recovery Correlated by the Inverse Linear Capillary Number--Water-Wet System	65
4.4	Recovery Correlated by the Inverse Radial Capillary Number--Water-Wet System	66
4.5	Recovery Correlated by the Inverse Linear Leverett Number--Oil-Wet System	69
4.6	Recovery Correlated by the Inverse Radial Leverett Number--Oil-Wet System	73
4.7	Recovery Correlated by the Inverse Linear Capillary Number--Oil-Wet System	74
4.8	Recovery Correlated by the Inverse Radial Capillary Number--Oil-Wet System	75

4.9 Recovery Correlated by the Inverse Gravity
Number--Oil-Wet System 76

4.10 Scaled Onset of Instability--Water-Wet System ... 80

4.11 Scaled Onset of Instability--Oil-Wet System 83

Nomenclature

- a Radius of the system
- A Cross-sectional area
- C Chuoke's constant
- C* Wettability number
- $C(S^*) = -\frac{1}{M_r} F_w(S^*) K_{ro}(S^*) \frac{d\pi_c(S^*)}{dS^*}$
- D Diameter of the system
- \vec{f}_w Vector of fractional flow of water
- f_{wd} Fractional flow as defined by Dietz
- $f_{w\xi}, \dots$ Fractional flow of water in the ξ, β, ψ directions
- $F_w(S^*)$ Fractional flow function = $\frac{M_r K_{rw}(S^*)}{M_r K_{rw}(S^*) + K_{ro}(S^*)}$
- \vec{g} Vector of gravity acceleration (pointing downward)
- $\vec{G}(S^*)$ Vector of gravity function = $\left[\frac{\vec{v}}{|\vec{v}|} - \frac{\vec{N}_g}{M_r} K_{ro}(S^*) \right] F_w(S^*)$
- h Formation thickness
- IOIP Initial oil in place
- $J(S_w)$ Leverett function of saturation = $\frac{P_c(S_w)}{\gamma} (K/\phi)^{1/2}$
- K Absolute permeability
- $K_o(S_w)$ Effective permeability to oil (function of saturation)

- $K_w(S_w)$ Effective permeability to water (function of saturation)
 K_{ob} Permeability to oil at some base saturation
 K_{wb} Permeability to water at some base saturation
 K_{or} Permeability to oil at residual water saturation
 K_{wr} Permeability to water at residual oil saturation
 $K_{ro}(S_w)$ Relative permeability to oil (function of saturation)
 $k_{rw}(S_w)$ Relative permeability to water (function of saturation)
 L Length of the system
 L_x, L_y Length in the x,y direction, respectively

Lt_l Linear Leverett number $\frac{\gamma(K\phi)^{1/2}}{V\mu_w L}$

Lt_r Radial Leverett number $\frac{\gamma(K\phi)^{1/2}}{V\mu_w D}$

m, λ, t Mass, length, time units used in dimensional analysis

M_g General mobility ratio $\frac{K_{wb} \mu_o}{K_{ob} \mu_w}$

M_r End-point mobility ratio $\frac{K_{wr} \mu_o}{K_{or} \mu_w}$

M_s Shock mobility ratio $\left[\frac{K_{or} K_{ro}(S_f)}{\mu_o} + \frac{K_{wr} K_{rw}(S_f)}{\mu_w} \right] / \frac{K_{or}}{\mu_o}$

M_R Ratio of mobilities $\frac{K_w(S_w)}{K_o(S_w)} \frac{\mu_o}{\mu_w}$

n Stability index

N_c Capillary number, dimensionless, equivalent to the linear capillary number

N_{cl}	Linear capillary number, dimensionless	$\frac{\sigma K_{wr}}{V_{hw} L}$
N_{cr}	Radial capillary number, dimensionless	$\frac{\sigma K_{wr}}{V_{hw} D}$
\vec{N}_g	Vector of gravity number, dimensionless	$\frac{K_{wr} \Delta \rho \vec{g}}{ \vec{v} \mu_w}$
P_c	Capillary pressure	
P_d	Displacement pressure	
P_o	Pressure in oil phase	
P_w	Pressure in water phase	
P_1, P_2	Inlet and outlet pressure, respectively	
q	Volumetric flow rate	
r, θ, x	Cylindrical coordinates	
S^*	Normalized water saturation	$\frac{S_w - S_{wi}}{1 - S_{or} - S_{wi}}$
S_f	Saturation at the floodfront	
S_o	Oil saturation	
S_{or}	Residual oil saturation	
S_w	Water saturation	
S_{wd}	$= 1 - S_{or} - S_{wi}$	
S_{wi}	Residual water saturation	
S_w^*	Some particular saturation	
t	Time	
$ \vec{v} , v$	Superficial velocity	
\vec{v}	Vector of superficial velocity	
\vec{v}_o	Vector of superficial oil velocity	

\vec{v}_r, \dots	Component of velocity in the r, β , x directions, respectively
\vec{v}_w	Vector of superficial water velocity
v_{wn}	Velocity of water normal to the fluid-fluid interface
V_c	Critical superficial velocity
V_f	Velocity of floodfront
x,y,z	Rectangular cartesian coordinates
x_f	Location of floodfront
Y	Coordinate of the oil/water interface as a fraction of formation thickness
Y^*	Some particular coordinate of the oil/water interface as a fraction of formation thickness
α	Angle of inclination of the system with the horizontal
α'	Angle of inclination of the system with the vertical
γ	Interfacial tension
γ^*	Effective or pseudo-interfacial tension
δ	Wave number
ζ	Non-normalized dimensionless length
$\Delta\rho$	Water-oil density difference
θ	Contact angle
λ	Wavelength of perturbation
λ_c	Critical wavelength
λ_m	Most probable wavelength of disturbance
μ_o	Oil viscosity
μ_w	Water viscosity
ξ	Normalized dimensionless length
ξ_f	Location of floodfront in dimensionless form
π_c	Normalized capillary pressure, dimensionless

π_1	Buckingham pi-term
ρ_0	Oil density
ρ_w	Water density
σ	Capillary pressure normalizing parameter
τ	Normalized dimensionless time
τ^*	Dimensionless time for the moving boundary problem
T	Non-normalized dimensionless time
ϕ	Porosity, fraction
Φ	Non-normalized dimensionless radius
ψ	Normalized dimensionless radius
$\hat{\psi}, \hat{\beta}, \hat{\xi}$	Unit vectors in the dimensionless coordinate system
ω	Angle of dip with the horizontal of the fluid-fluid interface

1. Introduction

With the ever-increasing demand for energy, it is of prime importance to employ and expand the technology currently available to the oil industry.

Waterflooding, the most important secondary recovery process which has been utilized for decades, is, as yet, not fully understood. This incomplete knowledge of the process may lead to disastrous results, if the economics of the project are marginal. Consequently, the effect of the interplay of viscous, capillary and gravity forces on the recovery of oil from a reservoir must be known.

1.1 Purpose of This Study

The problem of conducting meaningful laboratory tests on a model, with the purpose of relating the results to a prototype, has been the objective of many researchers. The number of variables which control the displacement process is numerous and the task is by no means trivial.

The purpose of this study was twofold. The first objective was to establish a set of scaling groups which included all of the variables in the problem as it is understood today. The approach used to reach this first objective was:

- 1) - to review the results of the methods of dimensional and inspectional analysis found in the literature,

- 2) to derive the scaling groups in a multi-dimensional system using a current capillary pressure model, and
- 3) to verify certain scaling groups experimentally.

The second objective was to investigate further, and verify, the criterion which determines the onset of floodfront perturbations. The specific areas of interest were:

- 1) Water-wet, residual water saturation system.
 - a) Better locate the onset of instability experimentally,
 - b) Investigate the possibility of a second region in the recovery curve, at a high value of the stability number, where the recovery is insensitive to frontal perturbations, and
 - c) Extend the data collected by Peters (1979) to small and large values of the stability number.
- 2) Oil-wet, no residual water saturation system.
 - a) Attempt to locate the onset of instability in the recovery curve, as suggested by the theory.
 - b) Better define the second region in the recovery curve for high values of the stability number and determine its magnitude.

- c) Extend the data collected by Peters (1979) to both small and large values of the stability number.

The purpose of extending the data collected by Peters (1979), to small and large values of the stability number, was to verify the suggestion that the recovery is independent of the stability number for these magnitudes. It was also intended to investigate further any possible anomalies which might appear in the data.

1.2 Stabilization and Stability--Terminology Defined

Throughout the literature, the terms 'stabilization' and 'stability' appear often. In view of the fact that both terms apply to the behaviour of the floodfront, it is important to understand the physical interpretation of these terms in order to avoid confusion.

'Stabilization' occurs when the frontal region of the saturation profile has attained a fixed configuration invariant with time. This saturation profile should approach that predicted by Buckley-Leverett (1941) theory.

During the life of a waterflood, frontal perturbations (viscous fingering) may arise. The displacement is considered to be 'stable' if these frontal perturbations are attenuated. Thus a 'stable' displacement may be either 'stabilized' or 'unstabilized', depending on the magnitude of certain variables which control the displacement process.

2. Theory and Literature Review

2.1 Theory of Immiscible Displacement

2.1.1 Fundamental Equations

The partial differential equation describing the displacement of one fluid by another through a porous medium may be derived by combining Darcy's law and the equations of continuity for each phase.

Darcy's law, in a general three-dimensional form, for the simultaneous flow of two immiscible and incompressible fluids through a homogeneous and isotropic porous medium may be written as:

$$\vec{v}_w = - \frac{K_w(S_w)}{\mu_w} (\text{grad } P_w - \rho_w \vec{g}) \quad 2.1$$

and

$$\vec{v}_o = - \frac{K_o(S_w)}{\mu_o} (\text{grad } P_o - \rho_o \vec{g}) \quad 2.2$$

for each phase.

If the porous medium is considered to be non-deformable, then the equations of continuity may be written as (Buckley and Leverett, 1942):

$$\text{div } \vec{v}_w = - \phi \frac{\partial S_w}{\partial t} \quad 2.3$$

and

$$\text{div } \vec{V}_0 = -\phi \frac{\partial S_0}{\partial t} = \phi \frac{\partial S_w}{\partial t} \quad 2.4$$

for each phase. Note that conservation of mass requires that the saturations must sum to unity, viz:

$$S_w + S_0 = 1 \quad 2.5$$

A capillary pressure definition (Leverett, 1941)

$$P_c(S_w) = P_0 - P_w \quad 2.6$$

is required to link Equations 2.1 and 2.2.

2.1.2 Relative Permeability and Mobility Ratio

Before proceeding with the derivation of the partial differential equation, it is convenient to introduce the concepts of relative permeability and mobility ratio. Relative permeability is defined as the effective permeability to a specific fluid divided by some base permeability, viz:

$$K_{rw}(S_w) \equiv \frac{K_w(S_w)}{K_{wb}} \quad 2.7$$

and

$$K_{ro}(S_w) \equiv \frac{K_o(S_w)}{K_{ob}} \quad 2.8$$

There are three different base permeabilities which are generally used throughout the literature (Craig, 1971):

- 1) The absolute air permeability;
- 2) The absolute water permeability;
- 3) The permeability to oil at residual water saturation.

Equations 2.1 and 2.2 both contain a term of the form (k/μ) . This term is defined as the mobility of the fluid. As will be demonstrated in a later section, a mobility ratio will be defined. Suffice it to state the general form of the ratio of mobilities as:

$$M_R \equiv \frac{K_w(S_w)}{\mu_w} \frac{\mu_o}{K_o(S_w)} \quad 2.9$$

The ratio of mobilities may be defined as the water mobility divided by the oil mobility. Using the definitions of relative permeability given by Equations 2.7 and 2.8 yields:

$$M_R = \frac{K_{rw}(S_w)}{K_{ro}(S_w)} \frac{K_{wb}}{K_{ob}} \frac{\mu_o}{\mu_w} \quad 2.10$$

A general mobility ratio may be defined as:

$$M_g \equiv \frac{K_{wb}}{K_{ob}} \frac{\mu_o}{\mu_w} \quad 2.11$$

It has been stated in the literature (Bentsen, 1976) that defining the relative permeability in terms of a single base permeability may not be desirable. If this is done,

then a non-dimensionalizing procedure will select the viscosity ratio as the scaling group. However, it is generally thought that the mobility ratio is a better scaling group (Craig, 1971).

After the manner of Perkins and Collins (1960), in which a different base permeability is used to normalize the two effective permeabilities, Equations 2.7 and 2.8 may be written as:

$$K_{rw}(S_w) = \frac{K_w(S_w)}{K_{wr}} \quad 2.12$$

and

$$K_{ro}(S_w) = \frac{K_o(S_w)}{K_{or}} \quad 2.13$$

where K_{wr} and K_{or} are the permeabilities to water at residual oil saturation and to oil at residual water saturation respectively. Furthermore, these relative permeabilities may be defined in terms of a normalized water saturation (S^*):

$$K_{rw}(S^*) = \frac{K_w(S^*)}{K_{wr}} \quad 2.14$$

$$K_{ro}(S^*) = \frac{K_o(S^*)}{K_{or}} \quad 2.15$$

Figures 2.1 and 2.2 illustrate typical and normalized relative permeabilities, respectively.

FIG: 2.1 TYPICAL RELATIVE PERMEABILITY CURVES

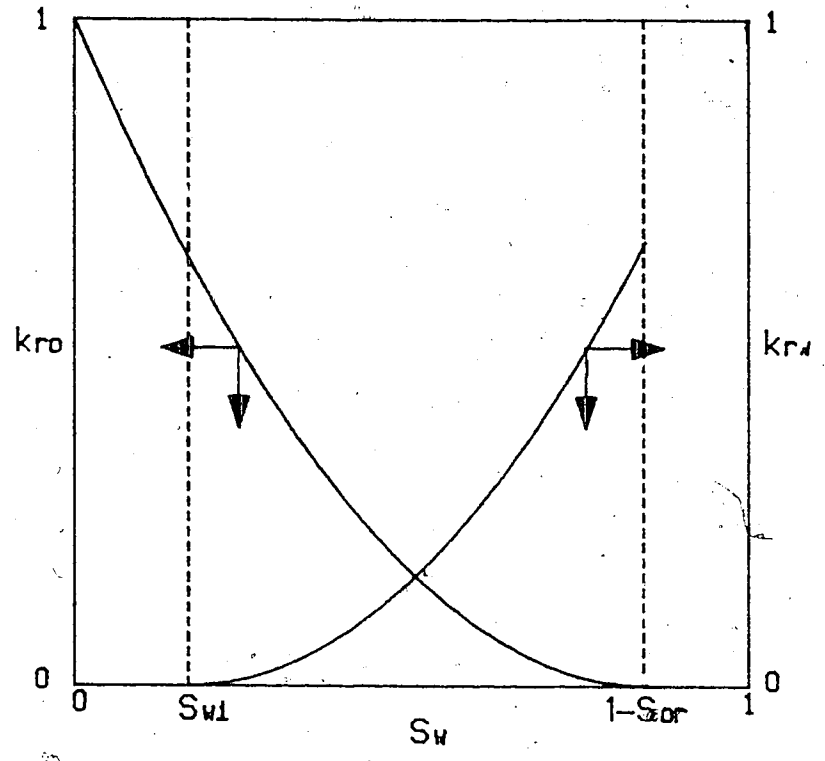
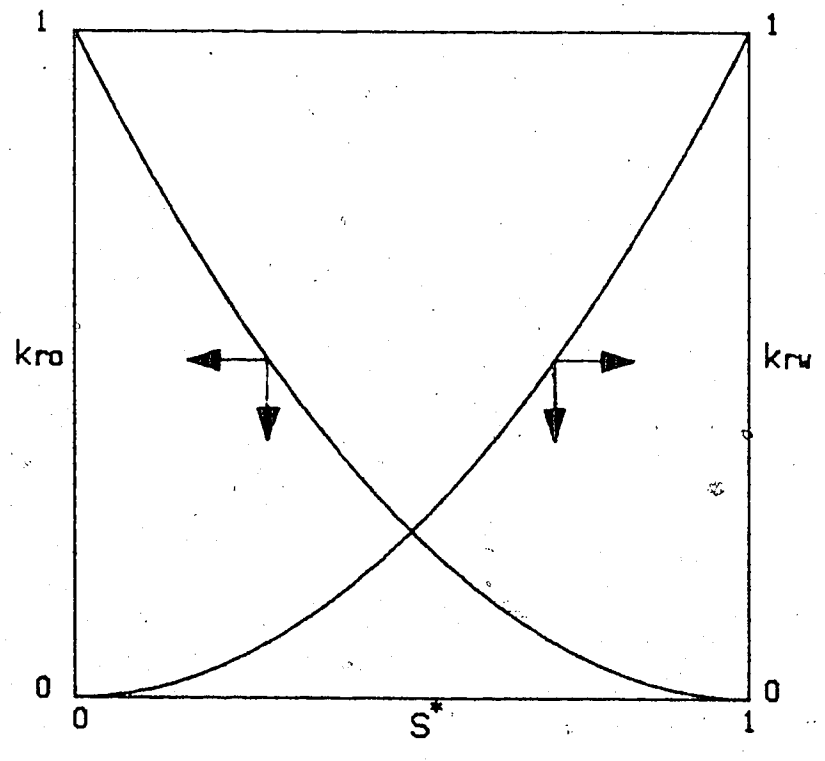


FIG. 2.2: TYPICAL NORMALIZED RELATIVE PERMEABILITY CURVES



2.1.3 Partial Differential Equation

The equations describing the fluid displacement problem may now be combined (see Appendix A.1 for details) to yield the result:

$$\begin{aligned} & \frac{K_{ob}}{\mu_o} \operatorname{div} \left[F_w(S_w) K_{ro}(S_w) \frac{dP_c(S_w)}{dS_w} \operatorname{grad} S_w \right] \\ & - \frac{K_{ob}}{\mu_o} \operatorname{div} \left[F_w(S_w) K_{ro}(S_w) \Delta \rho \vec{g} \right] \\ & + \vec{v} \cdot \frac{dF_w(S_w)}{dS_w} \operatorname{grad} S_w + \phi \frac{\partial S_w}{\partial t} = 0 \end{aligned} \quad 2.16$$

where

$$F_w(S_w) = \left(1 + \frac{K_{ro}(S_w)}{K_{rw}(S_w)} \frac{K_{ob} \mu_w}{K_{wb} \mu_o} \right)^{-1} \quad 2.17$$

and

$$\Delta \rho \equiv \rho_w - \rho_o \quad 2.18$$

This result is a generalization of the non-linear, parabolic partial differential equation derived by Rapoport (1955) and is not subject to an analytical solution. The equation accounts explicitly for the viscous, gravitational, and capillary forces.

2.1.4 Fractional Flow Equation

If the fractional flow of water is defined as:

$$\vec{f}_w \equiv \vec{v}_w / |\vec{v}| \quad 2.19$$

then Equation A.1.15 becomes:

$$\begin{aligned} \vec{f}_w = & \frac{F_w(S_w)}{|\vec{v}|} K_{ro}(S_w) \frac{K_{ob}}{\mu_o} \frac{dP_c(S_w)}{dS_w} \text{grad } S_w \\ & - \frac{F_w(S_w)}{|\vec{v}|} K_{ro}(S_w) \frac{K_{ob}}{\mu_o} \Delta \rho \vec{g} + F_w(S_w) \frac{\vec{v}}{|\vec{v}|} \end{aligned} \quad 2.20$$

and Equation 2.3 becomes:

$$\text{div } \vec{f}_w = - \frac{\phi}{|\vec{v}|} \frac{\partial S_w}{\partial t} \quad 2.21$$

Equations 2.20 and 2.21 also describe the fluid displacement problem.

2.1.5 Capillary Pressure Models

Several capillary pressure models have been proposed throughout the literature. Of particular note are the:

- 1) Leverett J-function (1941)

$$J(S_w) = \frac{P_c(S_w)}{\gamma} \left(\frac{K}{\phi} \right)^{1/2} \quad 2.22$$

- 2) Modified Leverett J-function (Rose and Bruce, 1949)

$$J(S_w) = \frac{P_c(S_w)}{\gamma \cos \theta} \left(\frac{K}{\phi} \right)^{1/2} \quad 2.23$$

3) Bentsen and Anli (1976)

$$P_c(S^*) = - \sigma \ln S^* + P_d \quad 2.24$$

The J-function attempts to correlate the physical properties of the rock and fluid. The expression given by Equation 2.23 includes the wetting angle. The J-function is restricted to correlating satisfactorily data obtained from unconsolidated porous media or certain lithological classifications (Brown, 1951). Bentsen and Anli (1976) proposed the model given by Equation 2.24 in an attempt to overcome the restrictions of the J-function.

The capillary pressure normalizing parameter incorporates the effects of interfacial tension, wettability and pore-size distribution. Both the displacement pressure and capillary pressure normalizing parameter must be determined experimentally.

In normalized form, the capillary pressure equation may be written as:

$$\pi_c(S^*) = \ln S^* \quad 2.25$$

where

$$\pi_c(S^*) = \frac{P_c(S^*) - P_d}{\sigma} \quad 2.26$$

or

$$P_c(S^*) = \sigma \pi_c(S^*) + P_d \quad 2.27$$

Figures 2.3 and 2.4 illustrate typical and normalized capillary pressure curves, respectively. In physical terms, the area under the capillary pressure curve represents the work done in creating new boundary surface.

In view of the fact that the model parameters are available experimentally, the Bentsen and Anli (1976) model will be used throughout this study in any mathematical derivations presented. Moreover, Golaz (1979) showed that the capillary pressure normalizing parameter retained the same value, regardless of the capillary pressure model used.

2.2 Immiscible Displacement Mechanisms

The fluid displacement problem introduced in Section 2.1 may be represented by various displacement mechanisms. The Muskat model is the simplest and easiest to apply in an analysis. The mathematical development of the stability theories is based on the Muskat theory.

2.2.1 Muskat Displacement Mechanism

With the assumption that the region in which an appreciable saturation gradient exists is small, then the porous medium can be divided into two parts: one containing only oil and irreducible water, and the second containing only water and immobile residual oil. Furthermore in the first region, which is located ahead of the front, only oil

FIG: 2.3 TYPICAL CAPILLARY PRESSURE CURVE

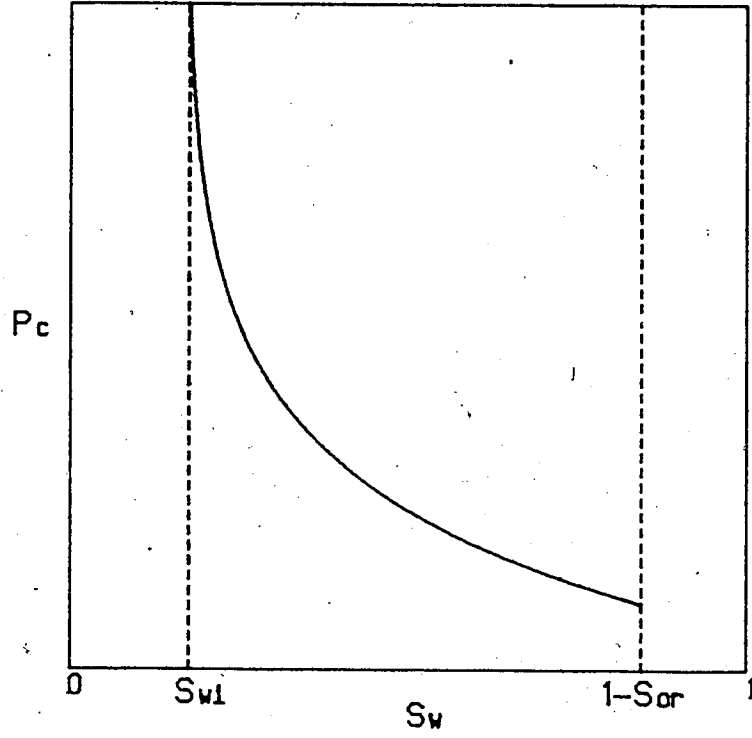
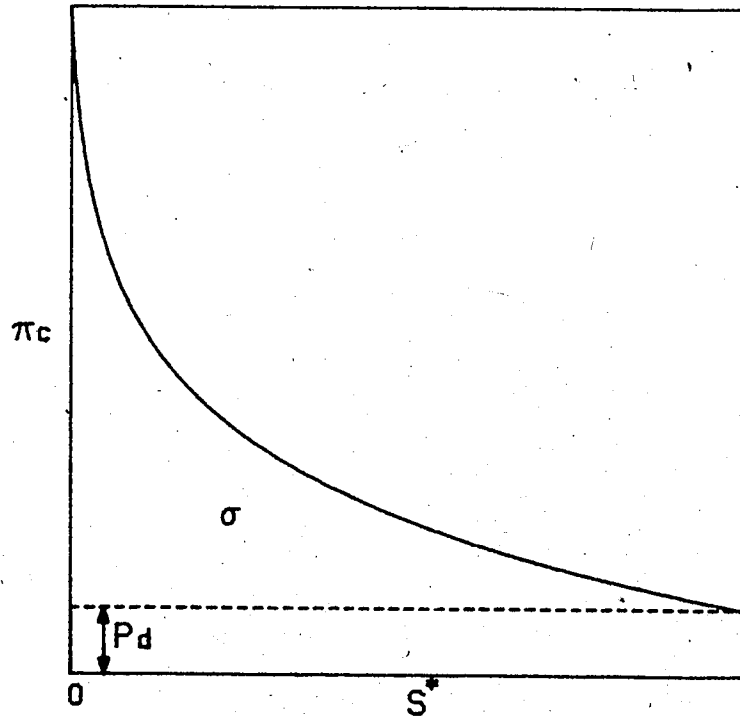


FIG. 2.4: TYPICAL NORMALIZED CAPILLARY PRESSURE CURVE



is mobile; and in the second region, which is located behind the front, only water is mobile. Figure 2.5 illustrates schematically the saturation distribution in such a system.

The surface separating these two regions may be interpreted as a saturation discontinuity. The velocity of this interface is given by:

$$v_f = \frac{v_{wn}}{\phi(1 - S_{or} - S_{wi})} \quad 2.28$$

Applying Darcy's law and the equation of continuity, and providing that gravity and capillary pressure is neglected, the problem may be formulated as:

$$\frac{\partial^2 P_w}{\partial x^2} = 0 \quad 0 < x < x_f \quad 2.29$$

$$\frac{\partial^2 P_o}{\partial x^2} = 0 \quad x_f < x < L \quad 2.30$$

$$P_o = P_w \quad x = x_f(t) \quad 2.31$$

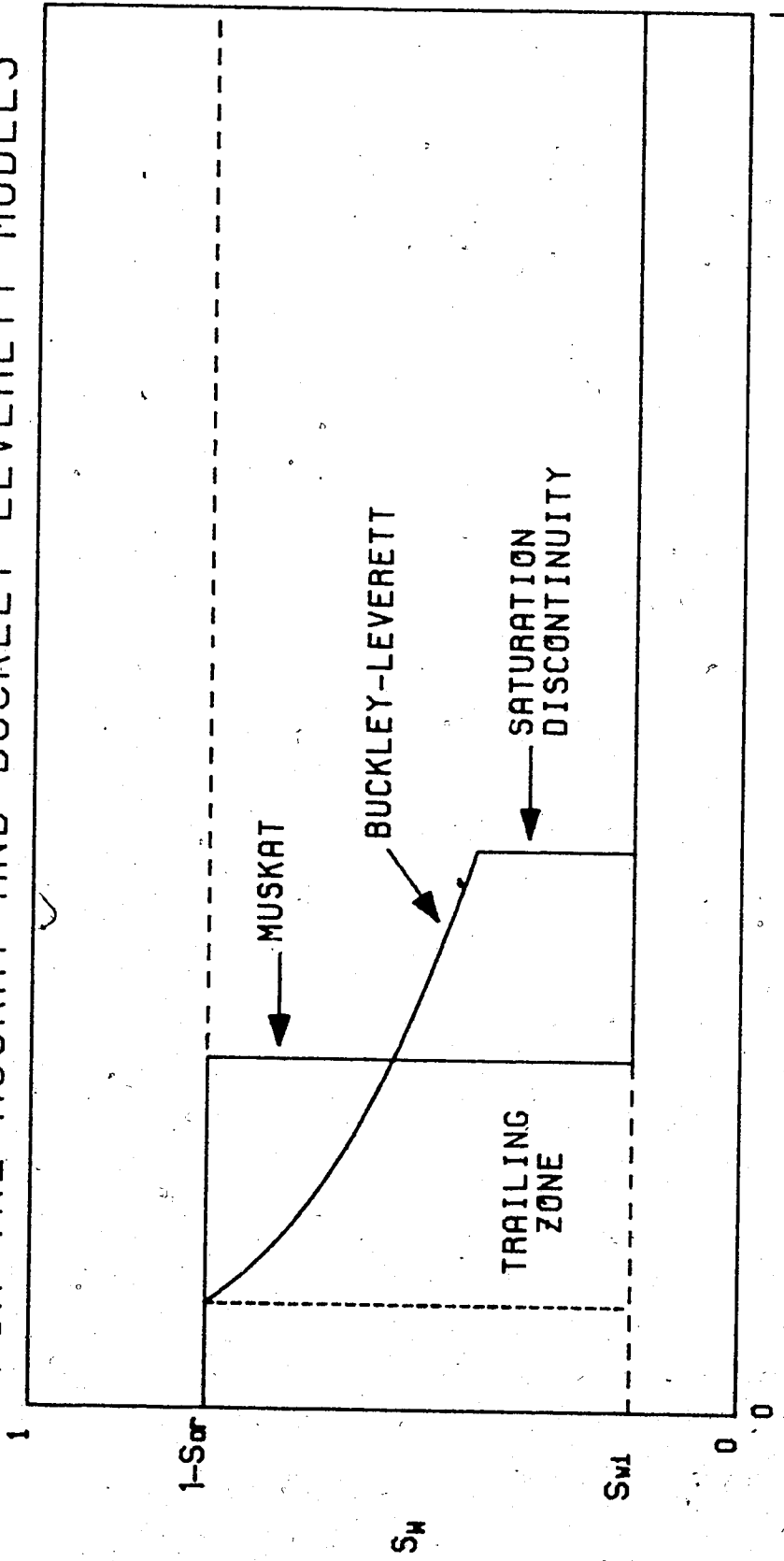
$$\frac{K_{wr}}{\mu_w} \frac{\partial P_w}{\partial x} = \frac{K_{or}}{\mu_o} \frac{\partial P_o}{\partial x} \quad x = x_f(t) \quad 2.32$$

$$P_w = P_1 \quad x = 0 \quad 2.33$$

and

$$P_o = P_2 \quad x = L \quad 2.34$$

FIG. 2.5: SATURATION DISTRIBUTION FOR THE MUSKAT AND BUCKLEY-LEVERETT MODELS



X

Integrating Equations 2.29 and 2.30, and applying the boundary conditions result in:

$$P_w = C_1 x + C_2 \quad 2.35$$

$$P_o = C_1' x + C_2' \quad 2.36$$

where

$$C_1 = - \frac{\Delta P}{M_r L + (1 - M_r) x_f} \quad 2.37$$

$$C_2 = P_1 \quad 2.38$$

$$C_1' = - \frac{M_r \Delta P}{M_r L + (1 - M_r) x_f} \quad 2.39$$

$$C_2' = \frac{(1 - M_r) x_f \Delta P}{M_r L + (1 - M_r) x_f} + P_1 \quad 2.40$$

$$\Delta P = P_1 - P_2 \quad 2.41$$

The rate of advance of the front may be readily derived from these equations and

$$v_{wn} = - \frac{K_{wr}}{\mu_w} \frac{\partial P_w}{\partial x} \quad 2.42$$

$$v_{wn} = - \frac{K_{wr}}{\mu_w} C_1 \quad 2.43$$

Hence

$$v_f = \frac{dx_f}{dt} = \frac{K_{wr}\Delta P}{\phi\mu_w(1 - S_{or} - S_{wi})} \cdot \frac{1}{M_r L + (1 - M_r)x_f} \quad 2.44$$

Defining

$$\xi_f = \frac{x_f}{L} \quad 2.45$$

and

$$\tau^* = \frac{K_{wr}\Delta P}{\mu_w\phi(1 - S_{or} - S_{wi})M_r L^2} \quad 2.46$$

Equation 2.44 may be integrated with $\xi_f = 0$ @ $\tau^* = 0$ to yield:

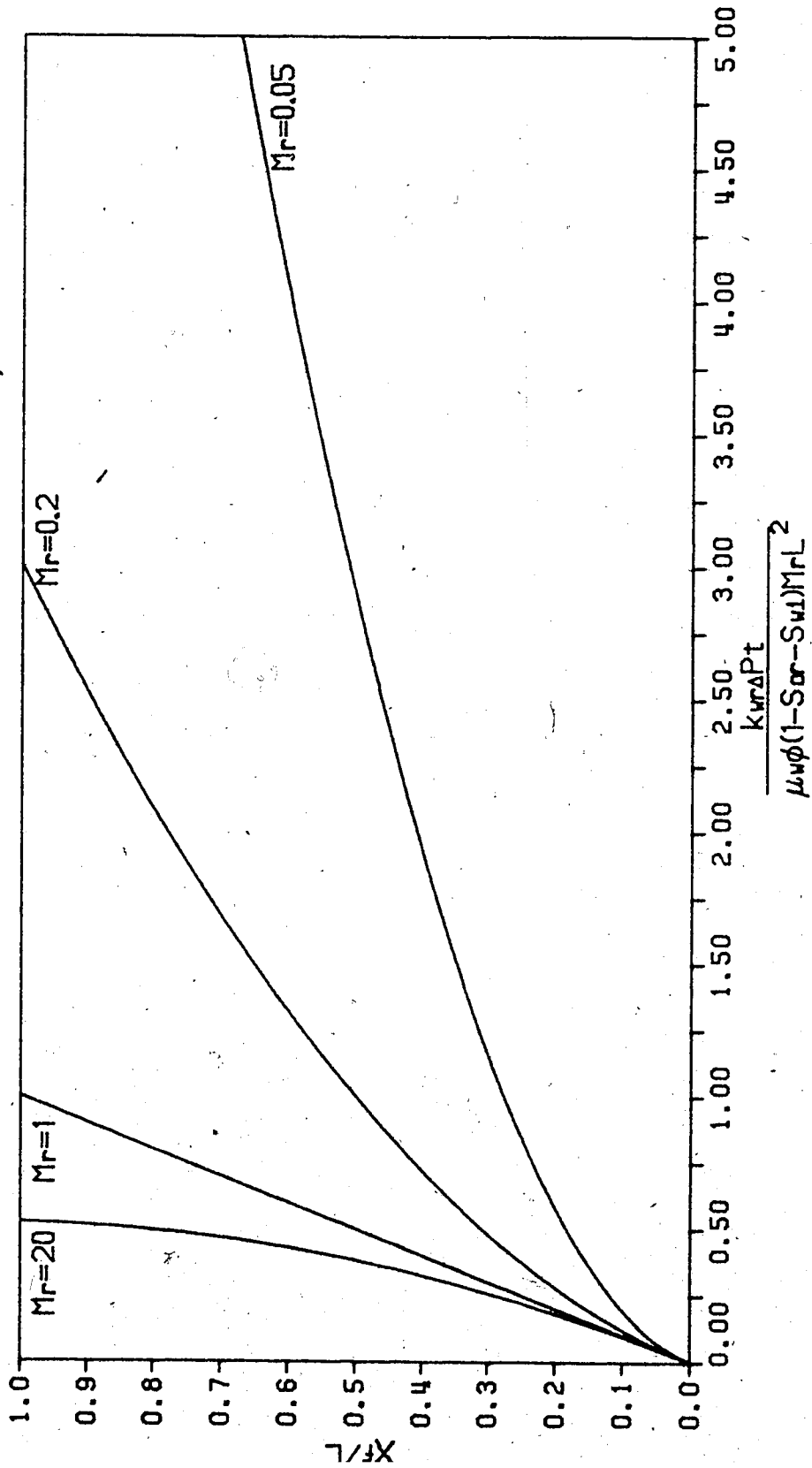
$$\xi_f = \frac{M_r - \sqrt{M_r^2 - 2M_r(M_r - 1)\tau^*}}{(M_r - 1)} \quad 2.47$$

Figure 2.6 illustrates the fractional distance traversed by the front for a linear displacement showing the effect of mobility ratio (Muskat, 1937).

2.2.2 Buckley-Leverett and Dietz Displacement Mechanisms

Under certain circumstances, the piston-like displacement discussed in the previous section may not describe the process adequately. The determination of the water saturation at breakthrough is fundamental to the establishment of over-all reservoir production. If the saturation in the trailing zone is not immediately reduced to the residual oil saturation, then the Muskat model cannot

FIG. 2.6: EFFECT OF MOBILITY RATIO ON--LINEAR SYSTEM (MUSKAT, 1937)



be applied. This trailing zone is illustrated in Figure 2.5.

There are two existing theories of immiscible displacement that have found acceptance in the literature. According to the theory suggested by Buckley and Leverett (1942), the invading water progresses with the formation of a front and a trailing zone (or transition zone with an appreciable saturation gradient). With the assumption that gravity, capillarity and variations in density are negligible, Buckley and Leverett (1942) wrote the following equation for the one-dimensional flow of two immiscible fluids:

$$\frac{\partial S_w}{\partial t} = - \frac{q}{\phi A} \frac{\partial f_w}{\partial x} \quad 2.48$$

The above equation may be derived from a material balance and Darcy's law. From Equation 2.48, the rate of advance of the front may be formulated as:

$$\left. \frac{dx}{dt} \right|_{S_w^*} = \frac{q}{\phi A} \left. \frac{df_w}{dS_w} \right|_{S_w^*} \quad 2.49$$

Equation 2.49 is the so called 'Buckley-Leverett' equation. The theory assumes that the oil and water flow simultaneously through the porous medium. Furthermore, the relative permeability curves must be known explicitly.

The theory of Dietz (1953) is designed for a two-dimensional flow system and assumes that the water invades the formation in the form of a tongue. It is further

assumed that the oil saturation in the invaded zone is instantaneously reduced to the residual oil saturation. Unlike the Buckley-Leverett theory, the oil and water flow separately: the oil, ahead of the front through a porous medium of constant relative permeability to oil; and the water, in the invaded zone with a constant relative permeability to water at residual oil saturation. The saturation distribution for the Buckley-Leverett and Dietz models is illustrated in Figure 2.7.

The analogous expressions to Equations 2.48 and 2.49 are:

$$\frac{\partial Y}{\partial t} = - \frac{q}{\phi A S_{wd}} \frac{\partial f_{wd}}{\partial x} \quad 2.50$$

and

$$\frac{\partial x}{\partial t} \Big|_{Y^*} = \frac{q}{\phi A} \frac{1}{S_{wd}} \frac{\partial f_{wd}}{\partial Y} \Big|_{Y^*} \quad 2.51$$

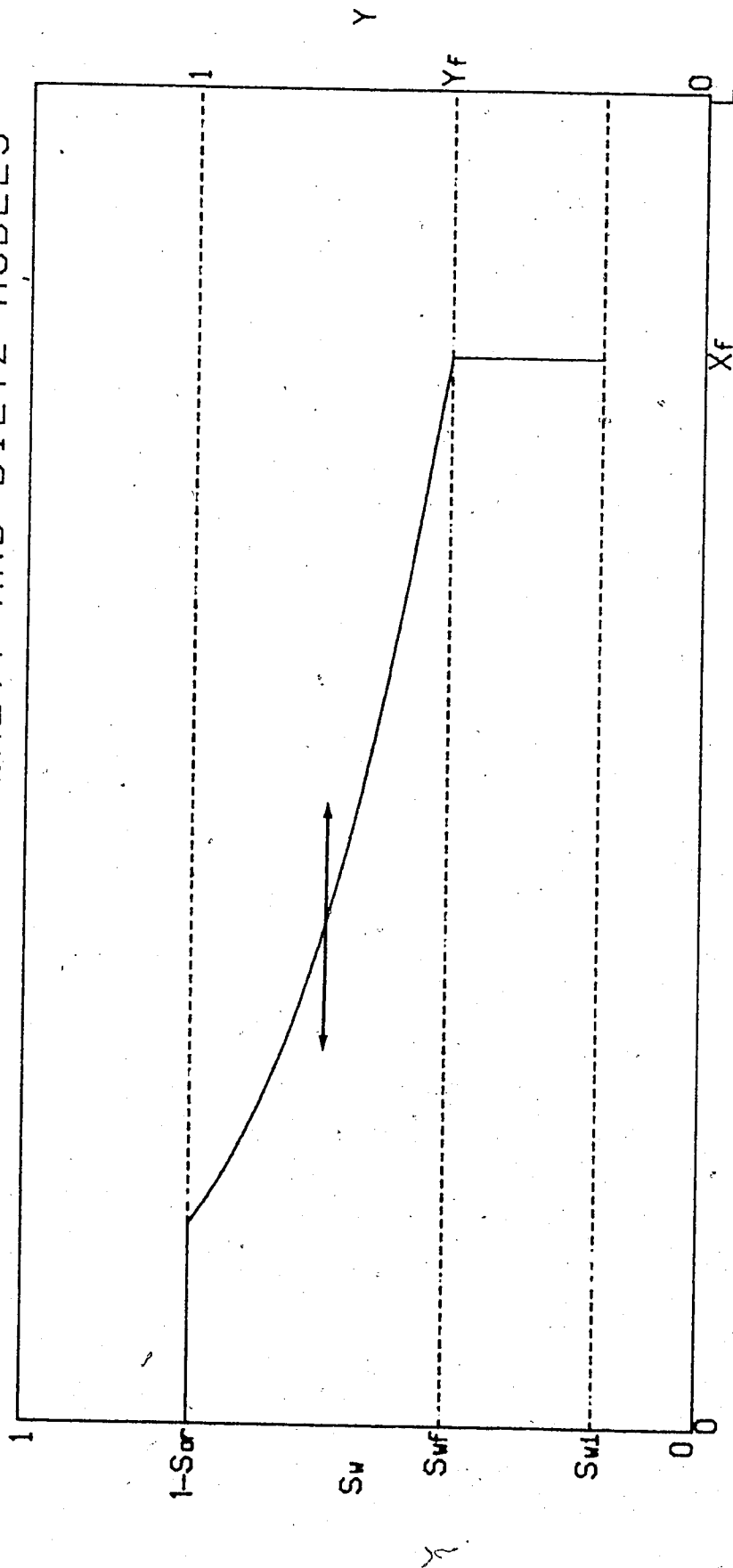
where

$$f_{wd} \equiv \frac{1}{1 + \frac{K_o}{K_w} \frac{\mu_w}{\mu_o} \left(\frac{1-Y}{Y} \right)} \quad 2.52$$

$$Y = y/h \quad 2.53$$

= coordinate of the oil/water interface as a

FIG. 2.7: SATURATION DISTRIBUTION FOR THE
BUCKLEY-LEVERETT AND DIETZ MODELS



fraction of formation thickness; its physical meaning being restricted to $0 \leq y \leq h$

$$S_{wd} = 1 - S_{or} - S_{wi} \quad 2.54$$

= the difference in saturation between the oil zone and water zone

The Dietz theory is simpler to apply than the Buckley-Leverett theory in view of that fact that only the end-point relative permeabilities need be known. Because the Dietz theory is not restricted to assuming a single tongue, the differences in the two theories diminish if a great many tongues exist. The two theories are identical, provided the relative permeabilities are defined as linear functions of saturation ($K_{rw} = S^*$, $K_{ro} = 1-S^*$).

2.3 Scaled Models and Scaling Groups

Dimensional models were first introduced to reservoir engineering by Leverett and co-workers (1942) in order to study the water-drive process. The resulting set of scaling groups enables the experimenter to:

- 1) vary the pertinent variables of the problem in a systematic way as a means of evaluating the process and
- 2) relate laboratory results to field applications.

2.3.1 Derivation of Scaling Groups

The scaling groups may be derived by either dimensional analysis or inspectional analysis techniques.

The dimensional analysis approach consists of considering all the variables involved in the process being studied, and combining these variables into dimensionless groups as dictated by Buckingham's (1915) pi-theorem. In an inspectional analysis, all equations which describe the process of interest are combined to form a single equation. The parameters form the scaling groups. If any of the equations are of the differential type, then inclusion of initial and boundary conditions is also required.

The dimensionless groups resulting from such an analysis may be divided into the following classes:

- 1) independent groups, or the dimensionless form of the independent variables;
- 2) dependent groups, or the dimensionless form of the dependent variables; and
- 3) similarity groups, which are independent constant groups.

Dimensional analysis does not require that the process be expressed by equations. Hence, complete knowledge of the process is not required. This is a distinct advantage over inspectional analysis. Special care must be taken to include all of the pertinent variables associated with the problem at hand. Furthermore, the resulting dimensionless groups may not have any clear physical interpretation and, in

general, the groups are not unique. An inspectional analysis of all the equations usually results in the scaling groups having a clear physical meaning.

The early work of Leverett, et al. (1942) has been built upon and used extensively. Presented in Appendix A.2 are the details of the derivation of the scaling groups for the immiscible fluid displacement problem, using the two methods mentioned above.

Englebarts and Klinkenberg (1951) extended the dimensional analysis of Leverett, et al. (1942). Their analysis yielded fewer pi-terms and, coupled with simpler experimental systems, obtained results of more general significance.

Rapoport and Leas (1953) presented their experimental results for linear waterfloods in which they systematically varied length, wetting phase viscosity, and flow rate.

Rapoport (1955) was the first to present the derivation of the scaling groups, using inspectional analysis, for a three-dimensional cartesian coordinate system. Geertsma, et al. (1956) derived the dimensionless groups for cold-water drive, hot-water drive and solvent injection by inspectional analysis. They then 'completed' the resulting set of pi-terms by means of dimensional analysis. This was done in an attempt to combine the advantages of both techniques.

Perkins and Collins (1960) recognized that previous derivations of the scaling groups required that the functional relationships of both relative permeability and

capillary pressure be identical in the model and prototype. They presented a new set of scaling groups in which the functional relationships were allowed to be different. This was done by redefining relative permeability and normalizing the water saturation. Consequently, the new set of scaling groups demanded that the functional dependence of relative permeability and capillary pressure be on normalized water saturation instead of water saturation.

Bentsen (1976) improved the work of Perkins and Collins (1960) for a linear displacement problem using the method of Hellums and Churchill (1961). The method used is essentially a modified inspectional analysis. However, the resulting scaling groups were difficult to interpret physically. Consequently, Bentsen (1976) redefined the pi-terms, thus attaching a physical significance to the dimensionless groups. A derivation extending the work of Bentsen (1976) to a cylindrical coordinate system is offered in the next section.

2.3.2 Dimensionless Form of the Fluid Displacement Equations

As a consequence of applying a modified inspectional analysis, Equations 2.20 and 2.21 take on the dimensionless form (Appendix A.2.3):

$$\frac{2L}{D} \psi \left[\frac{\partial}{\partial \psi} (\psi f_{w\psi}) + \frac{\partial f_{w\beta}}{\partial \beta} \right] + \frac{\partial f_{w\epsilon}}{\partial \epsilon} = - \frac{\partial S^*}{\partial \epsilon} \quad 2.55$$

and

$$\vec{f}_w = \vec{G}(S^*) - N_{cl} C(S^*) \left[\frac{2L}{D} \left(\frac{\partial S^*}{\partial \psi} \hat{\psi} + \frac{1}{\psi} \frac{\partial S^*}{\partial \beta} \hat{\beta} \right) + \frac{\partial S^*}{\partial \xi} \hat{\xi} \right] \quad 2.56$$

where

$$\vec{G}(S^*) = \left[\frac{\vec{v}}{|\vec{v}|} - \frac{N_g}{M_r} K_{ro}(S^*) \right] F_w(S^*) \quad 2.57$$

$$N_g = \frac{K_{wr} \Delta \rho \vec{g}}{|\vec{v}| \mu_w} \quad 2.58$$

$$C(S^*) = - \frac{1}{M_r} F_w(S^*) K_{ro}(S^*) \frac{d\pi_c(S^*)}{dS^*} \quad 2.59$$

$$S^* = \frac{S_w - S_{wi}}{1 - S_{or} - S_{wi}} \quad 2.60$$

$$M_r = \frac{K_{wr} \mu_o}{K_{or} \mu_w} \quad 2.61$$

$$F_w(S^*) = \frac{M_r K_{rw}(S^*)}{M_r K_{rw}(S^*) + K_{ro}(S^*)} \quad 2.62$$

$$N_{cl} = \frac{\sigma K_{wr}}{|\vec{v}| \mu_w L} \quad 2.63$$

$$N_{cr} = \frac{\sigma K_{wr}}{|\vec{v}| \mu_w D} \quad 2.64$$

$$\xi = \frac{x}{L} \quad 2.65$$

$$\psi = \frac{r}{a} \quad 2.66$$

$$\beta = \text{polar angle} \quad 2.67$$

$$\tau = \frac{|\vec{v}| t}{\phi L (1 - S_{or} - S_{wi})} \quad 2.68$$

In light of the previous discussion, the following classes of dimensionless groups arise:

1) Independent groups

$$\xi, \psi, \beta, \tau$$

2) Dependent groups

$$S^*, f_{w\psi}, f_{w\xi}, f_{w\beta}$$

3) Similarity groups

$$M_r, N_{cl}, \vec{N}_g, \frac{L}{D}$$

In addition to these groups there are the functions $K_{rw}(S^*)$, $K_{ro}(S^*)$ and $\pi_c(S^*)$. These have the properties of similarity groups and, consequently, must be the same in the model and prototype.

If the displacement is essentially linear, then the saturation gradient in the radial direction is small. Hence:

$$\frac{\partial S^*}{\partial \psi} = 0 \quad 2.69$$

and

$$\frac{\partial S^*}{\partial \beta} = 0 \quad 2.70$$

Furthermore, the pressure at any given cross-section will be uniform. This implies that:

$$\frac{\partial}{\partial \psi} (\psi f_{w\psi}) = 0 \quad 2.71$$

and

$$\frac{\partial}{\partial \beta} f_{w\beta} = 0 \quad 2.72$$

Hence Equations 2.55 and 2.56 reduce to:

$$\frac{\partial f_w}{\partial \xi} = - \frac{\partial S^*}{\partial \tau} \quad 2.73$$

and

$$f_w = G(S^*) - N_c C(S^*) \frac{\partial S^*}{\partial \xi} \quad 2.74$$

The above two equations are identical to those derived by Bentsen (1976) and apply only if there is no transverse flow.

2.3.3 Remarks on Scaling Groups

It is evident that in the design of a model, it is a difficult, if not impossible, task to meet the requirements of all the similarity groups simultaneously. It is desirable then to relax the groups.

Perkins and Collins (1960) showed that redefining the relative permeability curves in terms of the normalized water saturation was less restrictive than previous definitions. Van Daalen and van Domeselaar (1972) presented

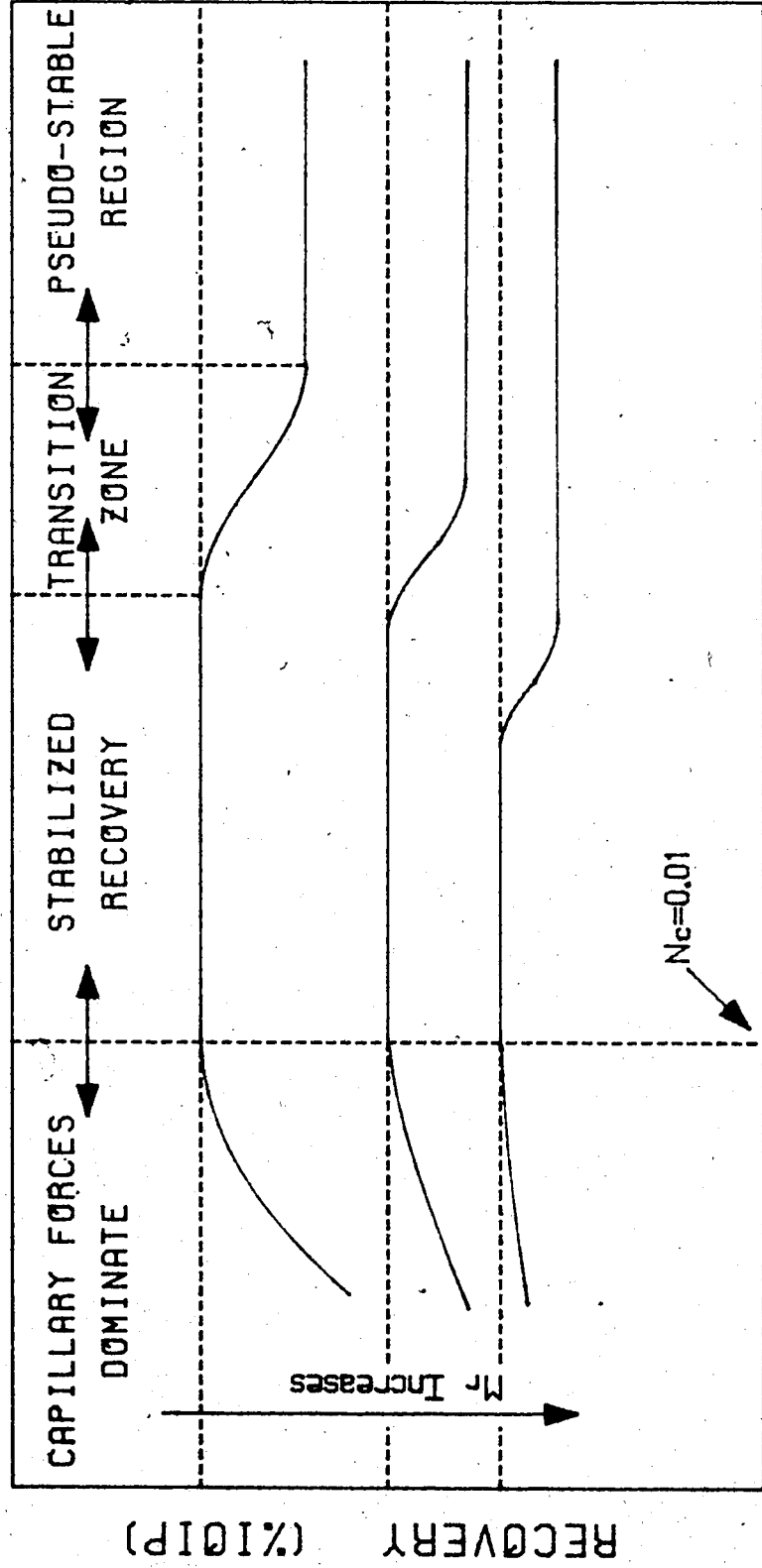
experimental evidence indicating that for small transition zones the functions $K_{rw}(S^*)$, $K_{ro}(S^*)$ and $\pi_c(S^*)$ did not influence the production behaviour. Under these circumstances, they do not have to be satisfied.

Bentsen (1976) suggested that the capillary number, if sufficiently small, may also be neglected. This group may be interpreted as a measure of the relative importance of the capillary forces to viscous forces. It was demonstrated both theoretically (Bentsen, 1978) and experimentally (Saeedi, 1979) that for a capillary number of less than 0.01, the recovery was independent of this group. The dependence of the recovery on the capillary number is illustrated in Figure 2.8, and the effect of mobility ratio is also shown.

The ratio $\sigma K_{wr} / |\vec{V}| \mu_w D$, similar to N_{cl} but representative of the capillary to viscous forces in the radial direction. This ratio may be neglected without restriction where no crossflow occurs. However, when gravity and viscous forces play an important role (gravity override and viscous fingering), crossflow is present. This group must then be taken into account. If the magnitude of the radial capillary number is small, say of the order of 0.01, then it may be anticipated that the fingers will have stabilized in the same sense that the floodfront is said to be stabilized (in the direction of bulk flow) when the linear capillary number is small.

Finally, it should be noted that the recovery at breakthrough for the immiscible fluid displacement problem

FIG. 2.8: VARIATION OF RECOVERY WITH RECIPROCAL CAPILLARY NUMBER SHOWING THE EFFECT OF MOBILITY RATIO



RECIPROCAL CAPILLARY NUMBER

is some complicated function of mobility ratio, gravity number, capillary number, geometric factor, and the effects of instability of the floodfront. The effects of instability of the floodfront are discussed in a later section. The recovery function may be represented as:

$$\text{Recovery} = f (M_r, \vec{N}_g, N_{cl}, L/D, N_s)$$

where N_s accounts for the effects of floodfront instability.

If the displacement is stable and stabilized, then:

$$\text{Recovery} = f (M_r, \vec{N}_g)$$

Furthermore, if gravity can be neglected, then the simplest case is:

$$\text{Recovery} = f (M_r)$$

2.4 Stability Theory of Immiscible Displacement

The theory presented in the preceding sections implicitly assumes that the floodfront has attained a stabilized configuration and that no frontal perturbations occur. Consequently, the stable model is incapable of predicting the waterflood performance of a prototype in a regime where viscous fingering dominates the recovery process. As a result, the instabilities associated with the model may not be properly accounted for in the prototype. Hence the need arises to develop a mathematical model which accounts explicitly for the floodfront perturbations.

2.4.1 Experimental Observations and Mathematical Descriptions of Instability

When one fluid is displaced by another fluid with a lower viscosity, the fluid-fluid interface is in an unstable state and has a tendency to 'break up'. The nature of this instability phenomenon was first observed by Englebarts and Klinkenberg (1951). The streamers which appeared in the visual models prompted them to coin the term 'viscous fingers'.

For an adverse viscosity ratio of 24, Englebarts and Klinkenberg (1951) observed a continuing decrease in recovery at breakthrough for both hydrophilic and oleophilic powders. This decrease in recovery was attributed to the onset of perturbations at the floodfront and growth of the incipient fingers toward the outlet, thus bypassing oil in the model.

Van Meurs (1957) described a technique which permitted complete visual observation of the displacement process. It was seen that, for a viscosity ratio of unity, the fluid-fluid interface was stable and the displacement efficiency was high. Further tests at an adverse viscosity ratio of 80 confirmed the observations of Englebarts and Klinkenberg (1951). Furthermore, van Meurs (1957) observed that the production of oil after breakthrough is due to the growth of the fingers already formed. These tests were performed in an oil-wet system containing no residual water saturation.

The results of the visual observations of the displacement process prompted van Meurs and van der Poel (1958) to attempt to describe the displacement process involving viscous fingering mathematically. This model, which parallels the theory of Buckley and Leverett (1942) in some respects, attempts to account for frontal perturbations. However, little recognition has been given to this theory in the literature.

Chuoque, et al. (1959) were the first to present a theoretical description of viscous fingering. With the assumption that the frontal disturbances may be represented by a Fourier decomposition, and using first order perturbation theory, they defined a stability index as:

$$n = \left\{ \delta \left[\left(\frac{\mu_o}{K_{or}} - \frac{\mu_w}{K_{wr}} \right) V + (\rho_o - \rho_w) g \cos \alpha' \right] - \gamma^* \delta^3 \right\} / \left(\frac{\mu_o}{K_{or}} + \frac{\mu_w}{K_{wr}} \right) \quad 2.75$$

For an excellent detailed derivation of Equation 2.75, the reader is referred to the work of Peters (1979).

In view of the fact that the sign of the stability index determines the stability classification, the necessary and sufficient condition for instability (n positive) is:

$$\left(\frac{\mu_o}{K_{or}} - \frac{\mu_w}{K_{wr}} \right) V + (\rho_o - \rho_w) g \cos \alpha' > \gamma^* \delta^2 \quad 2.76$$

A critical velocity may be defined such that the left hand

side of Equation 2.76 is equal to zero, that is:

$$\left(\frac{\mu_0}{K_{or}} - \frac{\mu_w}{K_{wr}} \right) V_c + (\rho_0 - \rho_w) g \cos \alpha' = 0 \quad 2.77$$

or

$$V_c = \frac{K_{wr} \Delta \rho g \cos \alpha'}{\mu_w (M_r - 1)} \quad 2.78$$

From Equations 2.76 and 2.77, there results:

$$\left(\frac{\mu_0}{K_{or}} - \frac{\mu_w}{K_{wr}} \right) (V - V_c) > \gamma^* \delta^2 \quad 2.79$$

or


$$\lambda > 2\pi \left[\frac{K_{wr} \gamma^*}{\mu_w (M_r - 1) (V - V_c)} \right]^{1/2} \quad 2.80$$

which is the condition for instability.

From Equation 2.80, a critical wavelength may be defined as:

$$\lambda_c = 2\pi \left[\frac{\frac{K_{wr}}{\mu_w} \gamma^*}{(M_r - 1) (V - V_c)} \right]^{1/2} \quad 2.81$$

Differentiation of Equation 2.75 with respect to δ , and equating to zero, determines the wavelength of the maximum instability, viz:



$$\lambda_m = 2\pi\sqrt{3} \left[\frac{\frac{k_{wr}}{\mu_w} \gamma^*}{(M_r - 1)(V - V_c)} \right]^{1/2} \quad 2.82$$

or

$$\lambda_m = \sqrt{3} \lambda_c \quad 2.83$$

To verify these theoretical findings, Chuoke, et al. (1959) used three types of experimental systems: a Hele-Shaw model inclined at 45°, a van Meurs model with no residual water and a van Meurs model with residual water.

Because in a Hele-Shaw model γ^* is equal to γ , the wavelengths of the maximum instability can be directly calculated. Excellent agreement between the calculated and measured wavelengths was obtained in the parallel-plate tests.

The displacement tests showed two trends consistent with the theory. It was observed by Chuoke, et al. (1959) that small fingers are formed, when the oil viscosity is high. Furthermore, the lower the bulk interfacial tension, the smaller the fingers.

Chuoke, et al. (1959) assumed a linear relationship between the effective interfacial tension, which is an unknown in porous media, and the bulk interfacial tension to be:

$$\gamma^* = C\gamma \quad 2.84$$

Hence, Equation 2.82 becomes:

$$\lambda_m = C \left[\frac{\frac{K_{wr}}{\mu_w} \gamma}{(M_r - 1)(V - V_c)} \right]^{1/2} \quad \bullet \quad 2.85$$

where C is Chuoke's constant which is of the order of $2\pi\sqrt{3}$. Chuoke, et al. (1959) found that the experimental data fitted Equation 2.85 well when C was taken to be equal to 30. However, this value of Chuoke's constant was only valid for an oil-wet system with no residual water.

Insufficient data were accumulated by Chuoke, et al. (1959) to arrive at a quantitative estimate of the system constant in a water-wet porous medium. However, it was speculated that Chuoke's constant would be much larger in this type of system.

In terms of field applications when instability occurs, the interpretation of model tests may be misleading. Consequently, Chuoke, et al. (1959) suggested that the similarity groups should contain the additional group $(\lambda_m/D)^2$ to account for the floodfront perturbations.

It was pointed out in Section 2.3.3 that it may not be feasible to satisfy simultaneously all the similarity groups. Chuoke, et al. (1959) suggested that if the wavelength is of the order of the diameter of the sandpack, exact scaling is required; otherwise it may be neglected.

De Haan (1959) presented further evidence confirming the theory of Chuoke, et al. (1959). In an oil-wet system, it was observed that a decrease in recovery occurred with an increase in the scaling factor, once fingering commenced. At

still higher rates, de Haan observed a levelling in the breakthrough recovery curve.

Outmans (1962) attempted an improvement to the first-order theory by including the non-linear terms in the equations describing the conditions at the interface. Of particular note is his conclusion that the shape and growth of the fingers cannot be calculated from the equations which arise from first-order theory. Consequently, the first order equations must be replaced by more complicated expressions. He suggests, if interfacial tension is negligible, that the conclusion from linear theory--that the rate of growth of the incipient finger will continue without bound--is incorrect. Finally, Outmans (1962) questioned the validity of the dynamic boundary condition at the interface suggested by Chuoke, et al. (1959). This boundary condition, which allows for capillarity at the interface, was redefined by Outmans (1962).

Using a first-order analysis, Rachford (1964) presented an extension to the theory proposed by Chuoke, et al. (1959). By including a saturation transition zone (Buckley-Leverett type displacement), Rachford (1964) concluded that laboratory tests scaled by the usual groups are also correctly scaled for the presence of viscous fingering in a water-wet system.

This first attempt to study the stability problem using Buckley-Leverett theory gave rise to highly non-linear perturbation equations. Rachford (1964), unable to solve

these equations, violated the nonlinearity of the perturbation equations and consequently his results may be questionable.

Perkins and Johnston (1969) studied immiscible fingering in linear Hele-Shaw and bead-packed models. It was observed that viscous fingering was severe in the system containing no residual water, whereas the viscous fingers were damped out before traveling very far in the systems with a residual water saturation. The damping mechanism was attributed to the movement of the two phases in the transverse direction to flow.

Hagoort (1974) also studied the displacement stability of a Buckley-Leverett type displacement. Included in the study were the effects of viscous and capillary forces, but gravity was neglected. In place of the conventional end-point mobility ratio, Hagoort (1974) defined a shock mobility ratio as:

$$M_s = \left[\frac{K_{or} K_{ro} (S_f)}{\mu_o} + \frac{K_{wr} K_{rw} (S_f)}{\mu_w} \right] / \frac{K_{or}}{\mu_o} \quad 2.86$$

It was found that the displacement is unstable provided that the shock mobility ratio is greater than unity, subject to the constraint that the wavelength of the finger is smaller than the diameter of the system. It was further concluded by Hagoort (1974) that a Buckley-Leverett type displacement is less prone to become unstable than a Muskat displacement.

Several researchers in this laboratory (Kloepfer, 1975;

Wiborg, 1976; Baird, 1978) conducted tests in unconsolidated sandpacks. It was observed that a dramatic decrease in recovery occurred at high rates. This decrease was attributed to the onset of instabilities. However, no physical evidence supporting the presence of viscous fingering was reported.

As recently as 1979, Peters (1979) investigated the stability problem of immiscible displacements in systems with and without a residual water saturation. Using a simple and novel technique, he was able to capture the viscous fingers and obtain permanent records via the use of photography.

Peters (1979) extended the theory of Chuoke, et al. (1959) by combining all of the pertinent variables of the stability problem to form a single dimensionless group. He concluded that this group would be capable of predicting the onset of instability. Proceeding in a manner analogous to Chuoke, et al. (1959), Peters (1979) showed that the stability index for a cylindrical coordinate system may be written as:

$$n = \frac{\delta_i \gamma^*}{a^2 \left(\frac{\mu_o}{K_{or}} + \frac{\mu_w}{K_{wr}} \right)} \left[\frac{(M_r - 1)(V - V_c) \mu_w a^2}{\gamma^* K_{wr}} - (\delta_i a)^2 \right] \quad 2.87$$

The subscript i indicates that the eigenvalues can take on different discrete values. Equation 2.87 is simply a

convenient rearrangement of Equation 2.75. As before, the necessary and sufficient condition for instability may be written as:

$$\frac{(M_r - 1)(V - V_c)\mu_w a^2}{\gamma^* K_{wr}} > (\delta_i a)^2 \quad 2.88$$

and the onset of instability is given by:

$$\frac{(M_r - 1)(V - V_c)\mu_w a^2}{\gamma^* K_{wr}} = (\delta_i a)^2 \quad 2.89$$

The possible discrete values of $\delta_i a$ are given by the zeros of the Bessel function, $J'_m(\delta_i a)$. The first non-zero value of $\delta_i a$ is 1.8412 at $m=1$, and consequently the onset of instability is defined as:

$$\frac{(M_r - 1)(V - V_c)\mu_w a^2}{\gamma^* K_{wr}} = (1.8412)^2 \quad 2.90$$

Equation 2.90 may be written as:

$$\frac{(M_r - 1)(V - V_c)\mu_w D^2}{C^* \gamma K_{wr}} = 13.56 \quad 2.91$$

where

$$C^* = \gamma^* / \gamma \quad 2.92$$

The dimensionless group, given by Equation 2.91, defines the onset of instability in a cylindrical sandpack.

Provided this group is less than 13.56, the displacement is unconditionally stable. In a rectangular coordinate system, the analogous expression to Equation 2.91 is given by:

$$\frac{(M_r - 1)(V - V_c)\mu_w L_x^2 L_y^2}{C^* \gamma K_{wr} (L_x^2 + L_y^2)} = \pi^2 \quad 2.93$$

It should be noted that the constant of proportionality, relating the bulk interfacial tension and effective interfacial tension, is not identical to that of Chuoke, et al. (1959). With this definition, Chuoke's constant now becomes:

$$C = 2\pi\sqrt{3C^*} \quad 2.94$$

From the photographic records of the viscous fingers, Peters (1979) estimated the most probable wavelength. Using Equation 2.85, he calculated a value for C and, hence, C^* (Equation 2.93) and γ^* (Equation 2.92). The system parameters obtained by Peters (1979) are shown in Table 2.1.

Table 2.1: System Parameters

(Peters, 1979)

Wettability	C	C^*	γ^* dynes/cm
Water-wet	190.45	306.25	7.442×10^3
Oil-wet	25.40	5.45	1.324×10^2

For a stability number greater than 1000, Peters (1979) observed that the recovery was insensitive to variations of the parameters in the stability number. This is in agreement with the observations of de Haan (1959). At a stability number greater than 1000, it was seen by Peters (1979) that numerous fingers with a small wavelength are present. The linear theory does not predict this second breakpoint in the recovery curve. This deficiency may be attributed to the fact that linear theory is inapplicable for disturbances with amplitudes much larger than their wavelength. It may also be because the current theory does not account for viscous dissipation effects. The introduction of viscosity into the analysis eliminates the tendency for the disturbances of small wavelength to increase without bound (Bellman and Pennington, 1954).

The experimental results of Peters (1979) agreed well with the estimate of Chuoke, et al. (1959). However, before the stability criterion may be applied, a complete set of experiments must be conducted in order to determine the system parameters. As a consequence of the extension of Chuoke's theory, Peters (1979) was successful in predicting the onset of instabilities. His experimental estimates of the system parameters were for a particular fluid-rock system and a complete investigation is pending.

3. Experimental Equipment, Materials and Procedure

3.1 Porous Media

3.1.1 Sand

The unconsolidated sandpacks used throughout this series of experiments was an Ottawa silica sand with a grain size range of 80-120 mesh (Fisher Scientific S-151). The sand was used as received from the supplier without any screening.

3.1.2 Coreholders

The sandpacks were housed in coreholders constructed of polyvinyl chloride (PVC) for low pressure usage (less than 100 psi) and of stainless steel for high pressure studies. The design of the coreholders was the same as those described in detail by Wiborg (1976).

Three lengths were used ranging from 23 cm to 110 cm with a choice of two diameters (2.4 cm and 4.8 cm). This set of coreholders allowed the study of geometrically dissimilar sandpacks.

3.1.3 Packing Procedure

Several techniques were used in packing the coreholders in an attempt to find a method which would yield sandpacks of consistent properties. It was found that the routine method of vibrating a dry core (Wiborg, 1976; Baird, 1978) and tamping with a hammer (Peters, 1979) produced sandpacks

with properties very much dependent on the length of time of vibration or tamping.

Consequently, the coreholders were packed with wet sand in the following manner. The coreholder was partially filled with clear distilled water followed by sand. The coreholder was vibrated throughout the filling process and an approximately constant 4 inch head of water was kept in the coreholder. The coreholder was then vibrated for at least 24 hours. After the vibration period, predried, compressed air at room temperature was passed through the sandpack for 48 hours to ensure the complete removal of the packing water. This method of packing is a modification of that used by Kloepfer (1975).

3.2 Fluids

Distilled water was used to create a residual water saturation, and distilled water doped with sodium fluorescein was used as the displacing fluid.

Only one oil was used during the tests. This was a Dow Corning 200 silicone-base oil. This oil was used because its density was almost equal to that of distilled water. The physical properties of interest for these two fluids are listed in Table 3.1 and were obtained from the report of Peters (1979).

TABLE: 3.1 Pertinent Fluid Properties At 21.5°C

	Density (gm/cc)	Viscosity (cp)
Distilled Water	0.9910	1.028
Dow Corning 200	0.9667	105.4

Interfacial Tension: 24.3 dynes/cm

Viscosity Ratio: 102.5

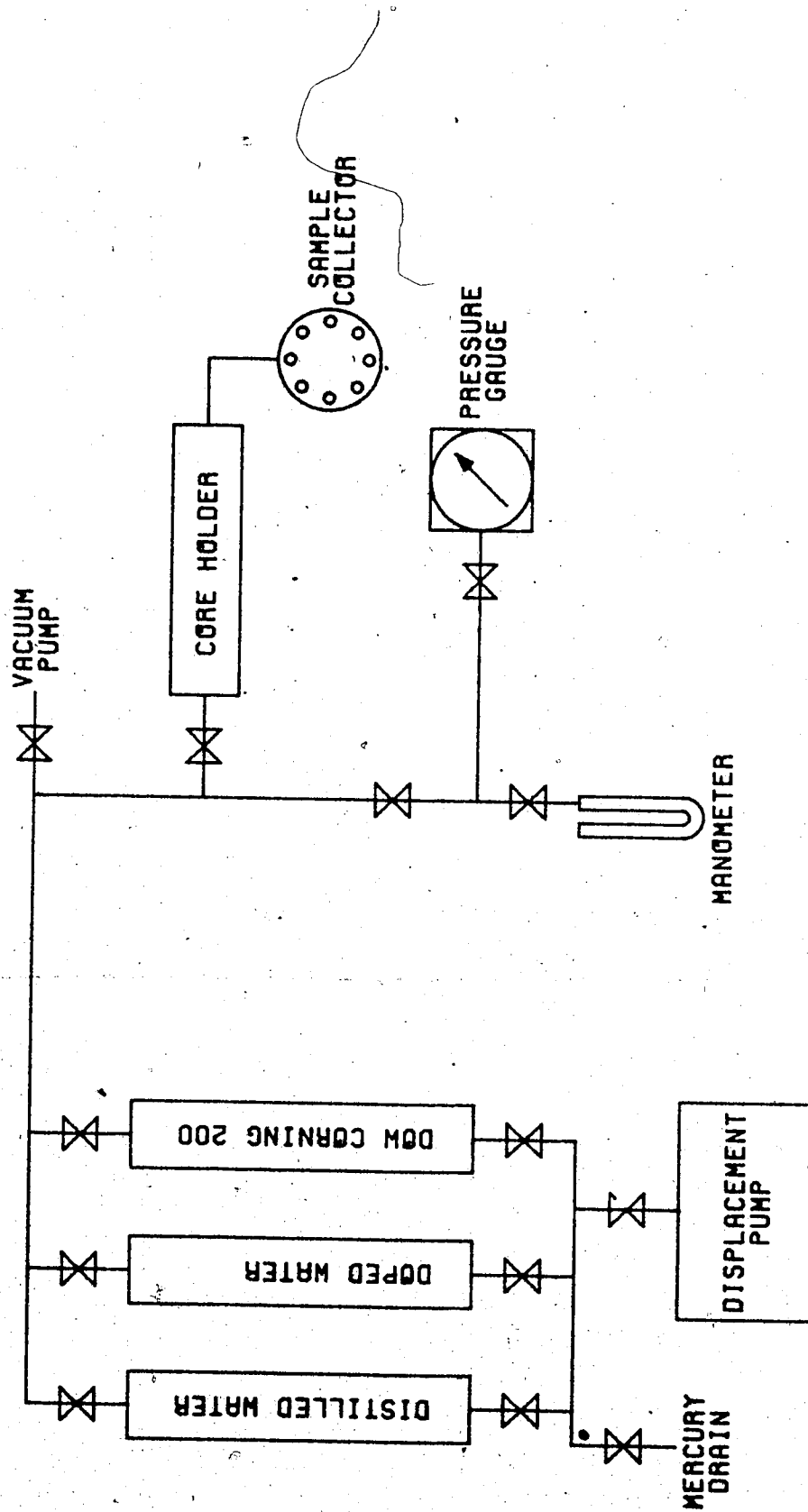
Water-oil Density Difference: 0.0243 gm/cc

3.3 Pumping System

Two dual positive-displacement Ruska pumps were used in this investigation. Both pumps were capable of delivery rates ranging from 2.5 cc/hr to 1120 cc/hr. A minor modification to the external-drive gearing on one of the pumps was done in order to attain a delivery rate of 0.5 cc/hr. The modification was the replacement of the two GB-60 gears by a GB-20 and GB-100 gear. Thus, when used in tandem, the pumping system delivered rates from 0.5 cc/hr to 2240 cc/hr. This range far surpassed that of other investigators (Kloepfer, 1975; Baird, 1978; Peters, 1979)

The pumps, charged with mercury, displaced the fluid of interest from a stainless steel fluid bomb into the coreholder. All lines were of high-pressure stainless steel tubing. The complete pumping system was designed to a working pressure of 1800 psi when using the stainless steel coreholders, and 100 psi for the PVC coreholders. Figure 3.1 is a schematic of the experimental set-up.

FIG. 3.1: SCHEMATIC OF DISPLACEMENT APPRATUS



3.4 Sandpack Property Determination

Prior to the waterflood, certain properties of each sandpack were measured. These measurements were performed by routine techniques and are only briefly described.

To determine the pore volume (porosity), the coreholder was first evacuated and then the initial fluid (depending on the wettability case desired) was introduced into the sandpack. The pore volume was then determined by both a material balance calculation and by weight. Taking into account the volume of fluid contained within the endcaps, agreement was within 2%.

This initial fluid was then flowed through the sandpack at several rates in order to estimate the absolute permeability using Darcy's law. In the case of water only flowing, a mercury manometer was used; for oil only flowing a Heise pressure gauge was used.

For the case of a water-wet system, the residual water saturation was then established by displacing the water with oil. The displacement was conducted at a high rate, with the coreholder in the vertical position, and the oil was introduced at the top.

It was suggested by Saeedi (1979) that the rate of injection of oil, while establishing the residual water saturation, should be higher than the injection rate of the subsequent waterflood. This procedure was suggested in order to ensure that the residual water would not be mobile. With this fact in mind, injection rates were set so that the

maximum pressure drop across the sandpack did not exceed 100 psi, the working pressure of the PVC coreholder.

Consequently, this restriction, in general, was sufficient to satisfy the suggestion of Saeedi (1979).

Subsequently, the permeability to oil at a residual water condition was measured in the same manner as above. It was observed that no water or sand was produced during this period.

3.5 Displacement Procedure

After the sandpack properties were measured, the flood was conducted in the following manner. The coreholder was placed in a horizontal position inside a cabinet maintained at 21.5°C. The inlet end was connected to the doped water bomb and a pressure gauge. A graduated cylinder was placed at the outlet to collect the effluent.

After an appropriate pumping rate was selected, the displacement was conducted until breakthrough of water. Breakthrough was that event when the first drop of water was produced. The use of the coloured water aided greatly in determining this point in time. At this time, both the pump reading and volume of effluent collected were recorded in order to verify the absence of leaks in the system, especially in the tests that were of long duration (2-3 weeks).

Vertical waterfloods were performed in the same manner as the horizontal floods. The orientation of the coreholder

was with the inlet end down, because the water density was slightly higher than that of the oil.

At the end of the test, the coreholder was disassembled completely, cleaned, and repacked with fresh sand before commencing another test.

3.6 Core Extraction Technique

The removal of the sand from the coreholder was investigated in order to develop a technique which was quick, simple and free of mess.

The method normally employed in this laboratory was to use a long auger to 'drill' out the core. A second method was to use hot water to flush out the sand from the coreholder. Both techniques proved to be time consuming and messy.

The following procedure was developed. After the outlet end-cap was removed, the coreholder was hung in a vertical position with the outlet end down. The Ruska pumping system, set at 560 cc/hr, was used to inject water into the coreholder. This had the effect of shifting the entire sandpack several centimeters. After the initial shift, the waterline was replaced by a 90-psi compressed airline. The compressed air ejected the entire sandpack from the coreholder into a bucket.

This technique of extracting the core was found to be both rapid (5-10 minutes) and relatively free of mess.

4. Presentation and Discussion of Results

There were two types of immiscible displacement tests carried out in this study. The first type was conducted in a water-wet porous medium with a residual water saturation. All tests of this type were horizontal displacements.

Secondly, the behaviour of an oil-wet porous medium was examined. This system contained no residual water and tests were conducted both horizontally and vertically. The fluid-rock system and the shape of the coreholders was identical to that used by Peters (1979) in order to make direct use of his data base.

4.1 Sandpack Properties

The techniques for packing each coreholder were outlined in Chapter 3. It was observed that the wet-packing method produced sandpacks of an absolute permeability in the range of 14 to 19 Darcys. However, the absolute permeability of the dry, vibrated cores was generally higher and quite unpredictable. Wide variations in permeability were seen, with one sandpack having a permeability of 32 Darcys. Similar observations were made for the permeability to oil at residual water saturation.

Both the porosity and residual water saturation appeared to be insensitive to the packing procedure used. The porosity of the sandpacks was, on the average, of the order of 36% and the residual water saturation was

approximately 11%.

Table 4.1 is a summary of the sandpack properties. The order of appearance of the data does not reflect the chronological sequence of the displacement tests.

The lower permeabilities obtained and the predictable results of the wet packing method may be attributed to the absence of static electricity and the stabilizing effect of water. The inherent sorting phenomenon associated with vibrating is consequently suppressed. From these observations, it may be concluded that the wet-packing method is superior to other techniques.

An experiment was designed in order to verify the complete removal of water from the sandpack during the packing procedure. The coreholder was prepared dry, then saturated and dried with compressed air. It was observed that, based on measurements of the weight of the coreholder, all the water was removed by the drying procedure.

Although no prescreening of the sand was attempted, it is suggested that a complete set of tests be arranged with sand from the same lot. It was observed that a change in lots corresponded to the dramatic change in permeability seen in Table 4.1 (Runs 18, 34, and 35).

4.2 Wettability of the Porous Media

When clean and uncontaminated, Ottawa silica sand is preferentially water-wet. However, the wettability of porous media depends on both the oil composition and rock type.

TABLE: 4.1
SUMMARY OF SANDPACK PROPERTIES

WATER-WET SYSTEM

RUN	LENGTH (CM)	DIAMETER (CM)	POROSITY (%)	ABS. PERM. (DARCY)	PERM. @SWI (DARCY)	SWI (%)
1D	113.1	2.390	36.36	21.04	17.25	10.4
2D	113.1	2.390	37.74	19.38	17.07	10.4
3D	113.1	2.390	37.19	19.72	14.61	11.5
4W	113.1	2.390	37.92	18.34	15.30	12.6
5W	26.9	2.390	38.01	18.26	16.59	10.8
6W	22.8	4.859	34.10	14.23	12.87	10.3
7W	22.6	4.815	37.28	17.91	15.28	10.2
8W	22.8	4.859	33.66	16.60	11.67	9.4
9W	53.2	4.850	32.32	15.38	14.90	10.7
10W	53.2	4.850	36.98	18.21	14.93	10.7
11W	53.2	4.850	35.83	18.37	14.51	13.2
12D	53.2	4.850	37.56	20.83	15.88	12.4
13D	110.4	4.864	33.65	19.17	16.98	10.7
14W	110.4	4.864	36.22	18.35	14.48	11.9

OIL-WET SYSTEM

RUN	LENGTH (CM)	DIAMETER (CM)	POROSITY (%)	ABS. PERM. (DARCY)
15D	113.1	2.390	37.29	18.83
16D	113.1	2.390	37.98	19.48
17D	113.1	2.390	37.09	19.90
18W	26.9	2.390	38.77	10.81
19D	22.6	4.815	35.50	17.15
20D	22.8	4.859	35.97	16.93
21W	53.2	4.850	35.25	17.70
22W	53.2	4.850	35.60	17.45
23W	53.3	4.811	35.80	18.02
24W	53.3	4.811	36.69	18.57
25W	53.3	4.811	38.58	21.98
26D	110.4	4.864	38.41	22.83
27D	110.2	4.828	36.67	19.78
28D	110.2	4.828	37.13	18.88
29D	110.2	4.828	39.20	31.70
30D	110.2	4.828	36.79	18.91
31D	110.4	4.864	36.63	19.51

Continued Next Page

TABLE: 4.1 CONTINUED
SUMMARY OF SANDPACK PROPERTIES

OIL-WET SYSTEM--VERTICAL FLOODS

RUN	LENGTH (CM)	DIAMETER (CM)	POROSITY (%)	ABS. PERM. (DARCY)
32W	22.8	4.859	36.97	18.56
33W	22.6	4.815	37.20	17.84
34W	22.6	4.815	38.12	10.75
35W	22.8	4.859	35.74	10.76

D Dry Packed
W Wet Packed

The effect of Dow Corning 200 fluid on the wettability of Ottawa silica sand was investigated by Baird (1978). For a water-wet system, his data suggested that Dow Corning fluid tends to shift the wettability of the Ottawa silica sand toward oil-wet. Thus, the Dow Corning fluid tends preferentially to wet the sand.

Based on Baird's (1978) findings, the porous media in this study were considered to be wet by the fluid of first contact. This is provided that the oil was not permitted to remain in contact with the sand for a long period of time. Consequently, for a displacement test where water was the first fluid to contact the sand, the system was considered to be water-wet. Furthermore, the porous media were considered to be oil-wet when Dow Corning 200 was the initial saturating fluid. It was beyond the scope of this study to establish a residual water saturation in the latter system.

4.3 Displacement Results

Immiscible displacement tests were carried out for both wettability types over a wide range of rates varying from 0.5 cc/hr to 480 cc/hr. The coreholders were of three lengths and two diameters. Due to the small pore volumes associated with the 2.4 cm coreholders, the flow rates were restricted to a maximum of 140 cc/hr for the longer core and to 40 cc/hr for the shorter-length sandpacks.

Table 4.2 is a summary of the results of the displacement tests carried out in this study. Included in the table are the results of the calculations of the various similarity groups pertinent to this study.

4.4 Scaling in Porous Media--Theoretical Results

In a scaled model study, it is not necessary to demand that the geometric factor be identical in both model and prototype, provided that the displacement is stable. However, the model and prototype should have the same shape because the derivation of the scaling groups was based on a particular coordinate system.

The meaning of the terms 'geometric factor' and 'geometric similarity' should not be confused. Geometric factor refers to the ratio of the overall dimensions (L/D) of the porous medium whereas geometric similarity refers to the scaling of the characteristic lengths of the porous medium.

The multi-dimensional modified inspectional analysis results in the emergence of two capillary numbers in the set of similarity groups. This important result does not arise if the displacement problem is assumed to be linear. The linear capillary number dictates the stabilization of the front in the direction of bulk flow. The radial capillary number, which is important only if an appreciable saturation gradient exists in the radial direction--such as in the case of viscous fingering--controls the spreading or growth of

TABLE: 4.2
SUMMARY OF DISPLACEMENT TESTS

WATER-WET SYSTEM

RUN	Q CC/HR	V CM/SEC	REC %IBT	1/Ltr	1/Nct	1/Ncr	Ng	Ns	
1	140.00	8.668E-03	34.63	1.509E 00	3.190E-02	2.395E 00	5.060E-02	5.553E-02	3.343E 01
2	40.00	2.477E-03	39.71	4.411E-01	9.321E-03	7.428E-01	1.570E-02	1.790E-01	1.037E 01
3	3.13	1.935E-04	42.16	3.441E-02	7.272E-04	5.703E-02	1.205E-03	2.332E 00	7.963E-01
4	0.50	3.096E-05	41.99	5.654E-03	1.195E-04	9.811E-03	2.073E-04	1.355E-01	1.370E-01
5	25.00	1.548E-03	40.91	6.731E-02	5.980E-03	1.172E-01	0.041E-02	2.699E-01	6.879E 00
6	15.00	2.247E-04	40.19	9.904E-03	2.111E-03	1.850E-02	3.943E-03	1.449E 00	5.297E 00
7	50.00	7.628E-04	41.90	2.847E-02	6.053E-03	4.957E-02	1.054E-02	5.372E-01	1.403E 01
8	3.13	4.681E-05	44.03	1.923E-03	4.093E-04	3.304E-03	7.042E-04	8.112E 00	9.459E-01
9	480.00	7.217E-03	32.42	7.334E-01	6.686E-02	1.283E 00	1.170E-01	4.875E-02	1.568E 02
10	200.00	3.007E-03	36.85	2.625E-01	2.392E-02	4.515E-01	4.116E-02	1.385E-01	5.519E 01
11	50.00	7.518E-04	39.73	6.639E-02	6.052E-03	1.119E-01	1.020E-02	5.590E-01	1.368E 01
12	60.00	9.021E-04	40.21	7.307E-02	6.661E-03	1.184E-01	1.079E-02	5.282E-01	1.447E 01
13	0.50	7.475E-06	38.94	1.384E-03	6.096E-05	2.213E-03	9.746E-05	5.867E 01	1.311E-01
14	50.00	7.475E-04	42.00	1.364E-01	6.009E-03	2.312E-01	1.018E-02	5.616E-01	1.369E 01

OIL-WET SYSTEM

RUN	Q CC/HR	V CM/SEC	REC %IBT	1/Ltr	1/Nct	1/Ncr	Ng	Ns	
15	100.00	6.192E-03	13.48	1.125E 00	2.378E-02	1.911E 00	4.039E-02	6.957E-02	1.499E 03
16	60.00	3.715E-03	14.69	6.578E-01	1.390E-02	1.108E 00	2.342E-02	1.200E-01	8.697E 02
17	50.00	3.096E-03	15.89	5.488E-01	1.160E-02	9.042E-01	1.911E-02	1.471E-01	7.094E 02
18	5.00	3.096E-04	21.58	1.732E-02	1.539E-03	3.959E-02	3.517E-03	7.988E-01	1.306E 02
19	50.00	7.628E-04	16.80	2.982E-02	6.338E-03	5.177E-02	1.100E-02	5.144E-01	8.232E 02
20	0.50	7.490E-06	25.07	2.947E-04	6.280E-05	5.184E-04	1.105E-04	5.171E 01	8.339E 00
21	60.00	9.021E-04	17.21	8.182E-02	7.459E-03	1.393E-01	1.270E-02	4.489E-01	9.571E 02
22	40.00	6.014E-04	18.43	5.467E-02	4.984E-03	9.423E-02	8.590E-03	6.638E-01	6.472E 02
23	10.00	1.528E-04	30.37	1.366E-02	1.233E-03	2.323E-02	2.096E-03	2.698E 00	1.567E 02
24	0.50	7.640E-06	31.13	6.644E-04	5.997E-05	1.127E-03	1.017E-04	5.560E 01	7.602E 00
25	0.82	1.261E-05	61.88	9.826E-04	8.869E-05	1.571E-03	1.418E-04	3.989E 01	1.060E 01
26	80.00	1.196E-03	20.41	1.800E-01	8.365E-03	2.973E-01	1.309E-02	4.367E-01	9.894E 02
27	0.50	7.587E-06	30.63	1.322E-03	5.792E-05	2.172E-03	9.516E-05	5.965E 01	7.137E 00
28	0.82	1.252E-05	54.00	2.219E-03	9.720E-05	3.755E-03	1.645E-04	3.450E 01	1.234E 01
29	0.82	1.252E-05	47.91	1.666E-03	7.301E-05	2.235E-03	9.797E-05	5.793E 01	7.348E 00
30	0.50	7.587E-06	35.55	1.350E-03	5.914E-05	2.272E-03	9.954E-05	5.702E 01	7.466E 00
31	2.50	3.737E-05	45.75	6.576E-03	2.896E-04	1.087E-02	4.788E-04	1.194E 01	3.618E 01

Continued Next Page

TABLE: 4.2 CONTINUED
SUMMARY OF DISPLACEMENT TESTS

OIL-WET SYSTEM--VERTICAL FLOODS

RUN	Q CC/HR	V CM/SEC	REC @BT	1/Ltr	1/Ltr	1/Ncl	1/NCF	Ng	Ns
32	0.50	7.490E-06	41.52	2.776E-04	5.917E-05	4.728E-04	1.008E-04	5.669E 01	7.606E 00
33	0.50	7.628E-06	51.50	2.856E-04	6.071E-05	4.977E-04	1.058E-04	5.351E 01	7.913E 00
34	0.50	7.628E-06	26.59	3.634E-04	7.726E-05	8.259E-04	1.756E-04	3.224E 01	1.313E 01
35	1.25	1.873E-05	23.49	9.271E-04	1.976E-04	2.039E-03	4.345E-04	1.315E 01	3.280E 01

the 'front' in the radial direction.

Although not presented, the similarity groups which arise from a three-dimensional analysis in a Cartesian coordinate system include three capillary numbers. These may be interpreted in the same way as the linear and radial capillary numbers.

4.5 Scaling in Porous Media--Experimental Results

The breakthrough recovery was correlated with both the conventional similarity groups which arise from an inspectional analysis using the Leverett J-function (Appendix A.2.2), and those derived in this study (Appendix A.2.3). For each wettability type considered, it was assumed that the mobility ratio, relative permeability curves, and capillary pressure curves remained constant. Furthermore, it was assumed that gravity effects were negligible. The similarity groups of interest were:

- 1) $\gamma(K\phi)^{1/2}/V\mu_w L$ Linear Leverett number Lt_l
and its counterpart,
 $\sigma K_{wr}/V\mu_w L$ Linear capillary number N_{cl} ;
- 2) $\gamma(K\phi)^{1/2}/V\mu_w D$ Radial Leverett Number Lt_r
and its counterpart,
 $\sigma K_{wr}/V\mu_w D$ Radial capillary number N_{cr} ;
- 3) L/D Geometric factor.

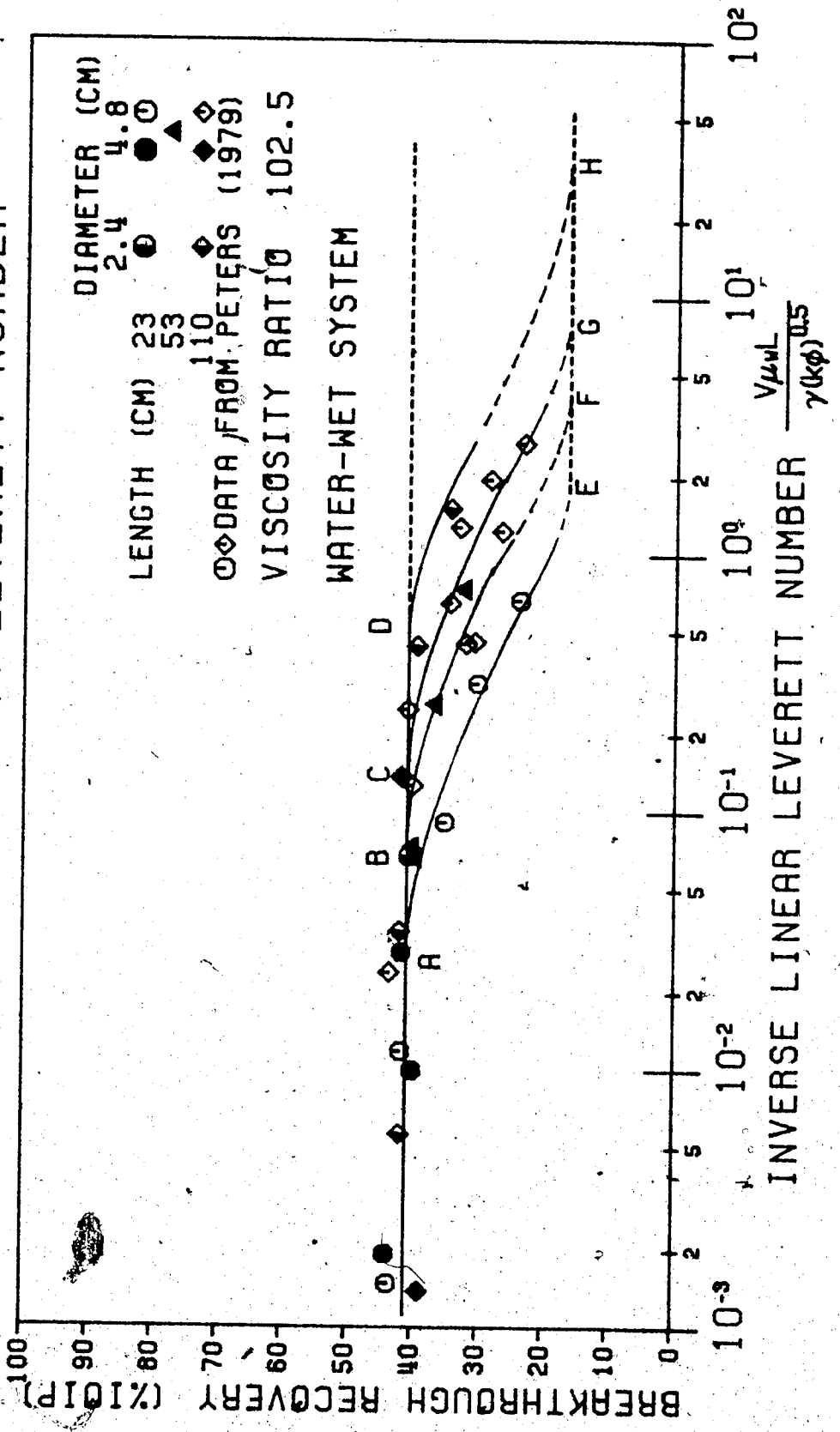
4.5.1 Water-wet System

In this type of system, the breakthrough recovery, when correlated with the inverse linear Leverett number, exhibited the behaviour shown in Figure 4.1. It was observed, as predicted by theory, that the breakthrough recovery is insensitive to variations in the similarity group, provided that the displacement is stable and stabilized. This region is represented by the horizontal line (and the dashed portion is an extension according to theory) at a recovery of 41% IOIP. Furthermore, regardless of the sandpack dimensions, all data correlated well. Thus the recovery is insensitive to the geometric factor in this region.

However, a deviation from this plateau is very apparent at higher values of the inverse linear Leverett number. This may be attributed to the viscous forces beginning to dominate the recovery process. The Points A, B, C and D correspond to the onset of instability at the floodfront for the various geometric factors considered in this study. These points correspond to a stability number of 13.56 and were determined experimentally.

For unstable displacements, a family of curves results. As shown in Figure 4.1, each member of the family corresponds to a particular L/D ratio. Thus, it appears that the geometric factor cannot be omitted as a scaling group when viscous fingering is present. Consequently in this

FIG. 4.1: RECOVERY CORRELATED BY THE INVERSE LINEAR LEVERETT NUMBER



intermediate zone, where the viscous forces begin to dominate, the linear flow assumption is no longer valid. Hence, scaling groups based on the assumption of a stable displacement may not be valid if instabilities are present, although they may still be useful if correctly interpreted.

Based on the results of Baird (1978), a second region (which may be considered as a pseudo-stable displacement region) of constant recovery is postulated. This region is represented by the lower dashed curve in Figure 4.1. Points E, F, G and H correspond to where the viscous forces completely dominate the recovery process, that is, for a stability number of 900. These points were calculated using estimated average sandpack and fluid properties. A typical calculation is presented in Appendix C. It may be speculated that beyond these points, the recovery is again insensitive to the magnitude of the parameters in the linear Leverett number. This speculation is based on the results of the oil-wet tests, which are presented in a later section. It should be noted that there is little experimental basis for the level at which the lower dashed portion of the recovery curve has been plotted. As will be seen in a later section, the level of the recovery is partially justified by the extrapolation of the recovery curve to a stability number of 900.

The pseudo-stable region could not be obtained experimentally due to the high displacement rates required, approximately 3200 cc/hr, and the small pore volumes of the

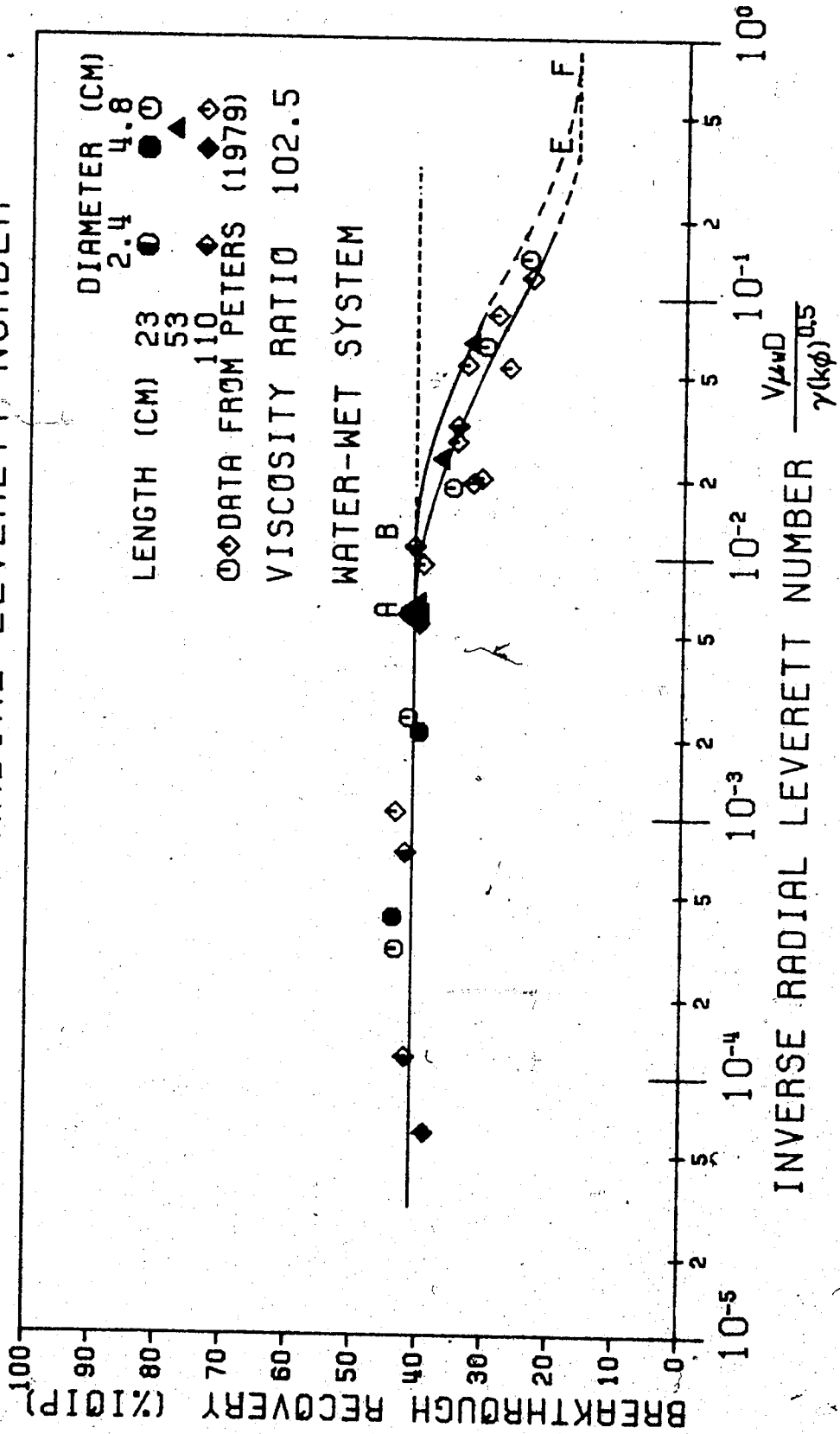
coreholders. The largest sandpack, with an estimated recovery of 17% IOIP, would break through in less than 1 minute at this rate. Consequently, data from this type of test were considered invalid.

The correlation of the breakthrough recovery with the radial Leverett number (shown in Figure 4.2) is acceptable, provided the sandpack diameters are approximately equal. Although it appears that the data correlate well, regardless of geometric factor, it should be noticed that Points A (for the 4.8 cm diameter sandpack) and B (2.4 cm diameter sandpack) both correspond to the onset of frontal perturbations. This 'good correlation' can be explained by the relatively small difference in magnitude of the sandpack diameters, and by the wide scatter of the data in the perturbed region.

Peters (1979) suggested that the radial Leverett number is the better scaling parameter in systems which contain a residual water saturation. This conclusion, however, was based on sandpacks of similar diameter. Despite the difficulty of the interpretation for the two reasons mentioned above, the data do not correlate well for different diameters.

From the above discussion, it can be concluded that neither the linear Leverett number nor the radial Leverett number is a good correlating group beyond the point where viscous forces begin to dominate the process. Thus, a model may be compared to a prototype provided the displacement is

FIG. 4.2: RECOVERY CORRELATED BY THE INVERSE RADIAL LEVERETT NUMBER



stable. Moreover, scaling the geometric factor is not important for such displacements.

Figures 4.3 and 4.4 are similar to the previous two figures, except that the correlation of the breakthrough recovery is made with the linear capillary and radial capillary numbers, respectively. It was assumed that the permeability to water at residual oil saturation was equal to the absolute permeability. The effect of this assumption is to shift the curve horizontally to the left. A test was undertaken in which the sandpack was flooded out to a water-oil ratio of 49. The permeability to water at residual oil saturation was estimated to be 6 Darcys. This result is in agreement with the experiments of Saeedi (1979). It is possible to assume that the permeability to water at residual oil saturation is some fixed fraction of the absolute permeability. However, this entails the implicit assumption that the ratio is fixed throughout the set of tests. No experimental evidence is available to support this assumption. For the sake of consistency, the absolute permeability was used in all calculations.

Both Figures 4.3 and 4.4 were constructed assuming the capillary pressure normalizing parameter to be of the order of 2.027×10^4 dynes/cm² (Saeedi, 1979). The validity of this assumption was verified by equating the Leverett number and capillary number, that is:

$$\frac{\gamma \sqrt{K\phi}}{V_{\mu_w} L} = \frac{\sigma K}{V_{\mu_w} L} \quad 4.1$$

FIG. 4.3: RECOVERY CORRELATED BY THE INVERSE LINEAR CAPILLARY NUMBER

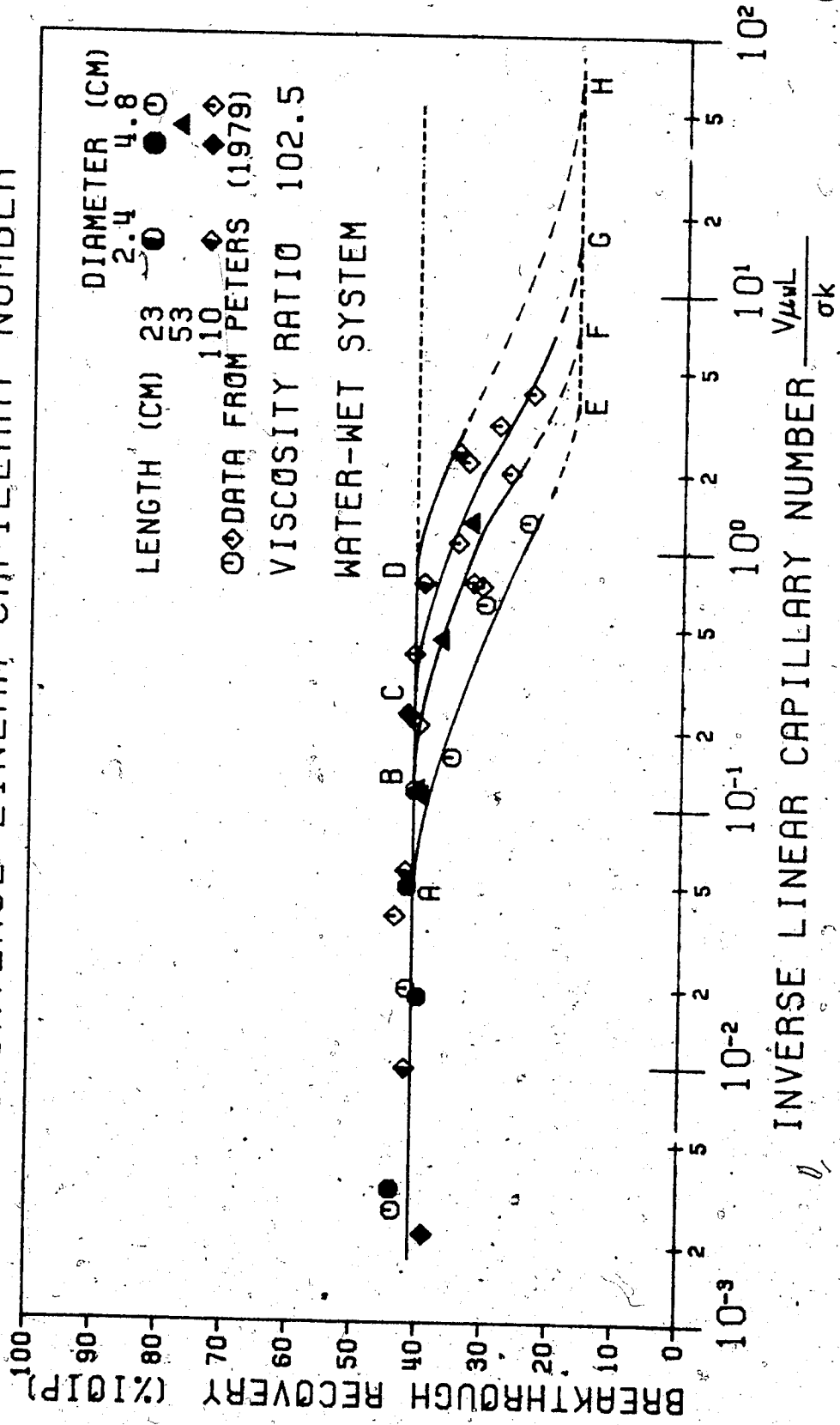
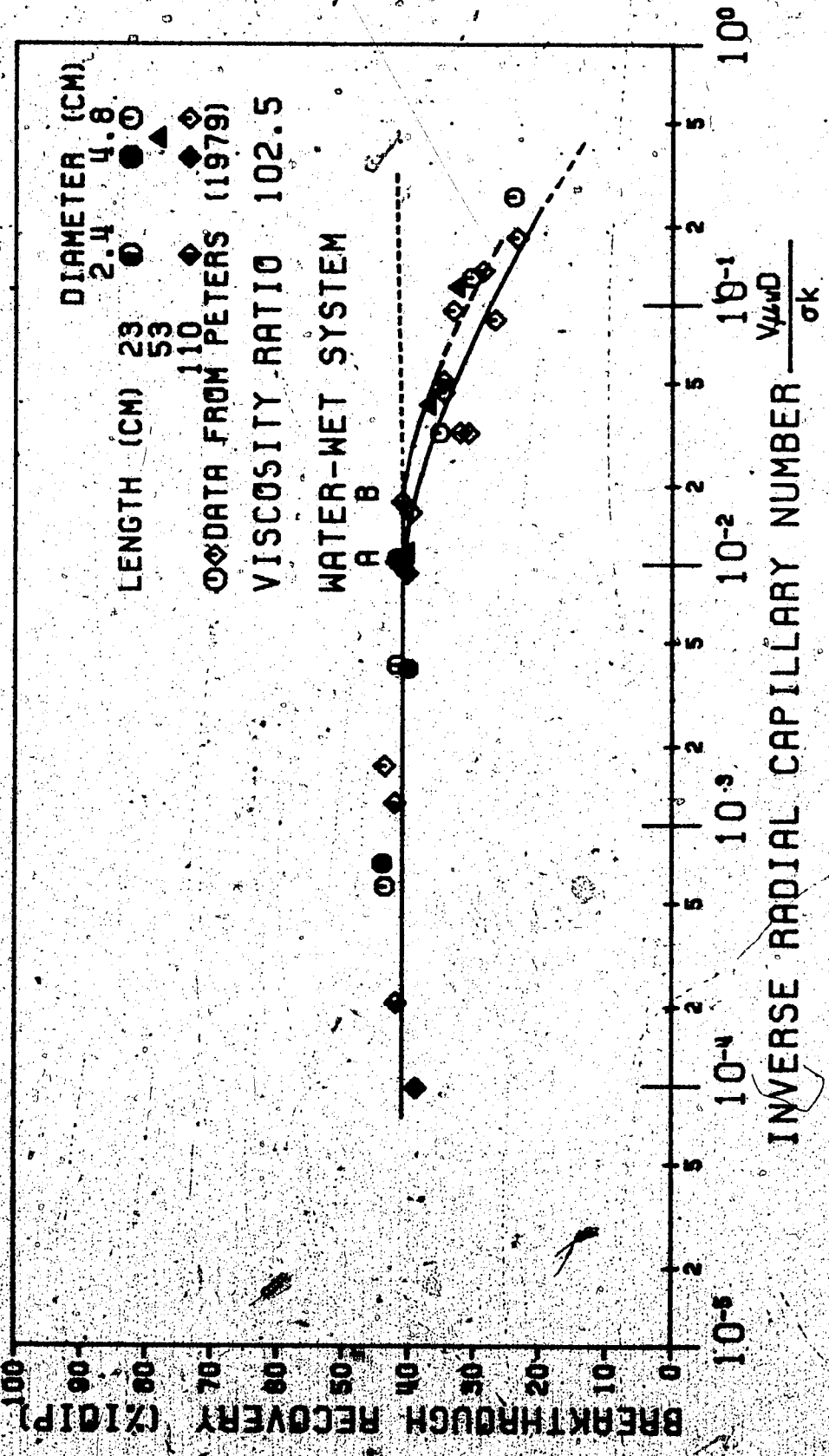


FIG. 4.4: RECOVERY CORRELATED BY THE INVERSE RADIAL CAPILLARY NUMBER



or

$$\sigma = \gamma \sqrt{\phi / K}$$

4.2

Using average properties, this estimation showed that the capillary pressure normalizing parameter is of the order of 3.5×10^4 dynes/cm².

Thus, the correlation with the capillary number shows that all the displacement tests carried out in this study were unstabilized as defined in Chapter 1, that is, the inverse linear capillary number was much less than 100. This conclusion could not be drawn by past researchers for the following reasons.

- 1) No estimate of the magnitude of the Leverett number delimiting a stabilized displacement was available.
- 2) The plateau observed in the Leverett correlation may be mistaken for a stabilized displacement wherein the results may be masked by 'end-effects' (Kyte and Rapoport, 1958). The observed plateau is due to an excessive build up of water at the outlet end. Consequently, the observed recovery is too high.
- 3) Figure 2.8 shows a typical recovery response curve. It can be seen that at a high mobility ratio and large values of the capillary number, the recovery is affected minimally by the

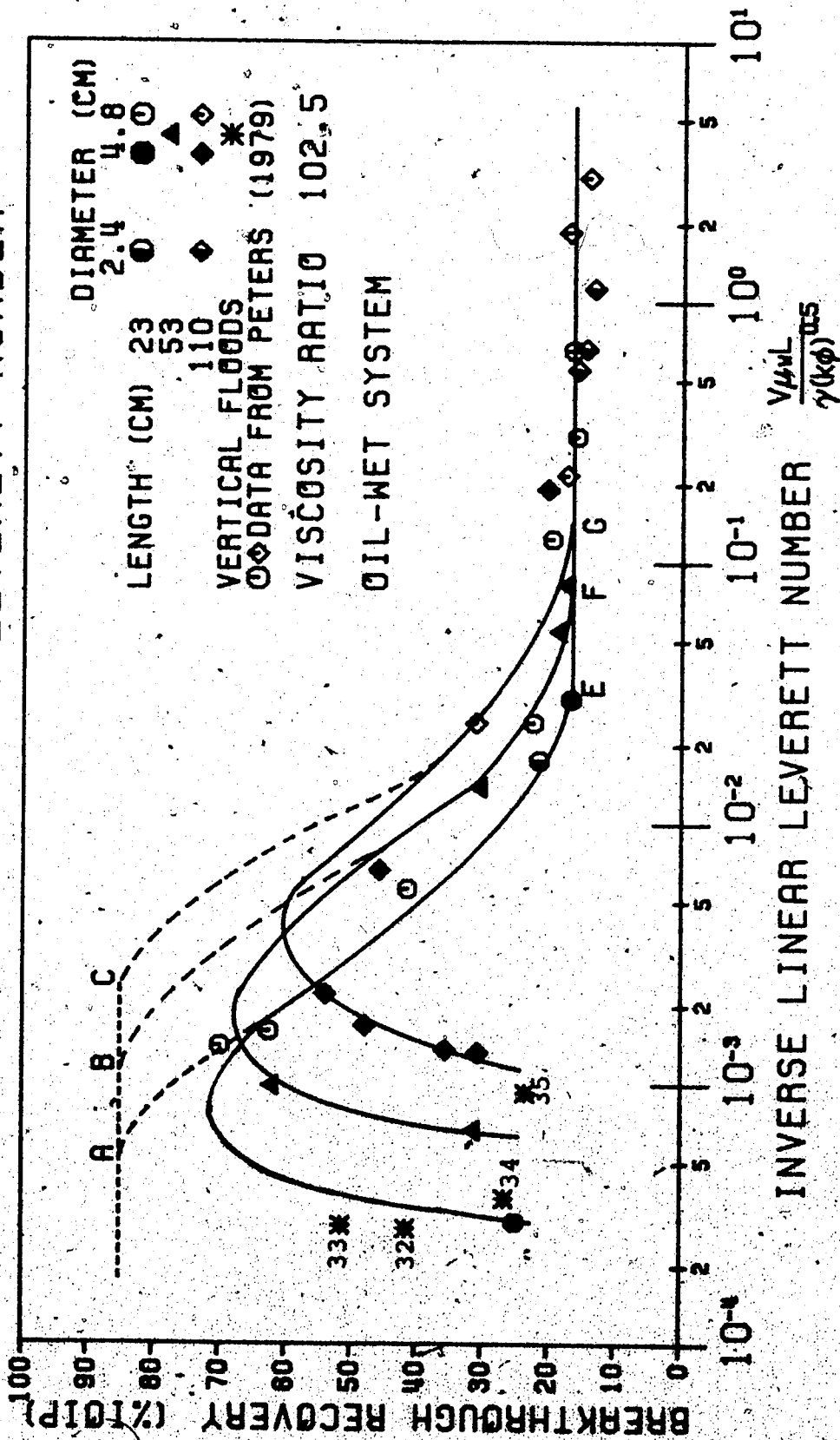
magnitude of the parameters in the Leverett number. Thus, the recovery is only a weak function of the Leverett number, provided the mobility ratio is high.

Figures 4.1 (a correlation of the recovery with the inverse Leverett number) and 4.3 (a correlation of the recovery with the inverse capillary number) are virtually identical. As a consequence, at least for this experimental system, the Leverett number and capillary number have the same physical significance. This suggests that the magnitude of the linear Leverett number should be of the order of 0.01 if the displacement is to be stabilized. In light of point 3 above, 'stabilization' may be defined as that point where the recovery response curve is within 5% of the steady-state recovery as predicted by Buckley-Leverett theory. However, it may not be convenient to use this definition due to difficulties in determining the Buckley-Leverett recovery.

4.5.2 Oil-wet System--Horizontal Displacements

The breakthrough recovery, for the oil-wet system, was correlated against the same scaling groups as for the water-wet system. Figure 4.5 shows the recovery correlated with the inverse linear Leverett number. The dashed curves in this figure indicate the 'expected' response for this type of system. Again, as for the water-wet case, the only experimental basis for the level of the recovery curve is from the extrapolation of the recovery curve to a stability

FIG. 4.5: RECOVERY CORRELATED BY THE INVERSE LINEAR LEVERETT NUMBER



number of 13.56. Points A, B, and C define the onset of frontal perturbations while Points E, F, and G indicate the complete dominance of the viscous forces. The 'expected' response may be justified by the same argument presented for the water-wet system.

In an attempt to explain the deviation from the 'expected' response, the sandpacks were extracted from the coreholders and a post-mortem was performed. It was observed that the waterflood suffered from gravity override by the injected water at low flow rates. It should be noticed that the effects of gravity are more pronounced in the longer sandpacks. Furthermore, the experimental results are masked by the compounded effects of frontal perturbations and a non-stabilized displacement. These compounded effects confuse the interpretation of the data. Any interpretation must be carefully undertaken.

In view of the fact that a water tongue was observed, the waterflood at low displacement rates was considered to behave according to the theory of Dietz (1953). Based on this theory, Hawthorne (1960) derived the following equation to calculate the slope of the fluid-fluid interface, viz:

$$\tan \omega = \frac{V \cos \alpha (u_w / K_{wr} - u_o / K_{or})}{g (\rho_w - \rho_o) + V \sin \alpha (u_w / K_{wr} - u_o / K_{or})} \quad 4.3$$

where the angles α and ω are the dip of the formation and interface with the horizontal, respectively. For a horizontal displacement and assuming that the end-point

permeabilities are equal to the absolute permeability, Equation 4.3 may be written as:

$$\tan \omega = \frac{V \Delta \mu}{K \Delta \rho g} \quad 4.4$$

where

$$\Delta \mu = \mu_w - \mu_o \quad 4.5$$

Equation 4.4 may be rewritten as:

$$\tan \omega = \frac{1}{N_g} \frac{\Delta \mu}{\mu_w} \quad 4.6$$

Using Equation 4.6 and the data from Run 16, the angle of the interface was estimated as 60°. The post-mortem of this sandpack enabled the angle to be estimated as approximately 55°, in fair agreement with the calculated angle.

The results of the water-wet tests showed that no correlation of all the data was possible in the intermediate zone (where the viscous forces begin to dominate the displacement process). It is also expected that this should be true in the oil-wet system. However, due to the effects of gravity, the data in this intermediate zone tend to fall along the same curve. This implies that a correlation is possible. However, the conclusion that the linear capillary number is a good correlating parameter in an oil-wet system is incorrect.

The existence of a second stabilized zone is clearly observed in Figure 4.5. In this region, all data correlated well, suggesting that the geometric factor does not affect the recovery.

Figure 4.6 is similar to Figure 4.2 and the same comments apply. Again, the effects of gravity are large for slow velocities and long cores. The dashed portion of the curve indicates the 'expected' recovery, if these effects are negligible.

Using the estimate of the capillary pressure normalizing parameter, Figures 4.7 and 4.8 were constructed. It should be noted that the capillary pressure normalizing parameter may be very different in an oil-wet system, as compared to a water-wet one. Typically, the capillary pressure normalizing parameter is one to two orders of magnitude smaller in an oil-wet system.

The breakthrough recovery, when plotted against the inverse gravity number (Figure 4.9) is remarkably similar in character to the radial scaling groups. It can be seen that, for small values of the inverse gravity number, the recovery is dramatically reduced. No interpretation is possible from the data at higher values of the inverse gravity number due to the effects of instabilities. However, it may be stated that the effects of gravity become negligible at high displacement rates.

FIG. 4.6: RECOVERY CORRELATED BY THE INVERSE RADIAL LEVERETT NUMBER

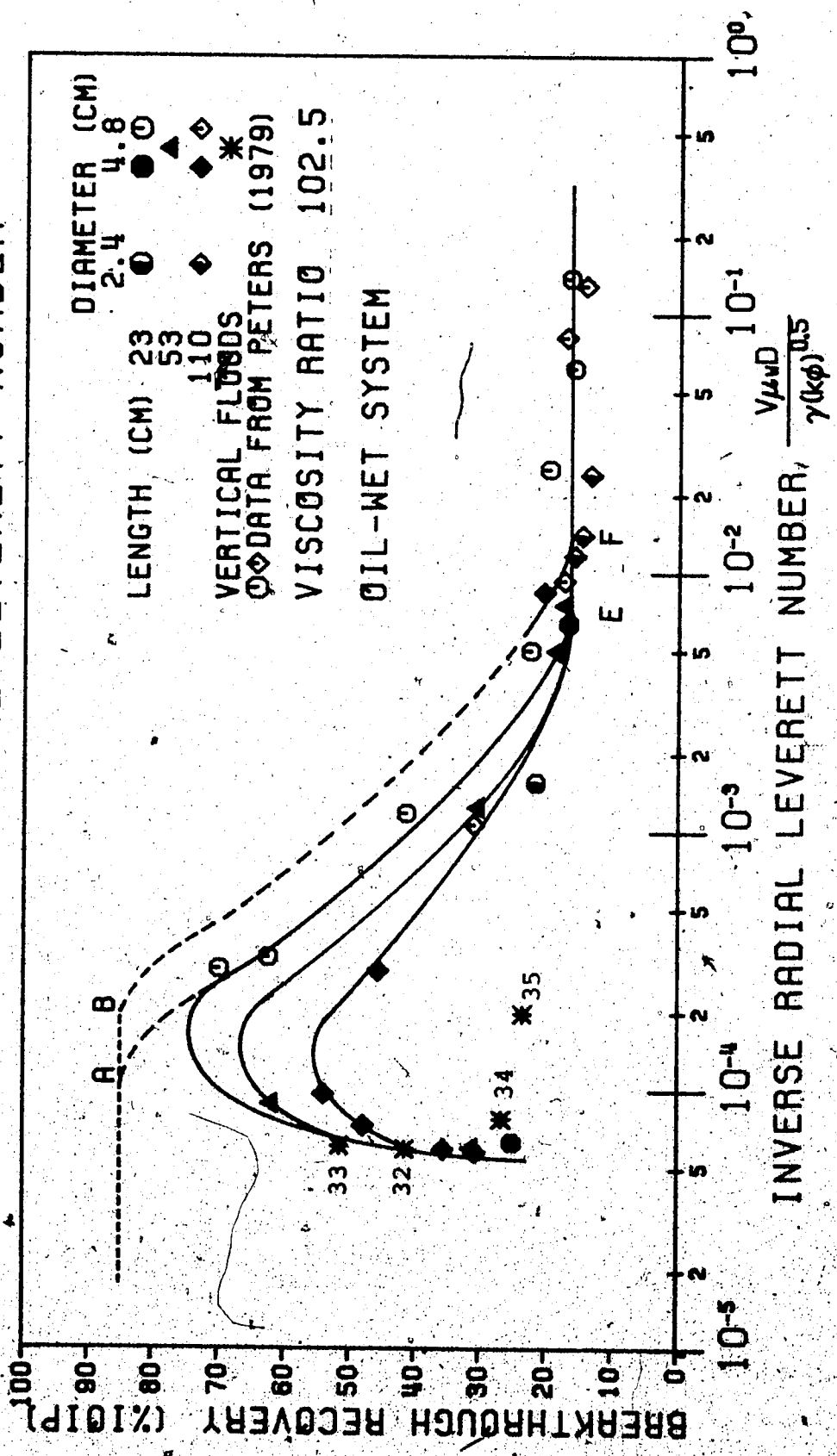


FIG. 4.7: RECOVERY CORRELATED BY THE INVERSE LINEAR CAPILLARY NUMBER

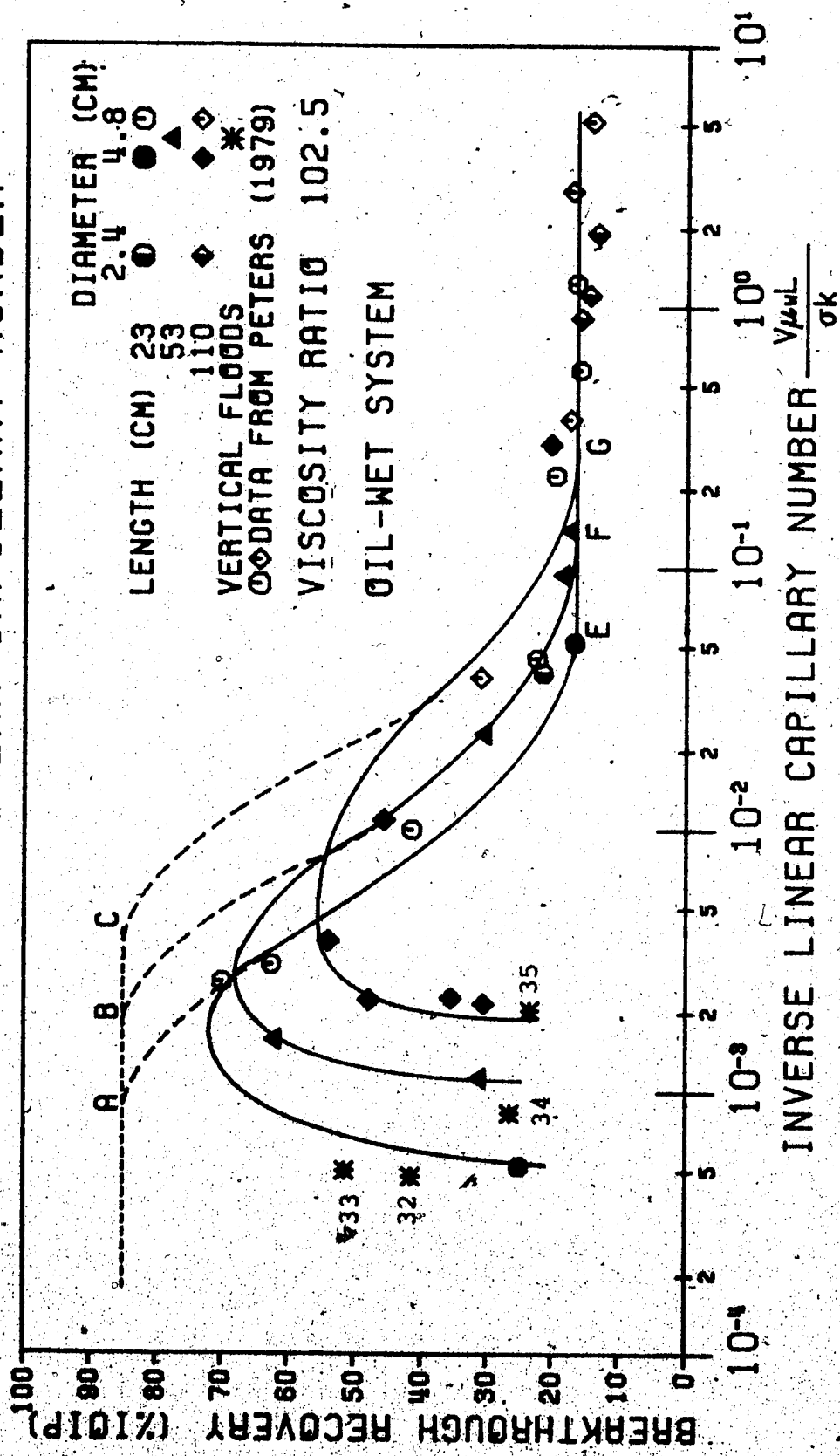
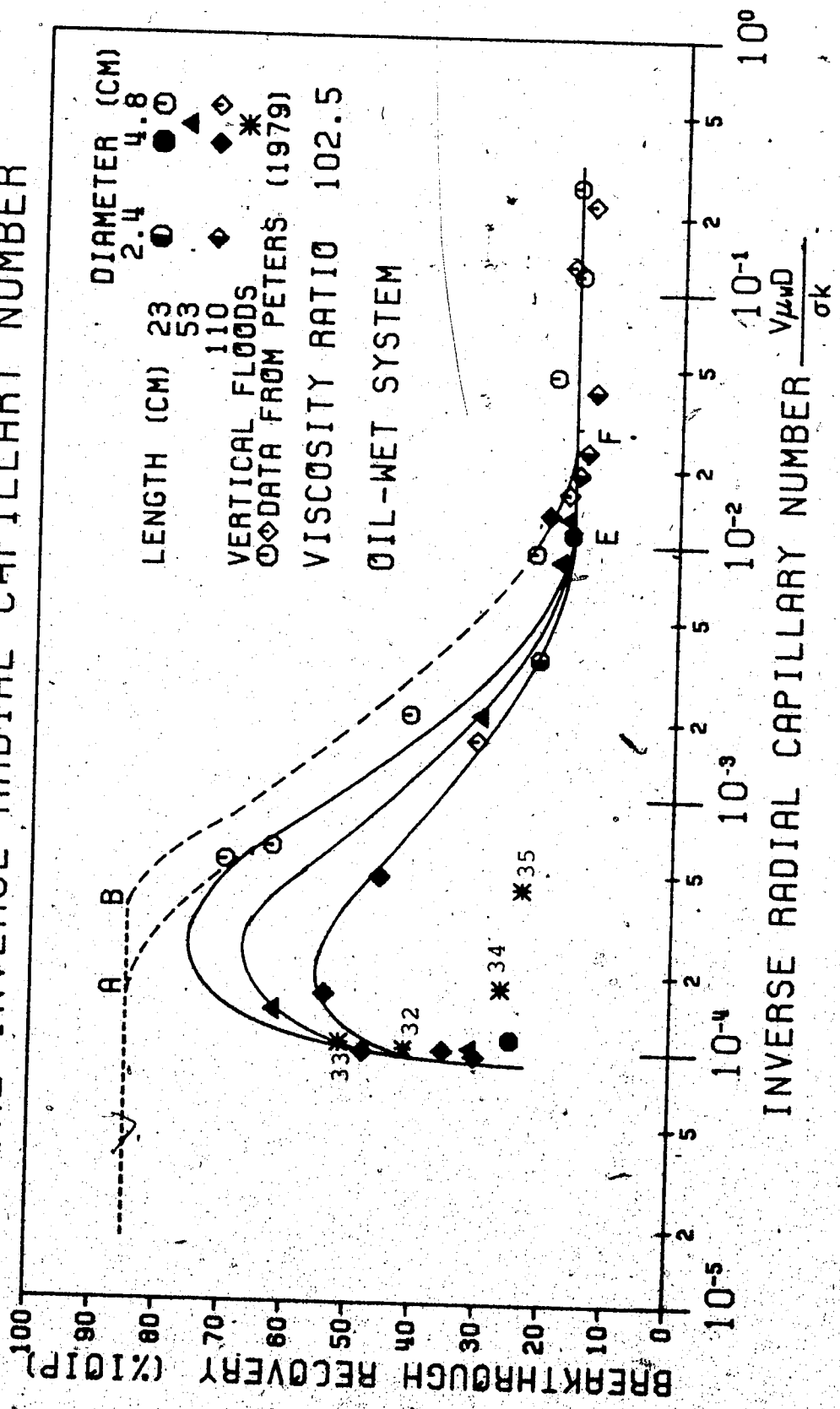


FIG. 4.8: RECOVERY CORRELATED BY THE INVERSE RADIAL CAPILLARY NUMBER



4.5.3 Oil-wet System--Vertical Displacements

In an attempt to obtain the 'expected' recovery shown in Figure 4.5, several vertical displacements were conducted. In a vertical flood, the effects of gravity underdrive are negated and consequently, the displacement should proceed as a plane horizontal front.

It was observed that all the vertical tests resulted in recoveries well below the 'expected' recovery. In order to gain insight into the apparent failure of the tests, an examination was conducted on the sandpacks. The following observations were made.

Run 32

This test was conducted in the short (4.8 cm diameter, 23 cm length) coreholder. It was seen that the areal sweep efficiency was high up to the last 7 cm of the sandpack. Between this point and the outlet, the areal sweep efficiency decreased rapidly. The sandpack was sliced in 1 cm sections. This revealed an almost circular water channel centred in the sandpack, the diameter of the circle decreasing toward the outlet. This peculiar behaviour, near the outlet, was attributed to the design of the end-cap. It was thought that the end-cap's effect was similar to that of a point sink, thus distorting the flow channel.

Run 33

This test was conducted in the same manner as the previous

test, except for a modification to the design of the end-cap in an attempt to 'remove' the sink effect. The result was to increase the recovery by approximately 10%. However, this test again fell short of the 'expected' 85% recovery. The post-mortem showed that the horizontal interface became distorted within 4 cm of the outlet. The effect of the end-cap was again influencing the flow path and a sectioning of the sandpack revealed an elliptically shaped flow channel open to water. Thus, the modification was only partially successful.

Run 34

This third test was conducted with a lower permeability, all other parameters being the same. As in the previous tests, this displacement was conducted at a velocity below the critical in order to avoid viscous fingering. The post-mortem of this sandpack showed that the flow path followed by the water was cylindrical in nature, that is, the flow tended to follow the perimeter of the coreholder.

The results of these three tests suggest that the behaviour of the waterflood is extremely sensitive:

- 1) to any heterogeneities in the porous medium; and
- 2) to the 'boundary conditions' of the system
(end-caps, walls of the coreholder)

if the superficial velocity is small.

Run 35

This test was conducted in the regime of unstable displacements. In addition to the effects mentioned above, it was observed that the flow paths were irregular.

4.6 Stability of Displacement Tests

Displacement tests, for both types of wettability, were conducted using sandpacks of various dimensions. It was seen in these series of tests that a displacement may fall into one of the following regimes:

- 1) stable displacement: no viscous fingers exists and there is a balance between viscous and capillary forces;
- 2) unstable displacement (transition zone): viscous forces begin to dominate the displacement and the displacement is characterized by a sharp decrease in recovery;
- 3) unstable displacement (pseudo-stable): the displacement is completely dominated by viscous forces and the recovery is insensitive to instabilities.

4.6.1 Water-wet System

Figure 4.10 is a graphical summary of the stability of the water-wet displacement tests performed on sandpacks having several geometric factors. It should be remembered that the stability number does not attempt to 'scale' the

displacement performance. Rather, it delimits the stability of the displacement process.

An objective of the study was to define better the onset of instability. To this end, displacement tests were carried out in the vicinity of a stability number of 13.56. As predicted by theory, the data from this study supports the findings of Peters (1979). It was observed that the recovery for this particular fluid-rock system was approximately 41% IOIP, provided that the displacement was stable. Beyond the onset of instability at the floodfront, a sharp decrease was observed, corresponding to the appearance of viscous fingers.

Due to the experimental limitations (high displacement rates required and small pore volumes of the sandpacks), it was not feasible to conduct tests beyond a stability number of 400. Thus, it was not possible to define the second breakpoint in the recovery curve. In order to define the pseudo-stable region, a more viscous oil is required because an increase in the mobility ratio has the effect of shifting the curve down and to the right.

The data base of Peters (1979) was extended by approximately one order of magnitude, to small values of the stability number. The displacement tests showed that the recovery is independent of a stability number, provided it is less than its critical value, 13.56. This portion of the curve corresponds to the nearly stabilized displacements discussed in Section 4.5.1.

4.6.2 Oil-wet System

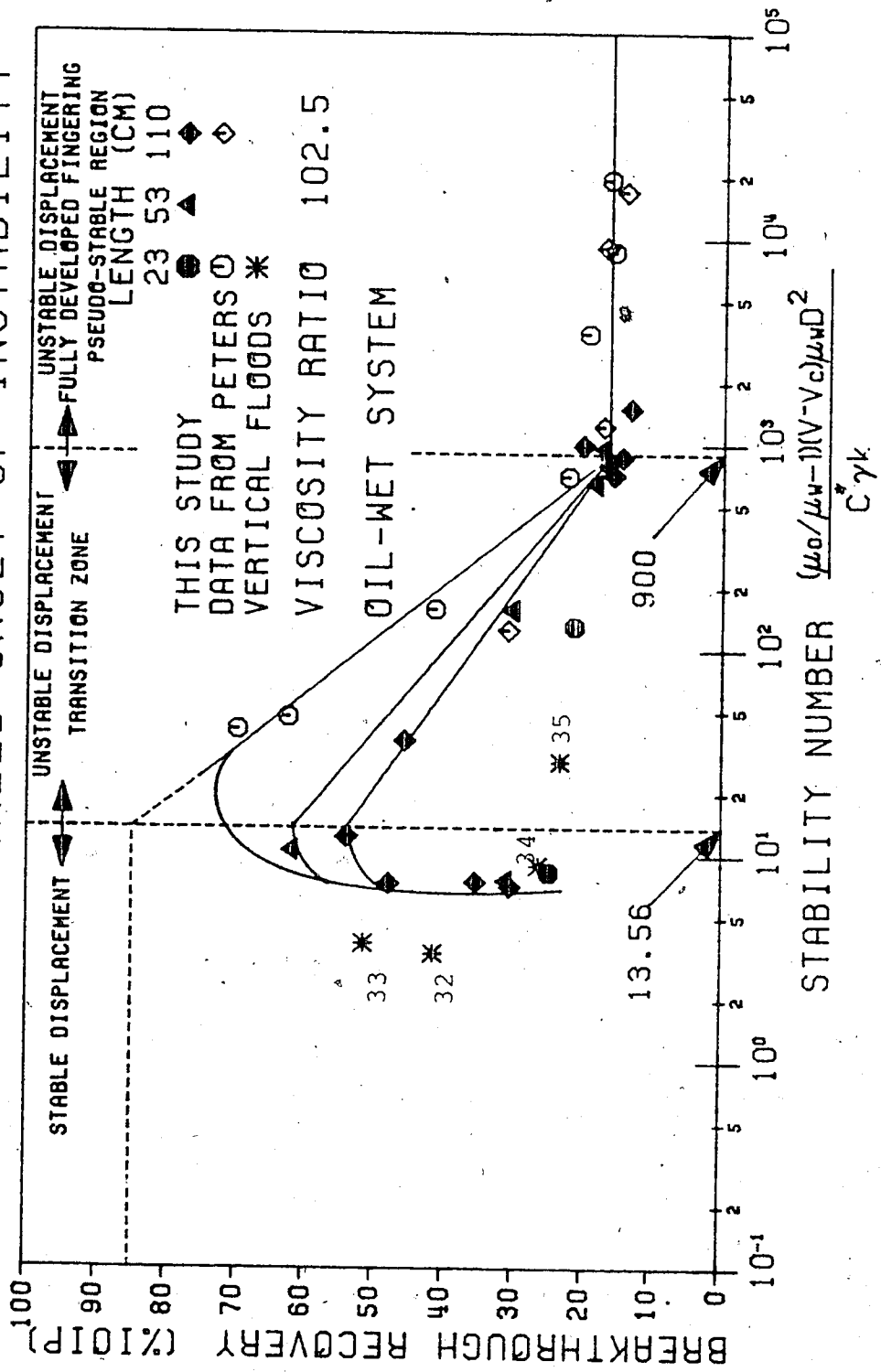
Figure 4.11 shows the scaled onset of instability for the oil-wet system studied. It was possible to extend the data base of Peters (1979) and obtain data in all three regions, as defined in the introductory comments of this section. The dashed portion of the curve indicates the 'expected' recovery as discussed in an earlier section. The vertical displacement results are also indicated.

According to the observations made in the water-wet system, all data should plot as one curve. However, the family of curves indicated in Figure 4.11 are a consequence of the effects of gravity override. It should be noted that the gravity effects are stronger in the longer length sandpacks. The effects of gravity are largest in the stable displacement region and lessen with increasing stability number (Note: increasing the stability number corresponds to increasing the superficial velocity).

At a stability number of 900, all data converge. It was mentioned in Chapter 2 that, as yet, there is no theory available to predict the onset of this pseudo-stable displacement region.

Beyond a stability number of 900, the recovery is independent of the stability number. Peters (1979) suggested that, in this region, the recovery should decline moderately. However, the additional data from this study indicates that the recovery is independent of the stability number in this region.

FIG. 4.11: SCALED ONSET OF INSTABILITY



5. Summary and Conclusions

The conclusions reached from this study may apply only to the particular geometry and fluid-rock system used here. A broad application of the results should be avoided until a more thorough investigation is undertaken.

A multi-dimensional modified inspectional analysis was undertaken in order to determine a set of similarity groups pertinent to the immiscible fluid displacement problem. The theoretical analysis led to the following conclusions.

1. The set of similarity groups which arise from a multi-dimensional modified inspectional analysis is:

$$\frac{\sigma K_{wr}}{V \mu_w L}, \quad \frac{K_{wr} \Delta \rho g}{V \mu_w}, \quad \frac{K_{wr} \mu_o}{K_{or} \mu_w}, \quad \frac{L}{D}$$

$$K_{rw}(S^*), \quad K_{ro}(S^*), \quad \pi_c(S^*)$$

for a cylindrical coordinate system. Similarly, in a Cartesian coordinate system, the following similarity groups arise:

$$\frac{\sigma K_{wr}}{V \mu_w L}, \quad \frac{K_{wr} \Delta \rho g}{V \mu_w}, \quad \frac{L_x}{L}, \quad \frac{L_y}{L}$$

$$\frac{K_{wr} \mu_o}{K_{or} \mu_w}, \quad K_{rw}(S^*), \quad K_{ro}(S^*), \quad \pi_c(S^*)$$

2. The analysis suggests that it may not be necessary to demand that the geometric factor be identical in both

the model and the prototype, provided that the displacement is stable.

As a prelude to the experimental verification of the theoretical findings above, the core packing procedure was investigated. It was concluded that the wet packing technique is effective in preparing sandpicks of predictable and consistent properties. It should also be mentioned that, as gained through experience, a complete series of tests should be arranged with sand from a particular lot shipment.

The experimental part of this study, with respect to the scaling of the displacement problem, led to the conclusions below.

1. Neither the linear nor the radial scaling groups are good correlating parameters beyond the point where viscous forces begin to dominate the displacement process. This conclusion is valid for both wettability types studied. Thus, a model may be compared to a prototype, provided the displacement is stable. Moreover, scaling the geometric factor is not important for such displacements.
2. Scaling groups, based on the assumption of a stable displacement, may not be valid if instabilities are present. However, they do provide useful information, if correctly interpreted.
3. Scaling the geometric factor is not important when a

displacement is completely dominated by viscous forces (pseudo-stable displacement).

4. The magnitude of the linear Leverett number should be of the order of 0.01, if the displacement is to be stabilized. Furthermore, 'stabilization' of the floodfront may be defined as that point where the recovery is within 5% of the steady-state recovery as predicted by Buckley-Leverett theory.
5. The interpretation of experimental data, obtained for the oil-wet system at low displacement rates, is complicated by the effects of gravity override, by frontal instability, and by a non-stabilized displacement.
6. The vertical displacements, conducted at low superficial velocities, revealed that the behaviour of the waterflood is extremely sensitive to any heterogeneities in the porous medium and to the 'boundary conditions' of the system.

The stability of the displacements was also investigated. The following conclusions were drawn.

1. Water-wet, residual water saturation system.
 - a. The onset of instability, as predicted by first-order perturbations theory, at $N_s = 13.56$, (Peters, 1979) was verified. Furthermore, the onset was independent of the geometric factor.
 - b. Due to experimental limitations, it was not possible

to obtain data in the pseudo-stable region, where the recovery is insensitive to viscous fingering.

- c. Displacement tests conducted at very small values of the stability number confirmed that the recovery was independent of this group.

2. Oil-wet, no residual water saturation system

- a. The recovery at the onset of instability was seen to be different for the various sandpack lengths considered. This was attributed to the effects of gravity override.
- b. The onset of a pseudo-stable region was determined experimentally to occur at a stability number of 900.
- c. The recovery is independent of the stability number and geometric factor in the pseudo-stable region.

Recommendations

The following recommendations to the experimental design of the equipment are suggested.

1. The determination of water arrival, instead of water breakthrough, should be attempted. This could be made possible by the use of a transparent end-cap, by the use of radioactive tracers, or by the use of microwaves.
2. A hydraulic ram should be constructed in order that the sandpacks may be extracted from the long coreholders. This would allow the capturing of viscous fingers on photographic film.
3. The displacing and displaced fluids should be of 'equal' densities in order to eliminate gravity override.

The following recommendations for further study are suggested.

1. Displacement tests should be conducted in rectangular sandpacks in order to verify that scaling the geometric factors (L_x/L , L_y/L) is not necessary for stable and pseudo-stable displacements.
2. A set of scaling groups should be derived by the method of modified inspectional analysis for a radial coordinate system. Verification of this set of scaling groups, with a reservoir, should be undertaken.
3. The stability of an oil-wet system, containing a residual water saturation, should be investigated.
4. There is a need to modify the stability theory in order

to be able to predict the onset of the pseudo-stable region. It is suggested that the investigation parallel the work of Bellman and Pennington (1954).

5. A series of tests should be conducted in the pseudo-stable displacement region for a water-wet system. This could be accomplished either by increasing the mobility ratio, or by decreasing the interfacial tension, one order of magnitude. These tests should include several geometric factors.

References Cited

- Baird, H.J. (1978), "Waterflood Behavior of Viscous Oils", M.Sc. Thesis, University of Alberta
- Bellman, R. and Pennington, R.H. (1954), "Effects of Surface Tension and Viscosity on Taylor Instability", Quart. Appl. Math., 12, 151-162
- Bentsen, R.G. (1976), "Scaled Fluid-Flow Models With Permeabilities Differing From That of the Prototype", Jour. Can. Pet. Tech., (July-September), 15, 46-52
- Bentsen, R.G. (1978), "Conditions Under Which The Capillary Term May Be Neglected", Jour. Can. Pet. Tech., (Oct-Dec), 17, 25-30
- Bentsen, R.G. and Anji, J. (1976), "A New Displacement Capillary Pressure Model", Jour. Can. Pet. Tech., (July-September), 15, 75-79
- Brown, H.W. (1951), "Capillary Pressure Investigations", Trans. AIME, 192, 67-74
- Buckingham, E. (1915), "Model Experiments and the Forms of Empirical Equations", Trans. ASME, 37, 263
- Buckley, S.E. and Leverett, M.C. (1942), "Mechanism of Fluid Displacements in Sands", Trans. AIME, 146, 107-116
- Chuoque, R.L., van Meurs, P. and van der Poel, C., (1959) "The Instability of Slow, Immiscible, Viscous Liquid-Liquid Displacements in Permeable Media", Trans. AIME, 216, 188-194
- Craig, F.F. (1971), "The Reservoir Engineering Aspects of Waterflooding", Monograph Volume 3, AIME, Henry L. Doherty Series
- van Daalen, F. and van Domselaar, H.R. (1972), "Scaled Fluid-Flow Models with Geometry Differing from that of Prototype", Trans. AIME, 253, 220-228
- Dietz, D.N. (1953), "A Theoretical Approach to the Problem of Encroaching and Bypassing Edgewater", Koninkl. Ned. Akad. Wetenschap. Proc., B56, 83
- Englebarts, W.F. and Klinkenberg, L.J., (1951), "Laboratory Experiments on the Displacement of Oil by Water from Packs of Granular Materials", Proc. Third World Petroleum Congress, Sec. II, 544-554

- Geertsma, J., Croes, G.A. and Schwarz, N. (1956), "Theory of Dimensionally Scaled Models of Petroleum Reservoirs", Trans. AIME, 207, 118-127
- Golaz, P. (1979), "A Study of the Centrifuge Method of Capillary Pressure Measurement", M.Sc. Thesis, University of Alberta
- Greenkorn, R.A. (1964), "Flow Models and Scaling Laws for Flow Through Porous Media", Ind. Eng. Chem., 56, 32-37
- de Haan, H.J. (1959), "Effect of Capillary Forces in the Water-Drive Process", Proc. Fifth World Petroleum Congress, Sec. II, Paper 25, 1-13
- Hagoort, J., (1974), "Displacement Stability of Water Drives in Water-Wet Connate-Water-Bearing Reservoirs", Soc. Pet. Eng. Jour., (February) 63-74
- Hawthorne, R.G. (1960), "Two-Phase Flow in Two-Dimensional Systems--Effects of Rate, Viscosity and Density on Fluid Displacement in Porous Media", Trans. AIME, 219, 81-87
- Hellums, J.D. and Churchill, S.W. (1961), "Dimensional Analysis and Natural Circulation", Chem. Eng. Prog. Symposium Ser., 57, 75-80
- Kloepfer, J.G. (1975), "Viscous Fingering in Unconsolidated Cores", M.Sc. Thesis, University of Alberta
- Kyte, J.R. and Rapoport, L.A. (1958), "Linear Waterflood Behavior and End Effects in Water-Wet Porous Media", Trans. AIME, 213, 423-426
- Langhaar, H.L. (1951), "Dimensional Analysis and Theory of Models", John Wiley and Sons, Inc., New York
- Leverett, M.C. (1941), "Capillary Behavior in Porous Solids", Trans. AIME, 142, 159-172
- Leverett, M.C., Lewis, W.B. and True, M.E. (1942), "Dimensional-Model Studies of Oil Field Behavior", Trans. AIME, 146, 175-193
- Loomis, A.G. and Crowell, D.C. (1964), "Theory and Application of Dimensional and Inspectional Analysis To Model Study of Fluid Displacements in Petroleum Reservoirs", U.S. Bureau of Mines, Report of Investigation 6546

- van Meurs, P. (1957), "The Use of a Transparent Three Dimensional Model for Studying the Mechanism of Flow Processes in Oil Reservoirs", Trans. AIME, 210, 295-301
- van Meurs, P. and van der Poel, C. (1958) "A Theoretical Description of Water-Drive Processes Involving Viscous Fingering", Trans. AIME, 213, 103-112
- Muskat, M. (1937), "Flow of Homogeneous Fluids Through Porous Media", McGraw-Hill Book Co., New York; J.W. Edwards Inc., Ann Arbor (1946)
- Outmans, H.D. (1962), "Nonlinear Theory for Frontal Stability and Viscous Fingering in Porous Media", SPEJ, 165-176
- Perkins, F.M., and Collins, R.E. (1960), "Scaling Laws For Laboratory Flow Models of Oil Reservoirs", Trans. AIME, 219, 383-385
- Perkins, T.K. and Johnston, O.C. (1969), "A Study of Immiscible Fingering in Linear Models", SPEJ, 9, 39-46
- Peters, E.J. (1979), "Stability Theory and Viscous Fingering in Porous Media", Ph.D. Thesis, University of Alberta
- Rachford, H.H. Jr. (1964), "Instability in Water Flooding Oil from Water-Wet Porous Media Containing Connate Water", SPEJ, 133-148
- Rapoport, L.A. (1955), "Scaling Laws for Use in Design and Operation of Water-Oil Flow Models", Trans. AIME, 204, 143-150
- Rapoport, L.A. and Leas, W.J. (1953), "Properties of Linear Waterfloods", Trans. AIME, 198, 139-148
- Rose, W. and Bruce, W.A. (1949), "Evaluation of Capillary Character in Petroleum Reservoir Rock", Trans. AIME, 186, 127-142
- Saeedi, J. (1979), "A Comparison of Theoretical and Experimental Saturation Profiles in Porous Media", M.Sc. Thesis, University of Alberta
- Wiborg, R. (1975), "Frontal Instabilities When Waterflooding at Unfavourable Viscosity Ratios", M.Sc. Thesis, University of Alberta

Selected Bibliography

- Bentsen, R.G. (1979), "Secondary Recovery", Graduate Lectures, University of Alberta
- Bentsen, R.G. and Saeedi, J. (1979), "Liquid-Liquid Immiscible Displacements in Unconsolidated Porous Media", Presented at the 30th Annual Technical Meeting of the Petroleum Society of CIM in Banff, Canada
- Birkhoff, G. (1960), "Hydrodynamics--A Study in Logic, Fact and Similitude", Princeton University Press, Princeton
- Bobek, J.E., Mattax, C.C., and Denekas, M.O. (1958), "Reservoir Rock Wettability--Its Significance and Evaluation", Trans. AIME, 213, 155-160
- Collins, R.E. (1961), "Flow of Fluids Through Porous Materials", Reinhold Publishing Corp., New York
- Croes, G.A. and Schwarz, N. (1955), "Dimensionally Scaled Experiments and the Theories on the Water-Drive Process", Trans. AIME, 204, 35-42
- Duncan, W.J. (1953), "Physical Similarity and Dimensional Analysis", Edward Arnold and Co., London
- Fayers, F.J. and Sheldon, J.W. (1951), "The Effect of Capillary Pressure and Gravity on Two-Phase Fluid Flow in a Porous Medium", Trans. AIME, 216, 147-155
- Flock, D.L., Peters, E.J., Baird, H., Wiborg, R. and Kloefer, J. (1977), "The Influence of Frontal Instabilities During Viscous Oil Displacement", The Oil Sands of Canada-Venezuela, CIM Special Vol. 17, 380-385
- Focken, C.M. (1953), "Dimensional Methods and Their Applications", Edward Arnold and Co., London
- Hellums, J.D. and Churchill, S.W. (1964), "Simplification of the Mathematical Description of Boundary and Initial Value Problems", A.I.Ch.E. Jour., 10, 110-114
- Ipsen, D.C. (1960), "Units, Dimensions, and Dimensionless Numbers", McGraw-Hill Book Co., New York
- Jones-Parra, J., Stahl, C.D., and Calhoun, J.C. (1954), "A Theoretical and Experimental Study Of Constant Rate Displacements In Water Wet Systems", Producers Monthly, (January), 18-26

Nielsen, R.L. and Tek, M.R. (1963), "Evaluation of Scale-Up Laws for Two-Phase Flow Through Porous Media", SPEJ, (June)

Outmans, H.D. (1962), "Transient Interfaces During Immiscible Liquid-Liquid Displacement in Porous Media", SPEJ, 156-164

Peters, E.J. and Flock, D.L. (1979), "The Onset of Instabilities During Two-Phase Immiscible Displacement in Porous Media", Presented at the 54th Annual Fall Technical Conference of SPE of AIME

Scheidegger, A.E. (1974), "The Physics of Flow Through Porous Media", 3rd Edition, University of Toronto Press

Smith, C.R. (1966), "Mechanics of Secondary Oil Recovery", Reinhold Publishing Corporation, New York

Appendix A--Derivations

A.1 Derivation of Equation 2.16

Restating Equations 2.1 to 2.4 and 2.6:

$$\vec{v}_w = - \frac{K_w(S_w)}{\mu_w} (\text{grad } P_w - \rho_w \vec{g}) \quad \text{A.1.1}$$

$$\vec{v}_o = - \frac{K_o(S_w)}{\mu_o} (\text{grad } P_o - \rho_o \vec{g}) \quad \text{A.1.2}$$

$$\text{div } \vec{v}_w = - \phi \frac{\partial S_w}{\partial t} \quad \text{A.1.3}$$

$$\text{div } \vec{v}_o = - \phi \frac{\partial S_o}{\partial t} \quad \text{A.1.4}$$

$$P_c(S_w) = P_o - P_w \quad \text{A.1.5}$$

Equations A.1.1 and A.1.2 may be rearranged to:

$$-\frac{\vec{v}_w}{K_w(S_w)/\mu_w} = \text{grad } P_w - \rho_w \vec{g} \quad \text{A.1.6}$$

$$-\frac{\vec{v}_o}{K_o(S_w)/\mu_o} = \text{grad } P_o - \rho_o \vec{g} \quad \text{A.1.7}$$

Subtracting Equation A.1.6 from A.1.7 results in:

$$\frac{\vec{v}_w}{K_w(S_w)/\mu_w} - \frac{\vec{v}_o}{K_o(S_w)/\mu_o} = \text{grad } P_o - \text{grad } P_w + \rho_o \vec{g} - \rho_w \vec{g} \quad \text{A.1.8}$$

Defining

$$\Delta\rho \equiv \rho_w - \rho_o \quad \text{A.1.9}$$

and recalling that

$$\text{grad } P_c(S_w) = \text{grad } P_o - \text{grad } P_w \quad \text{A.1.10}$$

Equation A.1.8 becomes:

$$\frac{\vec{v}_w}{K_w(S_w)/\mu_w} - \frac{\vec{v}_o}{K_o(S_w)/\mu_o} = \text{grad } P_c(S_w) - \Delta\rho\vec{g} \quad \text{A.1.11}$$

Because the fluids are incompressible and immiscible then:

$$\vec{v} = \vec{v}_w + \vec{v}_o \quad \text{A.1.12}$$

Using this relation, Equation A.1.10 may be written as:

$$\begin{aligned} \vec{v}_w \left[\frac{1}{K_w(S_w)/\mu_w} + \frac{1}{K_o(S_w)/\mu_o} \right] \\ = \text{grad } P_c(S_w) - \Delta\rho\vec{g} + \frac{\vec{v}}{K_o(S_w)/\mu_o} \end{aligned} \quad \text{A.1.13}$$

Defining

$$\begin{aligned} F_w(S_w) &\equiv \frac{K_w(S_w)/\mu_w}{K_w(S_w)/\mu_w + K_o(S_w)/\mu_o} \\ &= \left(1 + \frac{K_o(S_w)}{K_w(S_w)} \frac{\mu_w}{\mu_o} \right)^{-1} \end{aligned} \quad \text{A.1.14}$$

then

$$\vec{v}_w = F_w(S_w) \frac{K_o(S_w)}{\mu_o} \text{grad } P_c(S_w) - F_w(S_w) \frac{K_o(S_w)}{\mu_o} \Delta \rho \vec{g} \quad \text{A.1.15}$$

Substituting the above into Equation A.1.3 results in:

$$\begin{aligned} \text{div} \left(F_w(S_w) \frac{K_o(S_w)}{\mu_o} \text{grad } P_c(S_w) \right) - \text{div} \left(F_w(S_w) \frac{K_o(S_w)}{\mu_o} \Delta \rho \vec{g} \right) \\ + \text{div} \left(F_w(S_w) \vec{v} \right) + \phi \frac{\partial S_w}{\partial t} = 0 \end{aligned} \quad \text{A.1.16}$$

From vector calculus:

$$\text{div} \left(F_w(S_w) \vec{v} \right) = F_w(S_w) \text{div } \vec{v} + \text{grad } F_w(S_w) \cdot \vec{v} \quad \text{A.1.17}$$

Addition of Equations A.1.3 and A.1.4 and noting that:

$$S_w + S_o = 1 \quad \text{A.1.18}$$

shows that

$$\text{div } \vec{v} = 0 \quad \text{A.1.19}$$

Hence Equation A.1.16 results in:

$$\begin{aligned} \text{div} \left(F_w(S_w) \frac{K_o(S_w)}{\mu_o} \text{grad } P_c(S_w) \right) - \text{div} \left(F_w(S_w) \frac{K_o(S_w)}{\mu_o} \Delta \rho \vec{g} \right) \\ + \vec{v} \cdot \text{grad } F_w(S_w) + \phi \frac{\partial S_w}{\partial t} = 0 \end{aligned} \quad \text{A.1.20}$$

Applying the chain rule to the partial derivatives yields:

$$\text{grad } P_c(S_w) = \frac{dP_c(S_w)}{dS_w} \text{ grad } S_w \quad \text{A.1.21}$$

and

$$\text{grad } F_w(S_w) = \frac{dF_w(S_w)}{dS_w} \text{ grad } S_w \quad \text{A.1.22}$$

Then, Equation A.1.20 may be written as:

$$\begin{aligned} \text{div} \left(F_w(S_w) \frac{K_o(S_w)}{\mu_o} \frac{dP_c(S_w)}{dS_w} \text{ grad } S_w \right) - \text{div} \left(F_w(S_w) \frac{K_o(S_w)}{\mu_o} \Delta \rho \vec{g} \right) \\ + \vec{v} \cdot \frac{dF_w(S_w)}{dS_w} \text{ grad } S_w + \phi \frac{\partial S_w}{\partial t} = 0 \quad \text{A.1.23} \end{aligned}$$

Finally, the introduction of relative and base permeabilities yields the desired result:

$$\begin{aligned} \frac{K_{ob}}{\mu_o} \text{div} \left(F_w(S_w) K_{ro}(S_w) \frac{dP_c(S_w)}{dS_w} \text{ grad } S_w \right) \\ - \frac{K_{ob}}{\mu_o} \text{div} \left(F_w(S_w) K_{ro}(S_w) \Delta \rho \vec{g} \right) \\ + \vec{v} \cdot \frac{dF_w(S_w)}{dS_w} \text{ grad } S_w + \phi \frac{\partial S_w}{\partial t} = 0 \quad \text{A.1.24} \end{aligned}$$

A.2 Derivations of Scaling Groups

The following section presents the details of the derivation of the scaling groups by the methods mentioned in Chapter 2.

A.2.1 Dimensional Analysis

Loomis and Crowell (1964) and Greenkorn (1964) presented a dimensional-analysis approach to determine the scaling groups for immiscible flow, and miscible flow with heat transfer, respectively. The former, however, omitted time in the analysis.

Presented below is a derivation of the scaling groups for the immiscible fluid displacement problem. The derivation follows closely the report of Loomis and Crowell (1964), except for a few small modifications tailored to the definitions of capillary pressure and relative permeability adopted in this study.

The variables which control the displacement process are:

- 1) Geometric:
 - a) length of the system
 - b) thickness of the system or diameter
 - c) angle of dip
- 2) Sand properties:
 - a) permeability to oil at residual water saturation

- b) permeability to water at residual oil saturation
- c) porosity
- 3) Fluid Properties:
 - a) water viscosity
 - b) oil viscosity
 - c) water density
 - d) oil density
 - e) capillary pressure normalizing parameter
- 4) Others:
 - a) time
 - b) gravity
 - c) superficial velocity

Upon neglecting inertial forces, the variables ρ_w , ρ_o , and g occur only in the combination $\Delta\rho g$, where:

$$\Delta\rho = \rho_w - \rho_o \quad \text{A.2.1}$$

The functional relationship of these variables may be written in the following implicit form:

$$f(L, h, \alpha, K_{or}, K_{wr}, \phi, \mu_w, \mu_o, \Delta\rho g, \sigma, V, t) = 0 \quad \text{A.2.2}$$

Applying the principle of dimensional homogeneity results in:

$$m^0 L^0 t^0 \frac{d}{d} L^{a_1} h^{a_2} \alpha^0 K_{or}^{a_3} K_{wr}^{a_4} \phi^0 \mu_w^{a_5} \mu_o^{a_6} (\Delta\rho g)^{a_7} \sigma^{a_8} V^{a_9} t^{a_{10}} \quad \text{A.2.3}$$

where $a_1, a_2, a_3, \dots, a_{10}$ are arbitrary constants.

Introducing the dimensions of the variables into the above equation yields:

$$m^0 \ell^0 t^0 \stackrel{d}{=} \ell^{a_1} \ell^{a_2} \ell^{2a_3} \ell^{2a_4} (m \ell^{-1} t^{-1})^{a_5} (m \ell^{-1} t^{-1})^{a_6} \\ (m \ell^{-2} t^{-2})^{a_7} (m \ell^{-1} t^{-2})^{a_8} (\ell t^{-1})^{a_9} t^{a_{10}} \quad \text{A.2.4}$$

$$\stackrel{d}{=} m^{(a_5 + a_6 + a_7 + a_8)} \ell^{(a_1 + a_2 + 2a_3 + 2a_4 - a_5 - a_6 - 2a_7 - a_8 + a_9)} \\ t^{(-a_5 - a_6 - 2a_7 - a_9 + a_{10})} \quad \text{A.2.5}$$

Equating co-efficients of $m, \ell,$ and t results in:

$$a_5 + a_6 + a_7 + a_8 = 0 \quad \text{A.2.6}$$

$$a_1 + a_2 + 2a_3 + 2a_4 - a_5 - a_6 - 2a_7 - a_8 + a_9 = 0 \quad \text{A.2.7}$$

$$-a_5 - a_6 - 2a_7 - a_9 + a_{10} = 0 \quad \text{A.2.8}$$

It must be established that the above set of equations is independent in order to determine the minimum number of pi-terms. In matrix form, Equations A.2.6 to A.2.8 may be written as:

$$\begin{pmatrix} 0 & 0 & 0 & 0 & 1 & 1 & 1 & 1 & 0 & 0 \\ 1 & 1 & 2 & 2 & -1 & -1 & -2 & -1 & 1 & 0 \\ 0 & 0 & 0 & 0 & -1 & -1 & -2 & -2 & -1 & 1 \end{pmatrix} \begin{pmatrix} a_1 \\ a_2 \\ \vdots \\ a_{10} \end{pmatrix} = \begin{pmatrix} 0 \\ 0 \\ \vdots \\ 0 \end{pmatrix} \quad \text{A.2.9}$$

A theorem from matrix algebra (Langhaar, 1951) states that the number of independent equations will be equal to the order of the highest order determinant of the matrix which is different from zero. The value of the determinant may be positive or negative.

The highest order of the determinant for the above co-efficient matrix is 3. It may be shown that it is possible to write the 3-d determinant which has a non-zero value. Thus, from Buckingham's (1915) pi-theorem, the minimum number of pi-terms is (the number of variables, 12; less the number of independent equations, 3) 9.

A possible solution to the above system of equations, expressing three of the co-efficients in terms of the others, is:

$$a_1 = -2a_2 - 2a_3 - 2a_4 + a_7 - a_9 \quad \text{A.2.10}$$

$$a_5 = -a_6 - a_7 - a_8 \quad \text{A.2.11}$$

$$a_{10} = a_7 + a_8 + a_9 \quad \text{A.2.12}$$

Substituting into Equation A.2.3 results in:

$$m^0 l^0 t^0 \underline{d} L^{(-a_2-2a_3-2a_4+a_7-a_9)} h^{a_2} \alpha^0 K_{or}^{a_3} K_{wr}^{a_4} \phi^0$$

$$\mu_w^{(-a_5-a_7-a_8)} \mu_o^{a_6} (\Delta\rho g)^{a_7} \sigma^{a_8}$$

$$v^{a_9} t^{(a_7+a_8+a_9)}$$

A.2.13

which upon rearranging yields:

$$m^0 l^0 t^0 \underline{d} (L^{-1}h)^{a_2} (L^{-2}K_{or})^{a_3} (L^{-2}K_{wr})^{a_4} (\mu_w^{-1}\mu_o)^{a_6}$$

$$(L\mu_w^{-1}\Delta\rho g t)^{a_7} (\mu_w^{-1}\sigma t)^{a_8} (L^{-1}vt)^{a_9} \alpha^0 \phi^0$$

A.2.14

From Equation A.2.14 arise the following pi-terms:

$$\pi_1 = \frac{h}{L}$$

A.2.15

$$\pi_2 = \frac{K_{or}}{L^2}$$

A.2.16

$$\pi_3 = \frac{K_{wr}}{L^2}$$

A.2.17

$$\pi_4 = \frac{\mu_o}{\mu_w}$$

A.2.18

$$\pi_5 = \frac{L\Delta\rho g t}{\mu_w}$$

A.2.19

$$\pi_6 = \frac{\sigma t}{\mu_w}$$

A.2.20

$$\pi_7 = \frac{Vt}{L} \quad \text{A.2.21}$$

$$\pi_8 = \alpha \quad \text{A.2.22}$$

$$\pi_9 = \phi \quad \text{A.2.23}$$

The foregoing pi-terms may be brought to the form below because it is permissible to multiply, divide or invert these terms, provided that a complete set of pi-terms contains every variable at least once, thus:

$$\pi_1 = \frac{L}{h} \quad \text{A.2.24}$$

$$\pi_2 = \frac{K_{or}}{L^2} \quad \text{A.2.25}$$

$$\pi_3 = \frac{K_{wr}}{L^2} \quad \text{A.2.26}$$

$$\pi_4 = \frac{K_{wr} \mu_o}{K_{or} \mu_w} \quad \text{A.2.27}$$

$$\pi_5 = \frac{K_{wr} \Delta \rho g}{V \mu_w} \quad \text{A.2.28}$$

$$\pi_6 = \frac{K_{wr} \sigma}{V \mu_w L} \quad \text{A.2.29}$$

$$\pi_7 = \frac{Vt}{\phi L} \quad \text{A.2.30}$$

$$\pi_8 = \alpha \quad \text{A.2.31}$$

$$\pi_9 = \phi \quad \text{A.2.32}$$

A.2.2 Inspectional Analysis

The equations describing the fluid displacement problem, as given by Equations 2.1 to 2.6, may be combined (see Appendix A.1) to yield:

$$\begin{aligned} & \frac{K_{ob}}{\mu_o} \operatorname{div} \left[F_w(S_w) K_{ro}(S_w) \frac{dP_c(S_w)}{dS_w} \operatorname{grad} S_w \right] \\ & - \frac{K_{ob}}{\mu_o} \operatorname{div} \left[F_w(S_w) K_{ro}(S_w) \Delta \rho \vec{g} \right] \\ & + \vec{v} \cdot \frac{dF_w(S_w)}{dS_w} \operatorname{grad} S_w + \phi \frac{\partial S_w}{\partial t} = 0 \end{aligned} \quad \text{A.2.33}$$

Upon substituting the following capillary pressure model (Bentsen and Anli, 1976);

$$P_c(S_w) = \sigma \pi_c(S^*) + P_d \quad \text{A.2.34}$$

and using the end-point relative permeability definitions as a function of normalized water saturation:

$$K_{rw}(S^*) = \frac{K_w(S^*)}{K_{wr}} \quad \text{A.2.35}$$

$$K_{ro}(S^*) = \frac{K_o(S^*)}{K_{or}} \quad \text{A.2.36}$$

Equation A.2.33 becomes:

$$\begin{aligned} & \frac{\sigma K_{or}}{\mu_0} \operatorname{div} \left[F_w(S^*) K_{ro}(S^*) \frac{d\pi_c(S^*)}{dS^*} \operatorname{grad} S^* \right] \\ & - \frac{K_{or}}{\mu_0} \operatorname{div} \left[F_w(S^*) K_{ro}(S^*) \Delta \rho \vec{g} \right] \\ & + \vec{v} \cdot \frac{dF_w(S^*)}{dS^*} \operatorname{grad} S^* + \phi \frac{\partial S^*}{\partial t} = 0 \end{aligned} \quad \text{A.2.37}$$

Expanding Equation A.2.37 in cylindrical coordinates (r, x, β) and retaining the gravity term results in:

$$\begin{aligned} & \frac{\sigma K_{or}}{\mu_0} \left\{ \frac{1}{r} \frac{\partial}{\partial r} \left[r F_w(S^*) K_{ro}(S^*) \frac{d\pi_c(S^*)}{dS^*} \frac{\partial S^*}{\partial r} \right] \right. \\ & + \frac{1}{r^2} \frac{\partial}{\partial \beta} \left[F_w(S^*) K_{ro}(S^*) \frac{d\pi_c(S^*)}{dS^*} \frac{\partial S^*}{\partial \beta} \right] + \frac{\partial}{\partial x} \left[F_w(S^*) K_{ro}(S^*) \frac{d\pi_c(S^*)}{dS^*} \frac{\partial S^*}{\partial x} \right] \left. \right\} \\ & - \frac{\Delta \rho \vec{g} K_{or}}{\mu_0} \left\{ \frac{1}{r} \frac{\partial}{\partial r} \left[r F_w(S^*) K_{ro}(S^*) \right] + \frac{1}{r^2} \frac{\partial}{\partial \beta} \left[F_w(S^*) K_{ro}(S^*) \right] \right. \\ & + \frac{\partial}{\partial x} \left[F_w(S^*) K_{ro}(S^*) \right] \left. \right\} + \phi \frac{\partial S^*}{\partial t} \\ & + \left[v_r \frac{\partial S^*}{\partial r} + \frac{v_\beta}{r} \frac{\partial S^*}{\partial \beta} + v_x \frac{\partial S^*}{\partial x} \right] \frac{dF_w(S^*)}{dS^*} = 0 \end{aligned} \quad \text{A.2.38}$$

The next step in an inspectional analysis is to define certain dimensionless variables. After the manner of Perkins and Collins (1960):

$$\phi \equiv \frac{r}{a} \quad \text{A.2.39}$$

$$\xi \equiv \frac{x}{L} \quad \text{A.2.40}$$

$$\vec{f} \equiv \frac{\vec{v}}{|\vec{v}|} \quad \text{A.2.41}$$

$$\tau \equiv \frac{|\vec{v}| t}{\phi L (1 - S_{or} - S_{wi})} \quad \text{A.2.42}$$

and

$$S^* \equiv \frac{S_w - S_{wi}}{1 - S_{or} - S_{wi}} \quad \text{A.2.43}$$

Substitution of Equations A.2.39 to A.2.43 into Equation A.2.38 yields:

$$\begin{aligned} & \frac{\sigma K_{or}}{\mu_o} \left\{ \frac{1}{a^2 \psi} \frac{\partial}{\partial \psi} \left[\psi F_w(S^*) K_{ro}(S^*) \frac{d\pi_c(S^*)}{dS^*} \frac{\partial S^*}{\partial \psi} \right] \right. \\ & \quad + \frac{1}{a^2 \psi^2} \frac{\partial}{\partial \beta} \left[F_w(S^*) K_{ro}(S^*) \frac{d\pi_c(S^*)}{dS^*} \frac{\partial S^*}{\partial \beta} \right] \\ & \quad \left. + \frac{1}{L^2} \frac{\partial}{\partial \xi} \left[F_w(S^*) K_{ro}(S^*) \frac{d\pi_c(S^*)}{dS^*} \frac{\partial S^*}{\partial \xi} \right] \right\} \\ & - \frac{\Delta \rho K_{or}}{\mu_o} \left\{ \frac{1}{a \psi} \frac{\partial}{\partial \psi} \left[\psi F_w(S^*) K_{ro}(S^*) |\vec{g}| \cos \alpha \right] \right. \\ & \quad \left. + \frac{1}{L} \frac{\partial}{\partial \psi} \left[F_w(S^*) K_{ro}(S^*) |\vec{g}| \sin \alpha \right] \right\} \\ & + \left\{ \frac{|\vec{v}| f_\psi}{a} \frac{\partial S^*}{\partial \psi} + \frac{|\vec{v}| f_\beta}{a} \frac{1}{\psi} \frac{\partial S^*}{\partial \beta} + \frac{|\vec{v}| f_\xi}{L} \frac{\partial S^*}{\partial \xi} \right\} \frac{dF_w(S^*)}{dS^*} \\ & + \frac{|\vec{v}|}{L} \frac{\partial S^*}{\partial \tau} = 0 \quad \text{A.2.44} \end{aligned}$$

The above equation may be rearranged as:

$$\begin{aligned}
 & \left(\frac{\sigma K_{wr}}{|\vec{v}| \mu_w D} \right) \left(\frac{L}{D} \right) \left(\frac{K_{or} \mu_w}{K_{wr} \mu_o} \right) \left\{ \frac{4}{\psi} \frac{\partial}{\partial \psi} \left[\psi F_w(S^*) K_{ro}(S^*) \frac{d\pi_c(S^*)}{dS^*} \frac{\partial S^*}{\partial \psi} \right] \right. \\
 & \quad \left. + \frac{4}{\psi^2} \frac{\partial}{\partial \beta} \left[F_w(S^*) K_{ro}(S^*) \frac{d\pi_c(S^*)}{dS^*} \frac{\partial S^*}{\partial \beta} \right] \right\} \\
 & + \left(\frac{\sigma K_{wr}}{|\vec{v}| \mu_w L} \right) \left(\frac{K_{or} \mu_w}{K_{wr} \mu_o} \right) \left\{ \frac{\partial}{\partial \xi} \left[F_w(S^*) K_{ro}(S^*) \frac{d\pi_c(S^*)}{dS^*} \frac{\partial S^*}{\partial \xi} \right] \right\} \\
 & - \left(\frac{K_{wr} \Delta p |\vec{g}| \cos \alpha}{|\vec{v}| \mu_w} \right) \left(\frac{K_{or} \mu_w}{K_{wr} \mu_o} \right) \left(\frac{L}{D} \right) \left\{ \frac{2}{\psi} \frac{\partial}{\partial \psi} \left[\psi F_w(S^*) K_{ro}(S^*) \right] \right\} \\
 & + \left(\frac{L}{D} \right) \left\{ 2 f_\psi \frac{\partial S^*}{\partial \psi} + \frac{2f_\beta}{\psi} \frac{\partial S^*}{\partial \beta} \right\} \frac{dF_w(S^*)}{dS^*} \\
 & + f_\xi \frac{\partial S^*}{\partial \xi} \frac{dF_w(S^*)}{dS^*} + \frac{\partial S^*}{\partial \tau} = 0
 \end{aligned} \tag{A.2.45}$$

From the dimensionless equation above, the dimensionless groups which arise are:

1) Independent dimensionless variables

$$\psi, \xi, \beta, \tau$$

2) Dependent dimensionless variables

$$S^*, f_\psi, f_\beta, f_\xi$$

3) Independent constant or similarity groups

$$\frac{\sigma K_{wr}}{|\vec{v}| \mu_w D}, \frac{\sigma K_{wr}}{|\vec{v}| \mu_w L}, \frac{L}{D}, \frac{K_{or} \mu_w}{K_{wr} \mu_o}, \frac{K_{wr} \Delta \rho \vec{g}}{|\vec{v}| \mu_w},$$

$$K_{rw}(S^*), K_{ro}(S^*), \pi_c(S^*)$$

A similar analysis, using the Leverett J-function to represent the capillary pressure, results in the following similarity groups:

$$\frac{\gamma \sqrt{K\phi}}{|\vec{v}| \mu_w D}, \frac{\gamma \sqrt{K\phi}}{|\vec{v}| \mu_w L}, \frac{L}{D}, \frac{K_{or} \mu_w}{K_{wr} \mu_o}, \frac{K_{wr} \Delta \rho \vec{g}}{|\vec{v}| \mu_w},$$

$$K_{rw}(S^*), K_{ro}(S^*), J(S^*)$$

A.2.3 Modified Inspectional Analysis

Restating Equations 2.20 and 2.21

$$\vec{f}_w = \frac{F_w(S_w)}{|\vec{v}|} \frac{K_{ob}}{\mu_o} K_{ro}(S_w) \frac{dP_c(S_w)}{dS_w} \text{grad } S_w$$

$$- \frac{F_w(S_w)}{|\vec{v}|} \frac{K_{ob}}{\mu_o} K_{ro}(S_w) \Delta \rho \vec{g} + F_w(S_w) \frac{\vec{v}}{|\vec{v}|} \quad \text{A.2.46}$$

$$\text{div } \vec{f}_w = - \frac{\phi}{|\vec{v}|} \frac{\partial S_w}{\partial t} \quad \text{A.2.47}$$

To complete the description of the fluid displacement problem, an appropriate set of initial and boundary conditions is required.

- 1) $S_w = S_{wi}$ $|\vec{f}_w| = 0$
- 2) $S_w = 1 - S_{or}$ $|\vec{f}_w| = 1$
- 3) $0 < S_w < 1$ $|\vec{f}_w| = 1, t = 0$

Condition 1 states that initially, throughout the sandpack, a residual water saturation equal to S_{wi} exists; condition 2 implies that the porous medium is flooded out to a residual oil saturation; and finally, condition 3 represents a 'jump discontinuity' in the fractional flow at the inlet.

This completes the description of the problem. For each variable in the problem, a dimensionless variable may be constructed by dividing the original variable by some arbitrary reference quantity of the same dimensions, viz:

$$\zeta \equiv \frac{x}{x_0} \quad \text{A.2.48}$$

$$\phi \equiv \frac{r}{r_0} \quad \text{A.2.49}$$

$$\epsilon \equiv \frac{\beta}{\beta_0} \quad \text{A.2.50}$$

$$T \equiv \frac{t}{t_0} \quad \text{A.2.51}$$

$$S^* \equiv \frac{S_w - A_0}{B_0} \quad \text{A.2.52}$$

where x_0 , r_0 , β_0 , t_0 , A_0 , and B_0 are arbitrary reference quantities. Equations A.2.48 to A.2.52 are then substituted into the fluid displacement equations, initial and boundary conditions. Consider first the conditions:

$$S_w = S^* B_0 + A_0 = S_{wi} \quad |\vec{f}_w| = 0 \quad \text{A.2.53}$$

or

$$S^* = \frac{S_{wi} - A_0}{B_0} \quad |\vec{f}_w| = 0 \quad \text{A.2.54}$$

Also,

$$S_w = S^* B_0 + A_0 = 1 - S_{or} \quad |\vec{f}_w| = 1 \quad \text{A.2.55}$$

Hence

$$S^* = \frac{1 - S_{or} - A_0}{B_0} \quad |\vec{f}_w| = 1 \quad \text{A.2.56}$$

Now for $|\vec{f}_w| = 0$, $S^* = 0$; and from Equation A.2.54

$$A_0 = S_{wi} \quad \text{A.2.57}$$

Also for $|\vec{f}_w| = 1$, $S^* = 1$; and from Equation A.2.56

$$B_0 = 1 - S_{or} - S_{wi} \quad \text{A.2.58}$$

The same may be done for Equations A.2.46 and A.2.47; but, before proceeding, a dimensionless form of the gradient and divergence must be examined. Recall that in a cylindrical coordinate system:

$$\text{grad } h \equiv \left(\frac{\partial}{\partial r} \hat{i} + \frac{1}{r} \frac{\partial}{\partial \beta} \hat{j} + \frac{\partial}{\partial x} \hat{k} \right) h \quad \text{A.2.59}$$

and

$$\text{div } \vec{\ell} \equiv \frac{1}{r} \left(\frac{\partial}{\partial r} r \ell_r + \frac{\partial}{\partial \beta} \ell_\beta + r \frac{\partial}{\partial x} \ell_x \right) \quad \text{A.2.60}$$

Upon substituting for the variables defined by Equations A.2.48 to A.2.50, Equations A.2.59 and A.2.60 become:

$$\text{grad } h = \frac{1}{r_0} \left(\frac{\partial}{\partial \phi} \hat{\phi} + \frac{1}{r_0 \beta_0 \phi} \frac{\partial}{\partial \epsilon} \hat{\epsilon} + \frac{1}{x_0} \frac{\partial}{\partial \zeta} \hat{\zeta} \right) h \quad \text{A.2.61}$$

and

$$\text{div } \vec{\ell} = \frac{1}{r_0 \phi} \left[\frac{\partial}{\partial \phi} (\phi \ell_\phi) + \frac{1}{\beta_0} \frac{\partial}{\partial \epsilon} \ell_\epsilon + \frac{r_0 \phi}{x_0} \frac{\partial}{\partial \zeta} \ell_\zeta \right] \quad \text{A.2.62}$$

Recall Equation 2.24:

$$P_c(S^*) = \sigma \pi_c(S^*) + P_d \quad \diamond \quad \text{A.2.63}$$

to be used below.

Equations A.2.46 and A.2.47 may now be written in the following form:

$$\begin{aligned} \vec{f}_w = & \frac{F_w(S^*)}{|\vec{v}|} \frac{K_{or}}{\mu_0} K_{ro}(S^*) \sigma \frac{d\pi_c(S^*)}{dS^*} \left[\frac{1}{r_0} \frac{\partial S^*}{\partial \phi} \hat{\phi} \right. \\ & \left. + \frac{1}{r_0 B_0 \phi} \frac{\partial S^*}{\partial \epsilon} \hat{\epsilon} + \frac{1}{x_0} \frac{\partial S^*}{\partial \zeta} \hat{\zeta} \right] \\ & - \frac{F_w(S^*)}{|\vec{v}|} \frac{K_{or}}{\mu_0} K_{ro}(S^*) \Delta \rho \vec{g} + F_w(S^*) \frac{\vec{v}}{|\vec{v}|} \end{aligned} \quad \text{A.2.64}$$

and

$$\begin{aligned} \frac{1}{r_0 \phi} \left[\frac{\partial}{\partial \phi} (\phi f_{w\phi}) + \frac{1}{\beta_0} \frac{\partial f_{w\epsilon}}{\partial \epsilon} + \frac{r_0 \phi}{x_0} \frac{\partial f_{w\zeta}}{\partial \zeta} \right] \\ = - \frac{\phi B_0}{|\vec{v}| t_0} \frac{\partial S^*}{\partial T} \end{aligned} \quad \text{A.2.65}$$

Rearranging the above equations leads to:

$$\begin{aligned} \vec{f}_w = & F_w(S^*) K_{ro}(S^*) \frac{d\pi_c(S^*)}{dS^*} \left[\frac{\sigma K_{or}}{|\vec{v}| \mu_0 r_0} \frac{\partial S^*}{\partial \phi} \hat{\phi} \right. \\ & \left. + \frac{\sigma K_{or}}{|\vec{v}| \mu_0 r_0 \beta_0} \frac{1}{\phi} \frac{\partial S^*}{\partial \epsilon} \hat{\epsilon} + \frac{\sigma K_{or}}{|\vec{v}| \mu_0 x_0} \frac{\partial S^*}{\partial \zeta} \hat{\zeta} \right] \\ & + \left[\frac{\vec{v}}{|\vec{v}|} - \frac{K_{or} \Delta \rho \vec{g}}{|\vec{v}| \mu_0} K_{ro}(S^*) \right] F_w(S^*) \end{aligned} \quad \text{A.2.66}$$

and

$$\begin{aligned} \frac{|\vec{v}|t_0}{\phi B_0 r_0} \frac{1}{\phi} \frac{\partial}{\partial \phi} (\phi f_{w\phi}) + \frac{|\vec{v}|t_0}{\phi B_0 r_0 \beta_0} \frac{1}{\phi} \frac{\partial f_{w\epsilon}}{\partial \epsilon} + \frac{|\vec{v}|t_0}{\phi B_0 x_0} \frac{\partial f_{w\zeta}}{\partial \zeta} \\ = - \frac{\partial S^*}{\partial T} \end{aligned} \quad \text{A.2.67}$$

In the above two equations, the parameters and reference quantities have been grouped together to yield a description of the problem in terms of dimensionless variables. These dimensionless groups may then be equated to unity to form a set of algebraic equations. These algebraic equations may then be solved to determine the reference quantities, viz:

$$\frac{\sigma K_{or}}{|\vec{v}|_{\mu_0} r_0} = 1 \quad \text{hence } r_0 = \frac{\sigma K_{or}}{|\vec{v}|_{\mu_0}} \quad \text{A.2.68}$$

$$\frac{\sigma K_{or}}{|\vec{v}|_{\mu_0} \beta_0 r_0} = 1 \quad \text{hence } \beta_0 = 1 \quad \text{A.2.69}$$

$$\frac{\sigma K_{or}}{|\vec{v}|_{\mu_0} x_0} = 1 \quad \text{hence } x_0 = \frac{\sigma K_{or}}{|\vec{v}|_{\mu_0}} \quad \text{A.2.70}$$

and

$$\frac{|\vec{v}|t_0}{\phi B_0 r_0} = 1 \quad \text{hence } t_0 = \frac{\phi(1-S_{or}-S_{wi})}{|\vec{v}|} \frac{\sigma K_{or}}{|\vec{v}|_{\mu_0}} \quad \text{A.2.71}$$

Although identical expressions were found for x_0 and r_0 , this is not the case in general. These quantities should not be forced to be identical as this

would lead to a loss of valuable information.

Now, for the sake of convenience, the following dimensionless groups are defined:

$$N_{cr} \equiv \frac{\sigma K_{wr}}{2|\vec{v}| \mu_w a} = \frac{\sigma K_{wr}}{|\vec{v}| \mu_w D} \quad \text{A.2.72}$$

and

$$N_{cl} \equiv \frac{\sigma K_{wr}}{|\vec{v}| \mu_w L} \quad \text{A.2.73}$$

where a is the core radius and L is the length of the sandpack. Recall Equation 2.11 in terms of the end-point permeabilities:

$$M_r \equiv \frac{K_{wr}}{K_{or}} \frac{\mu_o}{\mu_w} \quad \text{A.2.74}$$

The dimensionless variables defined by Equations A.2.48 to A.2.52 now become:

$$\phi = \frac{M_r}{2N_{cr}} \frac{r}{a} \quad \text{A.2.75}$$

$$\zeta = \frac{M_r}{N_{cl}} \frac{x}{L} \quad \text{A.2.76}$$

$$\tau = \frac{M_r}{N_{cl}} \frac{|\vec{v}| t}{\phi(1 - S_{or} - S_{wi})L} \quad \text{A.2.77}$$

or

$$\tau = \frac{M_r}{2N_{cr}} \frac{|\vec{v}|t}{\phi(1 - S_{or} - S_{wi})a} \quad \text{A.2.78}$$

The physical interpretation of the variables ϕ , ζ and τ is not an obvious one. Defining the following variables:

$$\psi \equiv \frac{r}{a} = \frac{2\phi N_{cr}}{M_r} \quad \text{A.2.79}$$

$$\xi \equiv \frac{x}{L} = \frac{\zeta N_{cl}}{M_r} \quad \text{A.2.80}$$

and

$$\tau \equiv \frac{|\vec{v}|t}{\phi L(1 - S_{or} - S_{wi})} = \frac{TN_{cl}}{M_r} \quad \text{A.2.81}$$

It is now evident that ψ , ξ and τ have the physical interpretation of dimensionless radius, dimensionless length, and dimensionless time, respectively. Furthermore, dimensionless time corresponds to pore volumes of fluid injected into the system. As a consequence of the introduction of N_{cr} and N_{cl} , the number of parameters is no longer a minimum. That is, N_{cr} and N_{cl} are redundant.

The above derivation of the reference quantities is based on a Lagrangian formulation of the initial and boundary conditions. The result is to yield a differential equation which does not account for the length and diameter of the system. These dimensions are accounted for in the

non-normalized dimensionless lengths, ζ and ϕ :

$$0 \leq \zeta \leq \frac{|\vec{v}| \mu_0 L}{K_{or}} \neq 1$$

and

$$0 \leq \phi \leq \frac{|\vec{v}| \mu_0 D}{K_{or}} \neq 1$$

The derivation may also be carried out using the Eulerian form of the initial and boundary conditions. Two possible definitions will arise for the arbitrary reference quantities, viz:

$$1) \quad x_0 = \frac{\sigma K_{or}}{|\vec{v}| \mu_0}, \quad r_0 = \frac{\sigma K_{or}}{|\vec{v}| \mu_0}$$

$$2) \quad x_0 = L, \quad r_0 = D$$

The first definitions are the same as the ones which arise from the Lagrangian formulation. As a result of using the second definitions, the differential equation will account for the dimensions of the porous medium and the dimensionless distances will be normalized, viz:

$$0 \leq \psi \leq 1$$

and

$$0 \leq \xi \leq 1$$

As a consequence of the introduction of the definitions for

ψ and ξ (Equations A.2.79 and A.2.80), essentially equivalent results may be obtained.

The fractional flow equation and the equation of continuity may now be written in terms of ψ , ξ and τ , viz:

$$\begin{aligned} \vec{f}_w = & \left[\frac{\vec{v}}{|\vec{v}|} - \frac{K_{or} \Delta \rho \vec{g}}{|\vec{v}| \mu_o} K_{ro}(S^*) \right] F_w(S^*) \\ & + \frac{F_w(S^*) K_{ro}(S^*)}{M_r} \frac{d\pi_c(S^*)}{dS^*} \left[2N_{cr} \frac{\partial S^*}{\partial \psi} \hat{\psi} \right. \\ & \left. + \frac{2N_{cr}}{\psi} \frac{\partial S^*}{\partial \beta} \hat{\beta} + N_{cl} \frac{\partial S^*}{\partial \xi} \hat{\xi} \right] \end{aligned} \quad \text{A.2.82}$$

and

$$\frac{2N_{cr}}{\psi} \frac{\partial}{\partial \psi} (\psi f_{w\psi}) + \frac{2N_{cr}}{\psi} \frac{\partial f_{w\beta}}{\partial \beta} + N_{cl} \frac{\partial f_{w\xi}}{\partial \xi} = - N_{cl} \frac{\partial S^*}{\partial \tau} \quad \text{A.2.83}$$

Equations A.2.82 and A.2.83 may be simplified to:

$$\vec{f}_w = \vec{G}(S^*) - N_{cl} C(S^*) \left[\frac{2L}{D} \left(\frac{\partial S^*}{\partial \psi} \hat{\psi} + \frac{1}{\psi} \frac{\partial S^*}{\partial \beta} \hat{\beta} \right) + \frac{\partial S^*}{\partial \xi} \hat{\xi} \right] \quad \text{A.2.84}$$

$$\frac{2L}{D} \psi \left[\frac{\partial}{\partial \psi} (\psi f_{w\psi}) + \frac{\partial f_{w\beta}}{\partial \beta} \right] + \frac{\partial f_{w\xi}}{\partial \xi} = - \frac{\partial S^*}{\partial \tau} \quad \text{A.2.85}$$

where

$$\vec{G}(S^*) = \left[\frac{\vec{v}}{|\vec{v}|} - \frac{\vec{N}_g}{M_r} K_{ro}(S^*) \right] F_w(S^*) \quad \text{A.2.86}$$

$$\vec{N}_g = \frac{K_{wr} \Delta \rho \vec{g}}{|\vec{v}| \mu_w} \quad \text{A.2.87}$$

$$C(S^*) = - \frac{1}{M_r} F_w(S^*) K_{ro}(S^*) \frac{d\pi_c(S^*)}{dS^*} \quad \text{A.2.88}$$

$$S^* = \frac{S_w - S_{wi}}{1 - S_{or} - S_{wi}} \quad \text{A.2.89}$$

$$M_r = \frac{K_{wr}}{K_{or}} \frac{\mu_o}{\mu_w} \quad \text{A.2.90}$$

$$F_w(S^*) = \frac{M_r K_{rw}(S^*)}{M_r K_{ro}(S^*) + K_{ro}(S^*)} \quad \text{A.2.91}$$

Appendix B--Experimental Results From the Literature

TABLE: B.1
SUMMARY OF SANDPACK PROPERTIES
DATA FROM PETERS (1979)

WATER-WET SYSTEM

RUN	LENGTH (CM)	DIAMETER (CM)	POROSITY (%)	ABS. PERM. (DARCY)	PERM. @SWI (DARCY)	SWI (%)
1	22.9	4.809	38.98	16.43	15.82	11.2
2	23.6	4.844	36.37	18.36	17.99	8.7
3	112.8	4.961	38.38	21.89	18.05	9.2
4	23.7	4.809	38.94	18.93	18.33	11.3
5	110.5	4.825	38.91	20.52	18.50	10.8
6	110.0	4.805	37.61	21.91	19.40	10.5
7	23.6	4.844	37.49	14.19	11.03	15.3
8	116.1	4.961	34.66	18.28	15.57	8.3
9	113.0	4.958	39.62	22.99	19.90	8.6
10	115.9	4.958	35.86	19.22	15.49	12.5
11	22.8	4.843	37.52	16.23	15.19	11.2
12	110.4	4.805	37.46	20.85	18.48	10.0
13	115.9	4.972	37.80	18.54	15.53	9.3
14	110.0	4.805	38.11	22.50	18.62	8.9
15	112.8	4.972	35.48	22.72	20.90	9.9

OIL-WET SYSTEM

RUN	LENGTH (CM)	DIAMETER (CM)	POROSITY (%)	ABS. PERM. (DARCY)
19	22.9	4.809	41.33	17.26
20	23.6	4.844	37.89	15.05
21	22.9	4.809	39.64	18.02
22	110.5	4.825	38.46	22.63
23	23.5	4.843	38.25	16.20
24	23.5	4.809	38.04	16.34
25	115.6	4.972	37.01	18.36
26	23.7	4.809	38.20	15.62
27	22.9	4.844	39.82	16.18
28	110.0	4.825	38.13	24.79
29	115.7	4.961	37.49	18.62

TABLE: B.2
SUMMARY OF DISPLACEMENT TESTS
DATA FROM PETERS (1979)

WATER-WET SYSTEM

RUN	Q CC/HR	V CM/SEC	REC %IDIP	BT	1/Lt1	1/Ltr	1/Nc1	1/Ncr	Ng	Ns
1	2.50	3.823E-05	43.63		1.473E-03	3.094E-04	2.738E-03	5.751E-04	9.831E-00	7.646E-01
2	20.00	3.015E-04	41.88		1.172E-02	2.406E-03	1.991E-02	4.087E-03	1.393E-00	5.474E-00
3	10.00	1.437E-04	43.68		2.382E-02	1.047E-03	3.805E-02	1.674E-03	3.485E-00	2.295E-00
4	160.00	2.447E-03	35.32		9.096E-02	1.846E-02	1.574E-01	3.194E-02	1.770E-01	4.247E-01
5	50.00	7.596E-04	40.30		1.265E-01	5.523E-03	2.102E-01	9.178E-03	6.180E-01	1.224E-01
6	100.00	1.532E-03	41.10		2.500E-04	1.092E-02	3.952E-01	1.726E-02	3.272E-01	2.293E-01
7	480.00	7.235E-03	30.40		3.152E-01	6.471E-02	6.184E-01	1.269E-01	4.487E-02	1.700E-02
8	160.00	2.299E-03	32.22		4.516E-01	1.930E-02	7.504E-01	3.207E-02	1.819E-01	4.398E-01
9	200.00	2.878E-03	30.89		4.588E-01	2.013E-02	7.268E-01	3.189E-02	1.828E-01	4.371E-01
10	240.00	3.453E-03	34.69		6.492E-01	2.777E-02	1.070E-00	4.577E-02	1.273E-01	6.274E-01
11	1120.00	1.689E-02	23.94		6.645E-01	1.411E-01	1.219E-00	2.590E-01	2.199E-02	3.467E-02
12	480.00	7.353E-03	26.81		1.237E-00	5.384E-02	2.001E-00	8.708E-02	6.487E-02	1.157E-02
13	480.00	6.867E-03	33.24		1.280E-00	5.492E-02	2.206E-00	9.464E-02	6.176E-02	1.301E-02
14	800.00	1.225E-02	28.62		1.960E-00	8.563E-02	3.079E-00	1.345E-01	4.200E-02	1.787E-02
15	1120.00	1.602E-02	23.43		2.711E-00	1.195E-01	4.088E-00	1.802E-01	3.244E-02	2.477E-02

OIL-WET SYSTEM

RUN	Q CC/HR	V CM/SEC	REC %IDIP	BT	1/Lt1	1/Ltr	1/Nc1	1/Ncr	Ng	Ns
19	2.50	3.823E-05	69.91		1.396E-03	2.932E-04	2.607E-03	5.474E-04	1.033E-01	4.090E-01
20	2.50	3.768E-05	62.50		1.586E-03	3.255E-04	3.037E-03	6.233E-04	9.137E-00	4.690E-01
21	10.00	1.529E-04	41.47		5.580E-03	1.172E-03	9.987E-03	2.097E-03	2.696E-00	1.567E-02
22	10.00	1.519E-04	31.02		2.423E-02	1.058E-03	3.812E-02	1.665E-03	3.408E-00	1.248E-02
23	40.00	6.032E-04	22.46		2.425E-02	4.997E-03	4.496E-02	9.266E-03	6.144E-01	6.972E-02
24	200.00	3.059E-03	19.71		1.228E-01	2.512E-02	2.261E-01	4.626E-02	1.222E-01	3.456E-03
25	80.00	1.145E-03	17.46		2.161E-01	9.297E-03	3.703E-01	1.593E-02	3.670E-01	1.230E-03
26	480.00	7.341E-03	16.05		3.039E-01	6.154E-02	5.724E-01	1.161E-01	4.868E-02	8.677E-03
27	1120.00	1.688E-02	16.66		6.486E-01	1.372E-01	1.228E-00	2.597E-01	2.193E-02	1.954E-04
28	800.00	1.215E-02	17.26		1.852E-00	8.122E-02	2.771E-00	1.216E-01	4.666E-02	9.112E-03
29	1120.00	1.609E-02	14.30		3.001E-00	1.287E-01	5.139E-00	2.204E-01	2.647E-02	1.698E-04

Appendix C--Sample Calculation of Extrapolated Data

This section demonstrates the calculations for Point E of Figure 4.1 for the inverse linear Leverett correlation. The magnitude of the stability number, N_s , corresponding to the point where the viscous forces completely dominate the displacement process, is 900. Thus,

$$N_s = \frac{\left(\frac{\mu_o}{\mu_w} - 1\right) V \mu_w D^2}{C^* \gamma K} = 900 \quad \text{C.1}$$

Solving for the velocity yields:

$$V = \frac{900 C^* \gamma K}{\left(\frac{\mu_o}{\mu_w} - 1\right) \mu_w D^2} \quad \text{C.2}$$

Recalling the definition of the inverse linear Leverett number:

$$\frac{1}{L t_d} = \frac{V \mu_w L}{\gamma (K\phi)^{0.5}} \quad \text{C.3}$$

and, upon substituting Equation C.2, gives the result:

$$\frac{1}{L t_d} = \frac{900 C^* \gamma K}{\left(\frac{\mu_o}{\mu_w} - 1\right) \mu_w D^2} \cdot \frac{\mu_w L}{\gamma (K\phi)^{0.5}} \quad \text{C.4}$$

Equation C.4 may be simplified to:

$$\frac{1}{L t_d} = \frac{900 C^* (K/\phi)^{0.5} L}{\left(\frac{\mu_o}{\mu_w} - 1\right) D^2} \quad \text{C.5}$$

The inverse linear Leverett number, in a water-wet,

connate-water-bearing system may now be estimated from Equation C.5. In particular, for Point E:

$$\begin{aligned}
 C^* &= 306.25 \\
 \left(\frac{h_o}{h_w} - 1 \right) &= 101.5 \\
 K &= 18 \text{ Darcys} = 1.78 \times 10^{-7} \text{ cm}^2 \\
 \phi &= 0.36 \\
 L &= 22.6 \text{ cm} \\
 D &= 4.815 \text{ cm}
 \end{aligned}$$

where L and D are the dimensions of a sandpack, and ϕ and K are the estimated average sandpack properties. With these values for the variables, the inverse linear Leverett number is 1.86×10^0 . The same type of calculation may be carried out for any other case desired.